NATIONAL ADVISORY COMMITTEE
FOR AERONAUTICS

TECHNICAL NOTE 3782

HANDBOOK OF STRUCTURAL STABILITY

PART I - BUCKLING OF COMPOSITE ELEMENTS

By Herbert Becker

New York University

Washington
July 1957

NATIONAL ADVISORY COMMITTEE FOR AERONAUTICS

TECHNICAL NOTE 3782

HANDBOOK OF STRUCTURAL STABILITY

PART II - BUCKLING OF COMPOSITE ELEMENTS

By Herbert Becker

SUMMARY

The local buckling of stiffener sections and the buckling of plates with sturdy stiffeners are reviewed, and the results are summarized in charts and tables. Numerical values of buckling coefficients are presented for longitudinally compressed stiffener sections of various shapes, for stiffened plates loaded in longitudinal compression and in shear, and for stiffened cylinders loaded in torsion. Although the data presented consist primarily of elastic-buckling coefficients, the effects of plasticity are discussed for a few special cases.

INTRODUCTION

The buckling behavior of simple plate elements is described in parts I and III of this "Handbook of Structural Stability" (refs. 1 and 2). Structural components often consist of two or more simple plate elements so arranged that the buckling stress of each is increased as a result of the support provided by contiguous neighbors. Such composite elements are termed stiffeners because they are frequently used to stiffen a plate in order to increase the buckling stress. A compact stiffener is described as "sturdy" when it is not subject to local buckling and therefore only the axial, bending, and torsional rigidities of the stiffener influence the behavior of the plate-stiffener combination under a specified loading. The data presented in this report on the buckling of stiffened plates pertain to sturdy stiffeners.

The report begins with a discussion of calculation of local buckling stress of stiffening elements. Stiffener structural shapes in common use, such as Z-, channel, and hat sections, have been analyzed for buckling and charts are presented to facilitate buckling-stress computations. For sections which buckle elastically, failure may occur at loads considerably in excess of buckling. Failure, or crippling, of stiffening elements is treated in reference 3.

When the proportions of a stiffener are such that it is sturdy with respect to the plate which it is stiffening, it acts essentially as an

elastic restraint to the plate. It may assist in the resistance to load, as do the spanwise stiffeners in a wing cover, or it may behave primarily as a support, such as a transverse rib. In either case, it is necessary to consider only its axial, bending, and rotational spring properties in calculating the buckling stress of a stiffened plate. Buckling of the composite will then occur either locally in the plate or generally, involving both the plate and stiffener. The information on buckling of stiffened plates appears in the section entitled "Buckling of Stiffened Plates Under Longitudinal Compression" for uniaxial load and in the section entitled "Buckling of Stiffened Plates Under Shear Load" for shear load.

The buckling of stiffened curved plates involves the complication of plate curvature in addition to all the parameters affecting buckling of stiffened flat plates. The buckling of unstiffened curved plates has been described in reference 2, in which it was shown that theory is in good agreement with test data for shear loading and in poor agreement with data for axial compression loading. For certain proportions, the curved plates approach cylinder behavior, which permits evaluation of the unstiffened-plate results in the limiting case. Analyses of stiffened curved plates are reported in the section entitled "Buckling of Stiffened Plates Under Longitudinal Compression" for axial loads and in the section entitled "Buckling of Stiffened Plates Under Shear Load" for shear loads. In addition, the limiting case of torsional buckling of a stiffened cylinder is described in the latter section. The results of the theory and test data are compared with the information on stiffened curved plates under shear.

The buckling stress of a stiffener or a stiffened plate may be found from the general relationship

$$\sigma_{cr} = \frac{k_b \pi^2 E}{12\left(1 - \nu_e^2\right)}\left(\frac{t}{b}\right)^2 \tag{1}$$

in which b pertains to a general dimension. It may be the width of a flange on an angle, the depth of the web on a channel, or the width of one of the sides of a rectangular tube. The buckling coefficient k_b is the coefficient to be used together with this dimension in equation (1).

The parameters upon which k_b depends are a/b or λ/b of the plate, the amount of elastic rotational restraint along the unloaded edges ϵ, the ratio of the area of the stiffener to that of the plate A/bt, the ratio of the bending rigidity of the stiffener to that of the plate EI/bD, and the curvature parameter for curved plates Z_b. The

figures discussed in the following sections show k_b as a function of these parameters.

The effects of material properties on the buckling of simple elements were covered in reference 1, in which stress-strain curves, Poisson's ratio, and cladding and plasticity-reduction factors are presented and discussed. Plasticity-reduction factors for curved plates and shells are described in reference 2. For convenience, a summary of pertinent information appears in the "Application Section" and tables 1 to 3.

This survey was conducted at New York University under the sponsorship and with the financial assistance of the National Advisory Committee for Aeronautics.

SYMBOLS

A	area of stiffener cross section, sq in.
a	length of unloaded edge on longitudinally compressed plates and simple elements or longer side of plates loaded in shear,[1] in.
b	length of loaded edge on longitudinally compressed plates and simple elements or shorter side of plates loaded in shear,[1] in.
D	flexural rigidity of plate per inch of width, $Et^3/\left[12\left(1 - \nu_e^2\right)\right]$, in-lb
d	width of bulb of bulb flange
E, E_s, E_t	Young's modulus, secant modulus, and tangent modulus, respectively, psi
G	shear modulus, psi
h	width of rectangular tube stiffener (see fig. 5(c))

[1]Symbols a and b pertain to dimensions between stiffeners on stiffened plates or to distances between parallel edges on unstiffened plates. Thus, buckling stress is found for a single element of a stiffened plate and not in terms of overall dimensions of the plate, except for curved stiffened plates under shear. In this latter case it is more convenient to utilize a and b as overall plate dimensions for ease of comparison with cylinder data.

I	bending moment of inertia of stiffener cross section, in.^{4}
J	torsional moment of inertia of stiffener cross section, in.^{4}
k	buckling coefficient
k_b	general buckling coefficient of stiffener pertaining to buckling stress of element of width b
k_c, k_s	buckling coefficients for compression and shear, respectively
L	length of cylinder, in.
M	moment applied to edges of rotationally restrained element, in-lb
n	number of longitudinal stiffeners on plate of total width nb, or number of circumferential rings on cylinder of length L
q	number of transverse buckles in longitudinally stiffened plate longitudinally compressed
R	radius of curvature of curved plate, in.
r	correction for presence of stiffener on one side of plate
S	plate stiffness (see fig. 2 for different types)
t	thickness, in.
Z_b	plate curvature parameter, $\left(b^2/Rt\right)\left(1 - \nu_e^2\right)^{1/2}$
Z_L	cylinder curvature parameter, $\left(L^2/Rt\right)\left(1 - \nu_e^2\right)^{1/2}$
Z_{nq}	factor in r dependent upon n and q (see fig. 12)
$\bar{z}$	distance of stiffener centroid from midsurface of plate, in.
ϵ	ratio of rigidity of elastic restraint to rotational rigidity of plate; also strain
η	plasticity-reduction factor
θ	rotation of edge of simple element, radians
λ	wave length of buckle in simple element or plate, in.

ν_e Poisson's ratio in elastic range

σ_{cr} general buckling stress; also, buckling stress of compressed element, psi

τ_{cr} buckling stress of element loaded in shear, psi

Subscripts:

cr buckling

e effective

f flange

L lip

T top web of hat-section stiffeners

w web

LOCAL BUCKLING OF STIFFENING ELEMENTS

Behavior of Stiffeners

When a plate under longitudinal load is supported by a stiffener in the direction of the load, the stiffener participates in resisting this load. As a result, the possible buckling modes of this composite are local instability of the plate alone, local buckling of one or more simple elements of the stiffener, general instability of the plate involving column action of the stiffener, or some combination of these modes. The analyses pertaining to stiffened plates apply to sturdy stiffeners only, and, consequently, the second mode is precluded by the analysis in those cases described in the last sections of the present paper. However, in order to insure the sturdiness of the stiffener, it is first necessary to determine its local buckling stress. This is the subject to be discussed in the present section, which presents the background for analysis of local buckling in stiffeners and includes charts for rapid calculation of buckling stress for several common shapes.

The local buckling stress of a stiffener is the same as that of its weakest element. Consequently, each simple element must be analyzed for buckling under longitudinal load. Often the weakest element is readily evident by inspection. The analysis of the element involves determining the nature of the supports and rotational restraints along the edges and

then computing the buckling stress of the element considered as a simple plate under longitudinal load with the appropriate boundary conditions.

In general, however, there is mutual restraint at a longitudinal joint among all the members meeting along such a line. If this restraint could be converted directly into a value of rotational restraint ϵ for the simple element being analyzed, then the buckling-coefficient charts of references 1 and 2 could be used to find the buckling stress of the simple element, and, consequently, the buckling stress of the stiffener. Because of the rotational interaction among the simple elements at each joint line, which arises from the preservation of the corner angles between element pairs $(\theta_1 = \theta_2 = \ldots = \theta_n)$, however, the restraint imposed by each upon the others cannot be found immediately. It is necessary to analyze the problem as one in the distribution of moment among the members of a statically indeterminate system. When this has been done, ϵ can be found and σ_{cr} can be calculated.

For the most part, the stiffness of one element in its own plane is sufficient to impart support to its adjacent elements perpendicular to their planes, although the corner angles may differ from 90°. Most simple elements of a stiffener behave in this manner. Lips and bulbs may be too weak to provide complete transverse support to an element (invariably a flange). They act as columns that tend to resist elastically the transverse deflections of the otherwise free edges of flanges and, consequently, cannot be included in the usual methods of analysis of the interaction buckling problem. However, a flange with a lip or bulb along its free edge may be analyzed as a stiffened plate to determine the rigidity of this composite, which then can be used in the interaction analysis.

Calculation of Buckling Stress

The buckling stress of each simple element of a stiffener may be found from equation (1). Charts of k_b for several stiffener sections in common use are presented in this report and are discussed below in the section on "Numerical Values of Buckling Stress." The general methods of constructing these charts and for finding the buckling stress of a new stiffener section involve a successive approximation procedure such as the moment-distribution method of Lundquist, Stowell, and Schuette (ref. 4) or the step-by-step procedure of Kroll, Fisher, and Heimerl (ref. 5).

The basis for the moment-distribution method is the joint-stiffness criterion, which requires that at buckling the sum of the stiffnesses of the simple elements meeting at a joint line must be zero. This is predicted upon a distribution of stiffnesses among the joint members such that all have the same longitudinal wave length. The vanishing of the joint stiffness at buckling follows from the fact that stiffness is equal

to M/θ. Since θ is the same for all simple elements at the joint line, stiffness is proportional to the moment carried by each element. However, since these moments must vanish at buckling for small deflections of the elements, the joint-stiffness criterion follows.

The moment-distribution analysis is simplified by the use of charts of element stiffness and carry-over factor prepared by Kroll for different types of boundary conditions along the unloaded edges (ref. 6). These are described in the following section on numerical values of buckling stress.

In essence, the step-by-step procedure for calculating the buckling stress of a simple element involves the arbitrary selection of a buckling stress together with several arbitrary values of buckle wave length. For each of these values, σ_{cr} is calculated from equation (1) until its minimum value is found. If this is different from the initially assumed buckling stress, the process is repeated until the assumed and calculated values agree. This is the buckling stress of the composite element.

Charts of $k_c(\lambda/b,\epsilon)$ are used (as presented in ref. 1) together with the rigidity tables of Kroll (ref. 6).

The buckling stress of a flange with a lip or bulb was investigated by Hu and McCulloch (ref. 7), Goodman and Boyd (ref. 8), and Goodman (ref. 9) who considered a large range of lip, bulb, and flange proportions. Gerard simplified the analysis by selecting the geometries usually encountered in design and defined the range of section proportions in which the element undergoes the transition from a flange to a web as the rigidity of the edge stiffener increases (ref. 10).

Roy and Schuette have demonstrated experimentally that the local buckling stress of the section is unaffected although the angle between adjacent elements is as small as 30° or as large as 120° (ref. 11). The principal effect of changing the corner angle from 90° is to decrease the section moment of inertia, which diminishes its column strength.

Numerical Values of Buckling Stress

The buckling stress of a stiffener is determined using the breakdown scheme of figure 1. Equation (1) is utilized to compute the numerical value of this stress for the weakest element after the buckling coefficient has been found according to a method such as that described in the preceding section. The different stiffnesses evaluated by Kroll in tabular form (ref. 6) are depicted in figure 2.

The effects of lips or bulbs are obtainable from figures 3(a) and 3(b) which present the charts developed by Gerard (ref. 10). The buckling

strain is shown as a function of the flange b/t and the edge-stiffener proportions, which permit determination of the rigidity of such a composite for use in the indeterminacy analysis. In this manner, these charts serve as an adjunct to Kroll's tables.

Buckling coefficients are presented for common stiffener shapes such as shown in figure 4, in which the dimensions of webs and flanges are shown for both formed and extruded shapes. The buckling-coefficient charts for channel, Z-, H-, and rectangular-tube stiffeners appear in figure 5. They were taken from the report of Kroll, Fisher, and Heimerl (ref. 5). The dashed lines on these charts define the section proportions at which both web and flange buckle simultaneously. Data for hat-section stiffeners appear in figure 6. The curves, adapted from those of Van Der Maas (ref. 12), cover a range of flange sizes for different widths of center and lateral webs of the hat section. It should be noted that hat and lipped Z- and channel sections are structurally equivalent.

Effects of Plasticity

The inelastic-buckling stress of a stiffener may be computed by a method such as the moment-distribution procedure of Lundquist, Stowell, and Schuette for elastic-buckling problems (ref. 4). This was done by Stowell and Pride (ref. 13), who obtained good agreement with experimental data (fig. 7), for H-section stiffeners. The plasticity-reduction factor for each simple element of the section was employed in computing the buckling stress for use in the moment-distribution procedure, in which the joint-stiffness criterion controls the theoretical buckling stress of the section.

It should be noted that the test data at the larger strains lie about 5 percent below the stress-strain curve, while the theory band is 3 percent below at the most. This analysis seems to indicate that the use of the plasticity-reduction factor for a clamped flange would be conservative. Use of the secant modulus for a simply supported flange would be slightly optimistic.

BUCKLING OF STIFFENED PLATES UNDER LONGITUDINAL COMPRESSION

General Background

As discussed in the preceding section, the general case of buckling of stiffened panels involves local instability of the stiffeners as well as the spring properties in compression, bending, and torsion. In this section the special case of sturdy stiffeners is discussed, and a brief description of the influence of torsional rigidity of the stiffener is

included. This is of significance since the design data presented in the charts pertain to stiffeners with no torsional rigidity.

A description of the buckling behavior of a supported and restrained rectangular plate may be found in reference 1 for flat plates and in reference 2 for curved plates. The stiffening elements, whose local buckling behavior was depicted in the preceding section of this report, provide these supports and restraints to the plates at intermediate positions in the plate spans. The effectiveness of these supports depends upon the axial, bending, and torsional rigidities of the plate and stiffeners. Representative arrangements of plate-stiffener combinations are shown in figure 8.

Behavior of Stiffened Plates Under Longitudinal Compression

The two instability modes to be considered in this section are local buckling of the plate between stiffeners and general instability of the composite element. In most cases the torsional rigidity of the stiffener is assumed to be negligibly small, thus excluding rotational restraint of the plate along the stiffener line.

The behavior of a plate buckling under longitudinal load and supported by deflectional and rotational springs is shown schematically in figure 9. Wave forms for the three limiting cases of perfectly flexible and perfectly rigid springs are shown. In general, the wave forms for finite spring rigidities do not change shape significantly, although the amplitudes of the waves may vary. When the stiffener rigidity is sufficient to enforce a node, the plate will receive no additional flexural support from the stiffener. This description parallels that for columns which was presented by Budiansky, Seide, and Weinberger (ref. 14).

Calculation of Buckling Stress

The buckling stress of a stiffened plate under longitudinal load is usually expressed in the form of equation (1) where b is the width of the plate between stiffeners. The buckling coefficient k_c is a function of the parameters of the composite element:

$$k_c = k_c\left(a/b,\ A/bt,\ EI/bD,\ Z_b\right) \tag{2}$$

Both the energy-integral approach and the differential-equation method of solution have been used to solve the problem of buckling of a stiffened plate. The essentials of both these procedures have been described in reference 1.

Numerical Values of Buckling Stress

The numerical values of buckling stress for stiffened flat plates and curved plates under longitudinal compression are as follows:

Stiffened flat plates.- Seide and Stein calculated the buckling coefficients for longitudinally loaded simply supported flat plates with one, two, three, and an infinite number of longitudinal stiffeners (ref. 15). The results appear in figure 10 in which k_c is shown as a function of a/b for a range of values of EI/bD. A summary of coefficients for infinitely long plates is presented in figure 11 for convenience in determining buckling stresses for long stiffened plates.

The calculations of Seide and Stein were based upon the assumption that the stiffener-section centroid was located at the midsurface of the plate. This is not usually the case in actual practice, in which the stiffener is commonly located on one side of the plate. This problem was investigated in general terms by Chwalla and Novak (ref. 16). Seide also evaluated this effect (ref. 17) and evolved a correction for the charts of figure 10 applicable to plates with one, two, or infinitely many stiffeners

$$r = \frac{(EI/bD)_e}{(EI/bD)} = 1 + \frac{A\bar{z}^2/I}{1 + \left(Z_{nq}A/bt\right)} \tag{3}$$

from which the effective bending rigidity ratio $(EI/bD)_e$ may be obtained. The function $Z_{nq} = f(\lambda/b, n, q)$ in figure 12, in which λ/b ($\lambda/b = a/qb$, where $q = 1$, 2, and 3) must match the value used to enter figure 10. A trial-and-error approach might be required since $(EI/bD)_e$ may occur at a different value of q in figure 10 than does EI/bD at the a/b originally used together with n ($n = 1$, 2, and ∞) to enter these charts. When there are three stiffeners on the plate, it is necessary to satisfy an equation, other than equation (3), appearing in Seide's report.

Budiansky and Seide investigated longitudinal compressive buckling of transversely stiffened simply supported plates (ref. 18). The data which pertain to $a/b = 0.20$, 0.35, and 0.50 appear in figure 13. The curves cover a range of stiffener torsional rigidity, in contrast with the curves for axially stiffened plates for which $GJ = 0$ in all cases.

The preceding data pertain to general instability of stiffened plates. Gallaher and Boughan (ref. 19) and Boughan and Baab (ref. 20) determined local buckling coefficients for idealized web-, Z-, and T-stiffened plates. The stiffener-web composites were idealized as shown in figure 14, in which the buckling coefficients are presented as functions of the proportions of the composite.

Stiffened curved plates.- The information for stiffened curved plates relates to that obtained from sections of circular cylinders. Batdorf and Schildcrout investigated the compressive buckling of a simply supported curved plate with a central circumferential stiffener having no torsional rigidity or axial stiffness (ref. 21). In addition to determining the theoretical buckling stress, which was done using linear theory, the percentage increase in buckling stress over the theoretical value was obtained and is shown in figure 15. Because of the low experimental values of buckling stress compared with the results of the linear theory, Batdorf and Schildcrout recommended applying the theoretical percentage increase to the experimental buckling stress, values of which may be found in reference 2. The maximum possible increase for a curved plate with a given value of a/b and Z_b is shown in figure 15(a), while an increase less than the maximum is obtainable from figure 15(b). Furthermore, the value of EI/bD required to cause a buckle node at the stiffener line is obtainable from these figures by cross-plotting.

Note that no gain is indicated when $a/b > 0.7$ or when Z_b is greater than the values shown in the table below.

a/b	0.600	0.500	0.417	0.333	0.250	0.167
Z_b	28.0	14.0	7.8	4.1	1.9	0.7

The charts of figure 15 were designed to permit an estimate of the increase in buckling stress to be expected in an axially compressed curved plate when the central circumferential stiffener has less bending rigidity than that required to enforce a node along the stiffener line. When the stiffener has this minimum rigidity, the length of the original plate may be considered to be halved, and the data in reference 2 should be used to obtain the buckling stress.

This approach also applies to plates with axial stiffeners, which were analyzed by Schildcrout and Stein (ref. 22). The curves for this type of panel appear in figure 16, in which k_c appears as a function of EI/bD for a range of values of a/b and Z_b. In order to account for the disparity of test data with theory for curved plates, Schildcrout and Stein recommend the following procedure:

(1) Determine the difference between the buckling stress of the stiffened panel (fig. 16) and that of the unstiffened panel (ref. 2).

(2) To this difference, add the larger of the two following stresses:

(a) The buckling stress of the unstiffened panel

(b) The buckling stress of the corresponding flat plate

When the curved plate width exceeds the length, use the curves for cylinders. Use the curved-plate buckling data only when the length exceeds the width.

Effects of Plasticity

Plasticity-reduction factors for stiffened panels depend upon the factors pertinent to each element of the composite. For example, the factor for supported plates would be expected to apply to the plate elements between stiffeners, whereas sturdy stiffeners behaving as columns should follow the tangent modulus. If these conditions hold in the composite, the elastic-range parameter EI/bD would become $E_tI/\eta bD$ in the inelastic range.

Gallaher and Boughan compared test data on Z-stiffened panels subject to local buckling with buckling stresses computed using the secant modulus as the plasticity-reduction factor and obtained the agreement shown in figure 17 (ref. 19). Some of the data pertain to plates with sturdy stiffeners. However, a large portion applies to composites in which the stiffeners buckled locally.

Effect of Torsional Rigidity of Stiffener

The buckling-coefficient charts discussed in the preceding paragraphs were prepared for stiffeners with no torsional rigidity. Actually all stiffeners have some torsional rigidity, and closed stiffeners, of which the hat section is typical, may function as fully rigid stiffeners in torsion for some applications. In reference 1 a chart based upon test data was presented depicting the effect on buckling stress as the torsional rigidity changes relative to the rigidity of the plate being stiffened. This has been reproduced here in figure 18, in which may be seen the comparative effects of stiffeners with large and small torsional rigidity.

The gain in plate buckling stress realizable with stiffeners of finite torsional rigidity depends upon the rotational restraint ϵ provided by the stiffener. This is related to the difference in buckling stress between stiffener and plate, where the stiffener is now considered to be a simple element of specified elastic properties, in order to satisfy the joint-stiffness criterion discussed in the section entitled "Local Buckling of Stiffening Elements." Thus,

$$\sigma_{cr} = f\left(\sigma_{cr_{stiffener}} - \sigma_{cr_{plate}}\right) \tag{4}$$

This is substantiated by figure 18, which shows little gain over simple support when the plate rigidity is high (low values of b/t).

BUCKLING OF STIFFENED PLATES UNDER SHEAR LOAD

Behavior of Stiffened Plates Under Shear

When transverse stiffeners are attached to a plate loaded in shear, they may be rigid enough to enforce nodes at the attachment lines or they may be so weak as to exert virtually no influence on the plate buckle pattern. The extreme case of weak stiffeners was examined by Schmieden (ref. 23), Seydel (ref. 24), and Wang (ref. 25) while rigid stiffeners were examined by Timoshenko (ref. 26).

The intermediate rigidity range was analyzed by Crate and Lo who demonstrated the manner in which the shear buckling stress of an infinitely long flat plate is increased longitudinally as stiffener rigidity rises until it is sufficient to enforce nodes along the attachment lines (ref. 27). During this process the buckle pattern of the plate changes from the wave form for an unstiffened plate of infinite length and of width $(n + 1)b$ to that of a plate width b. Test data obtained by Crate and Lo follow the theoretical trend of k_s as a function of EI/bD. The scatter is large with most of the data lying between the curves for simple support and clamped edges, as shown in figure 19(a).

Stein and Fralich analyzed buckling of long flat plates with transverse stiffeners subjected to shear load (ref. 28). The behavior is analogous to that of a longitudinally compressed plate with transverse stiffeners. In figure 19(b) test data are shown to agree with the theory of Stein and Fralich.

Stein and Jaeger analyzed buckling of a curved plate with a central stiffener placed either axially or circumferentially (ref. 29). Although the general behavior pattern corresponds to that for flat plates, the additional factor of curvature modifies the buckle pattern, which tends toward that of a cylinder in wide curved plates.

A stiffened cylinder represents a limiting case of stiffened curved plates. Most of the literature pertaining to this case covers test results, the major portion of which applies to weak stiffeners that buckle locally or to stiffeners rigid enough to enforce nodes and thereby cause the cylinder to behave as a group of plates. These cases are discussed in reference 2, which deals specifically with this problem.

Stein, Sanders, and Crate investigated the buckling of cylinders loaded in torsion and stiffened by rings with finite rigidity (ref. 30).

A large range of values of Z_L was covered for a corresponding large range of values of EI/bD. The theory was compared with test data with the results shown in figure 20, in which the theory is seen to be slightly optimistic.

Calculation of Buckling Stress

The buckling stress is expressed in the form of equation (1) in which the buckling coefficient k_s is a function of geometry and loading. As in the case of longitudinal load, the basic parameters for flat plates are a/b, A/bt, and EI/bD, while Z_b is an additional parameter for curved plates and Z_L applies to cylinders. In the theoretical investigations the stiffeners were assumed to possess no torsional rigidity, and the centroids were assumed to lie in the midsurface of the plate.

Numerical Values of Buckling Stress

The numerical values of buckling stress for stiffened flat and curved plates and cylinders in torsion under shear loads are as follows:

Stiffened flat plates.- The theory of Crate and Lo for long flat plates loaded in shear and stiffened longitudinally (ref. 27) is presented in figure 19(a), in which k_s is plotted as a function of EI/bD for both clamped and simply supported plates with one or two stiffeners. The results of Stein and Fralich (ref. 28) for transversely stiffened flat plates appear in figure 21. From this latter figure it may be seen that the minimum value of EI/bD required to enforce a node at the stiffener-attachment line increases rapidly with a/b. Approximate values are shown in the table below.

a/b	1	2	5
Minimum value of EI/bD for node	10	100	700

Stiffened curved plates.- The results of the theoretical investigation of Stein and Yaeger on curved plates loaded in shear and supported by a central stiffener (ref. 29) appear in the charts of figure 22. Both axial and circumferential stiffeners are considered together with wide plates and long plates. The results are plotted in the form of k_s as a function of EI/bD, in which b is the short side. This permits comparison with the curves for unstiffened plates presented in reference 2.

The curves are plotted for several values of Z_b and $a/b = 1, 1.5,$ and 2 (where, for this case, a and b are the overall plate dimensions). In addition, the limiting curves of infinite a/b for long plates and the cylinder curve for wide plates are included. The latter may be checked against the curves for cylinders to be discussed in the following paragraph and presented in figure 23.

Stiffened cylinders in torsion.- Stiffened cylinders in torsion represent a limiting case of stiffened wide plates in shear. Stein, Sanders, and Crate calculated the buckling stress as a function of the cylinder and stiffener parameters (ref. 30). The curves appear in figure 23, in which k_s is shown as a function of EI/bD for a large range of values of Z_L and for one, two, three, and four intermediate rings. The curves pertaining to one ring may be seen to agree with the cylinder curves of figure 22(d) for wide plates with a central circumferential stiffener.

These results were obtained for stiffeners with no torsional rigidity, with the section centroid in the midsurface of the cylinder wall.

Effects of Plasticity

The plasticity-reduction factors for stiffened plates under shear may be found in references 1 and 2 for flat and curved plates with specific boundary conditions. This information should apply to plates with stiffeners rigid enough to enforce nodes along their attachment lines. No data exist, however, for plasticity-reduction factors for plates stiffened by elements of rigidity less than that required for a node.

APPLICATION SECTION

The use of buckling charts for stiffeners and stiffened plates has been described in the preceding sections. In this application section the results are summarized for rapid reference and the tables are explained.

Table 1 contains data for stiffening elements loaded in compression. Information on stiffened plates loaded in longitudinal compression appears in table 2, and data relating to stiffened plates loaded in shear are found in table 3. In all cases the buckling stress can be found from equation (1):

$$\sigma_{cr} = \eta \frac{k_b \pi^2 E}{12\left(1 - \nu_e^2\right)}\left(\frac{t}{b}\right)^2$$

Plasticity-reduction factors appear in the tables where they are applicable. For further information on plasticity-reduction factors and cladding reduction factors also, see references 1 and 2. For information on failure of stiffeners see reference 3.

For ring-stiffened cylinders in torsion,

$$\sigma_{cr} = \frac{k_t \pi^2 E}{12\left(1 - \nu_e^2\right)}\left(\frac{t}{L}\right)^2$$

For this case, k_t depends upon Z_L instead of Z_b.

It should be noted that a and b are the overall plate dimensions for stiffened plates under shear. This permits comparison with the data for ring-stiffened cylinders in torsion.

Research Division, College of Engineering,
New York University,
New York, N. Y., April 15, 1955.

REFERENCES

1. Gerard, George, and Becker, Herbert: Handbook of Structural Stability. Part I - Buckling of Flat Plates. NACA TN 3781, 1957.

2. Gerard, George, and Becker, Herbert: Handbook of Structural Stability. Part III - Buckling of Curved Plates and Shells. NACA TN 3783, 1957.

3. Gerard, George: Handbook of Structural Stability. Part IV - Failure of Plates and Composite Elements. NACA TN 3784, 1957.

4. Lundquist, Eugene E., Stowell, Elbridge Z., and Schuette, Evan H.: Principles of Moment Distribution Applied to Stability of Structures Composed of Bars or Plates. NACA WR L-326, 1943. (Formerly NACA ARR 3K06.)

5. Kroll, W. D., Fisher, Gordon P., and Heimerl, George J.: Charts for Calculation of the Critical Stress for Local Instability of Columns with I-, Z-, Channel, and Rectangular-Tube Section. NACA WR L-429, 1943. (Formerly NACA ARR 3K04.)

6. Kroll, W. D.: Tables of Stiffness and Carry-Over Factor for Flat Rectangular Plates Under Compression. NACA WR L-398, 1943. (Formerly NACA ARR 3K27.)

7. Hu, Pai C., and McCulloch, James C.: The Local Buckling Strength of Lipped Z-Columns With Small Lip Width. NACA TN 1335, 1947.

8. Goodman, Stanley, and Boyd, Evelyn: Instability of Outstanding Flanges Simply Supported at One Edge and Reinforced by Bulbs at Other Edge. NACA TN 1433, 1947.

9. Goodman, Stanley: Elastic Buckling of Outstanding Flanges Clamped at One Edge and Reinforced by Bulbs at Other Edge. NACA TN 1985, 1949.

10. Gerard, George: Torsional Instability of Hinged Flanges Stiffened by Lips and Bulbs. NACA TN 3757, 1956.

11. Roy, J. Albert, and Schuette, Evan H.: The Effect of Angle of Bend Between Plate Elements on the Local Instability of Formed Z-Sections. NACA WR L-268, 1944. (Formerly NACA RB L4I26.)

12. Van Der Maas, Christian J.: Charts for the Calculations of the Critical Compressive Stress for Local Instability of Columns With Hat Sections. Jour. Aero. Sci., vol. 21, no. 6, June 1954, pp. 399-403.

13. Stowell, Elbridge Z., and Pride, Richard A.: Plastic Buckling of Extruded Composite Sections in Compression. NACA TN 1971, 1949.

14. Budiansky, Bernard, Seide, Paul, and Weinberger, Robert A.: The Buckling of a Column on Equally Spaced Deflectional and Rotational Springs. NACA TN 1519, 1948.

15. Seide, Paul, and Stein, Manuel: Compressive Buckling of Simply Supported Plates with Longitudinal Stiffeners. NACA TN 1825, 1949.

16. Chwalla, E., and Novak, A.: The Theory of One-Sided Web Stiffeners. R.T.P. Translation No. 2501, British Ministry of Aircraft Production. (From Bautechnic - Suppl. der Stahlbau, vol. 10, no. 10, May 7, 1937, pp. 73-76.)

17. Seide, Paul: The Effect of Longitudinal Stiffeners Located on One Side of a Plate on the Compressive Buckling Stress of the Plate-Stiffener Combination. NACA TN 2873, 1953.

18. Budiansky, Bernard, and Seide, Paul: Compressive Buckling of Simply Supported Plates With Transverse Stiffeners. NACA TN 1557, 1948.

19. Gallaher, George L., and Boughan, Rolla B.: A Method of Calculating the Compressive Strength of Z-Stiffened Panels That Develop Local Instability. NACA TN 1482, 1947.

20. Boughan, Rolla B., and Baab, George W.: Charts for Calculation of the Critical Compressive Stress for Local Instability of Idealized Web- and T-Stiffened Panels. NACA WR L-204, 1944. (Formerly NACA ACR L4H29.)

21. Batdorf, S. B., and Schildcrout, Murry: Critical Axial-Compressive Stress of a Curved Rectangular Panel With a Central Chordwise Stiffener. NACA TN 1661, 1948.

22. Schildcrout, Murry, and Stein, Manuel: Critical Axial-Compressive Stress of a Curved Rectangular Panel With a Central Longitudinal Stiffener. NACA TN 1879, 1949.

23. Schmieden, C.: The Buckling of Stiffened Plates in Shear. Translation No. 31, U. S. Experimental Model Basin, Washington Navy Yard, June 1936.

24. Seydel, Edgar: Wrinkling of Reinforced Plates Subjected to Shear Stresses. NACA TM 602, 1931.

25. Wang, Tsun Kuei: Buckling of Transverse Stiffened Plates Under Shear. Jour. Appl. Mech., vol. 14, no. 4, Dec. 1947, p. A-269 - A-274.

26. Timoshenko, S.: Theory of Elastic Stability. First ed., McGraw-Hill Book Co., Inc., 1936.

27. Crate, Harold, and Lo, Hsu: Effect of Longitudinal Stiffeners on the Buckling Load of Long Flat Plates Under Shear. NACA TN 1589, 1948.

28. Stein, Manuel, and Fralich, Robert W.: Critical Shear Stress of Infinitely Long, Simply Supported Plate With Transverse Stiffeners. NACA TN 1851, 1949.

29. Stein, Manuel, and Yaeger, David J.: Critical Shear Stress of a Curved Rectangular Panel With a Central Stiffener. NACA TN 1972, 1949.

30. Stein, Manuel, Sanders, J. Lyell, Jr., and Crate, Harold: Critical Stress of Ring-Stiffened Cylinders in Torsion. NACA Rep. 989, 1950.

TABLE I

STIFFENER ELEMENTS IN COMPRESSION

[See fig. 1 for breakdown of typical sections into their component elements]

Fig.	Section	Buckling coefficient	Plasticity-reduction factor
5(a)	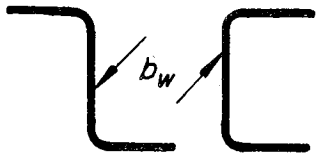	k_w	$(E_s/E)(1-\nu_e^2)/(1-\nu^2)$ is about 5 percent optimistic
5(b)	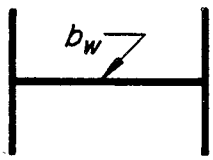	k_w	None reported
5(c)	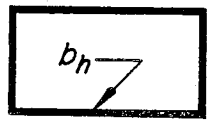	k_h	None reported
6	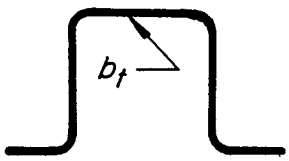	k_f	None reported

TABLE 2

STIFFENED PLATES UNDER LONGITUDINAL COMPRESSION

[See fig. 8 for sketches of plate-stiffener arrangements; $GJ = 0$]

Fig.	Section (a)	Plasticity-reduction factor
10	End view  $n = 1, 2, 3, \infty$	When stiffeners enforce nodes, $\eta = \left(\frac{1-\nu_e^2}{1-\nu^2}\right)\left(\frac{E_s}{E}\right)\left[\frac{1}{2} + \frac{1}{4}\left(1 + 3\frac{E_t}{E_s}\right)^{1/2}\right]$
14(a)	End view  Infinitely wide	
14(b)	End view  Infinitely wide	
14(c) 14(d)	End view  Infinitely wide	
15	End view  Side view 	When stiffeners enforce nodes, use data in ref. 2
16	End view 	

a_n, number of stiffeners on plate; ●, sturdy stiffener;
⟡, transverse support with no restraint of lateral movement.

TABLE 3

STIFFENED PLATES UNDER SHEAR

[See fig. 8 for sketches of plate-stiffener arrangements. GJ = 0]

Fig.	Section (a)	Plasticity-reduction factor
19(a)	End view  n = 1, 2, ∞ Longplates only	When stiffeners enforce nodes, $\eta = (E_s/E)\left(1-\nu_e^2\right)\Big/\left(1-\nu^2\right)$
21	End view 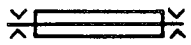 Side view 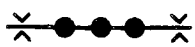 Long plates only	
22(a) and 22(b)	End view 	
22(c) and 22(d)	End view 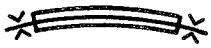 Side view 	
23	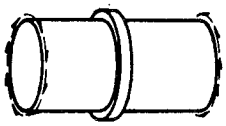 n = 1, 2, 3, 4 Simply supported ends	

a_n, number of stiffeners on plate; ●, sturdy stiffener;
 , transverse support with no restraint of lateral movement.

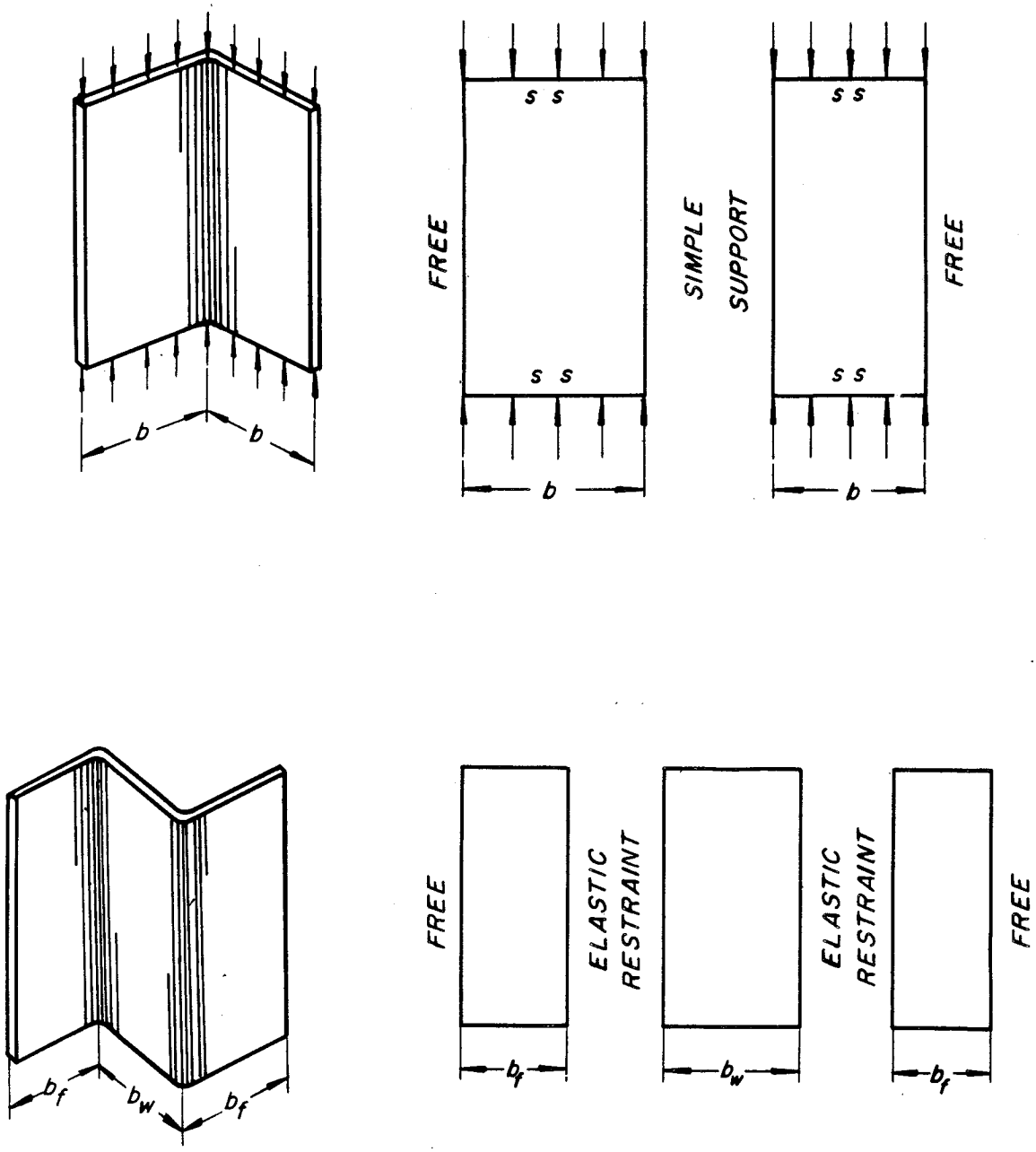

Figure 1.- Breakdown of angle and Z-stiffeners into component plate elements. ss, simply supported.

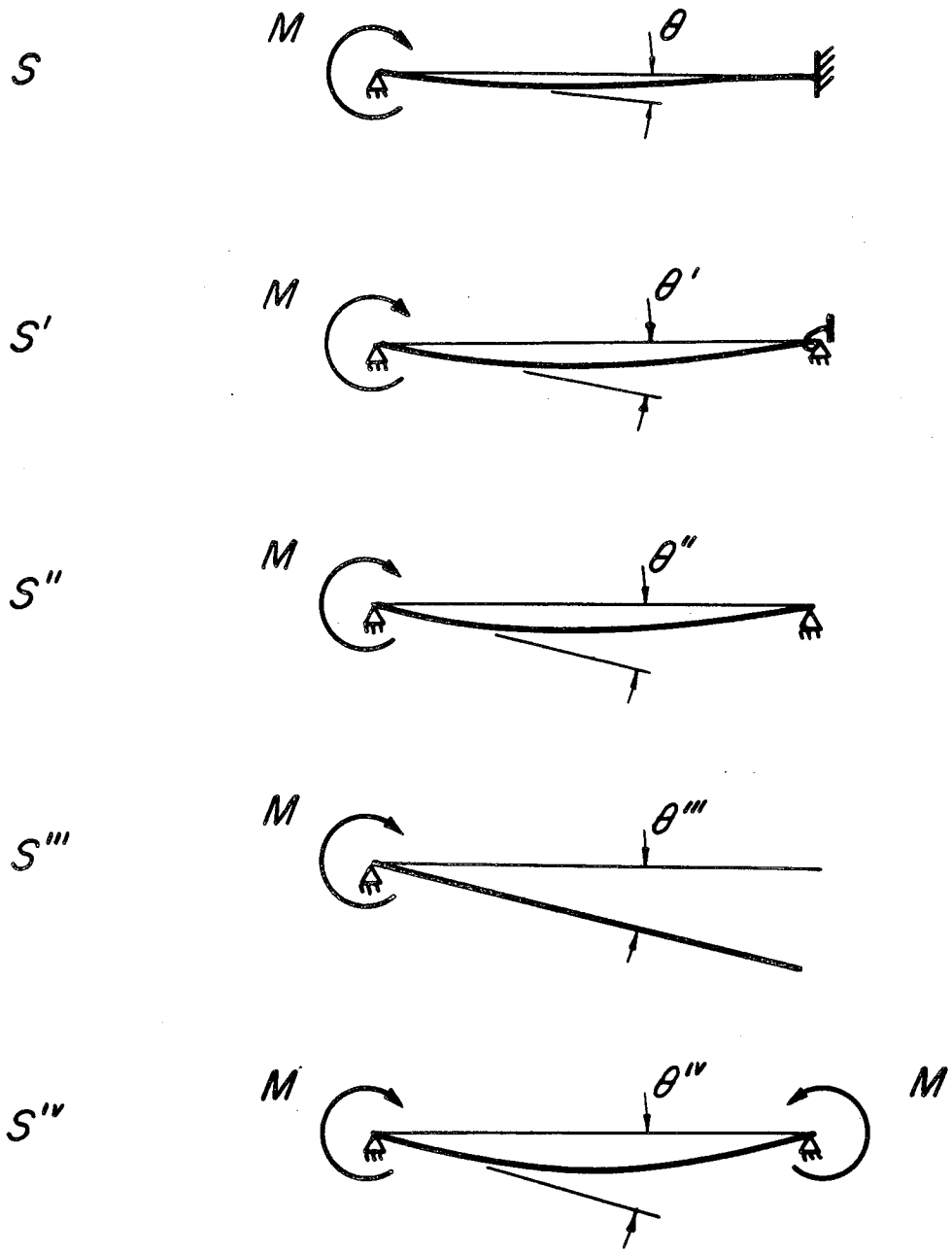

Figure 2.- Rotational stiffnesses of flat plates with different boundary conditions. Moments vary sinusoidally along plate length.

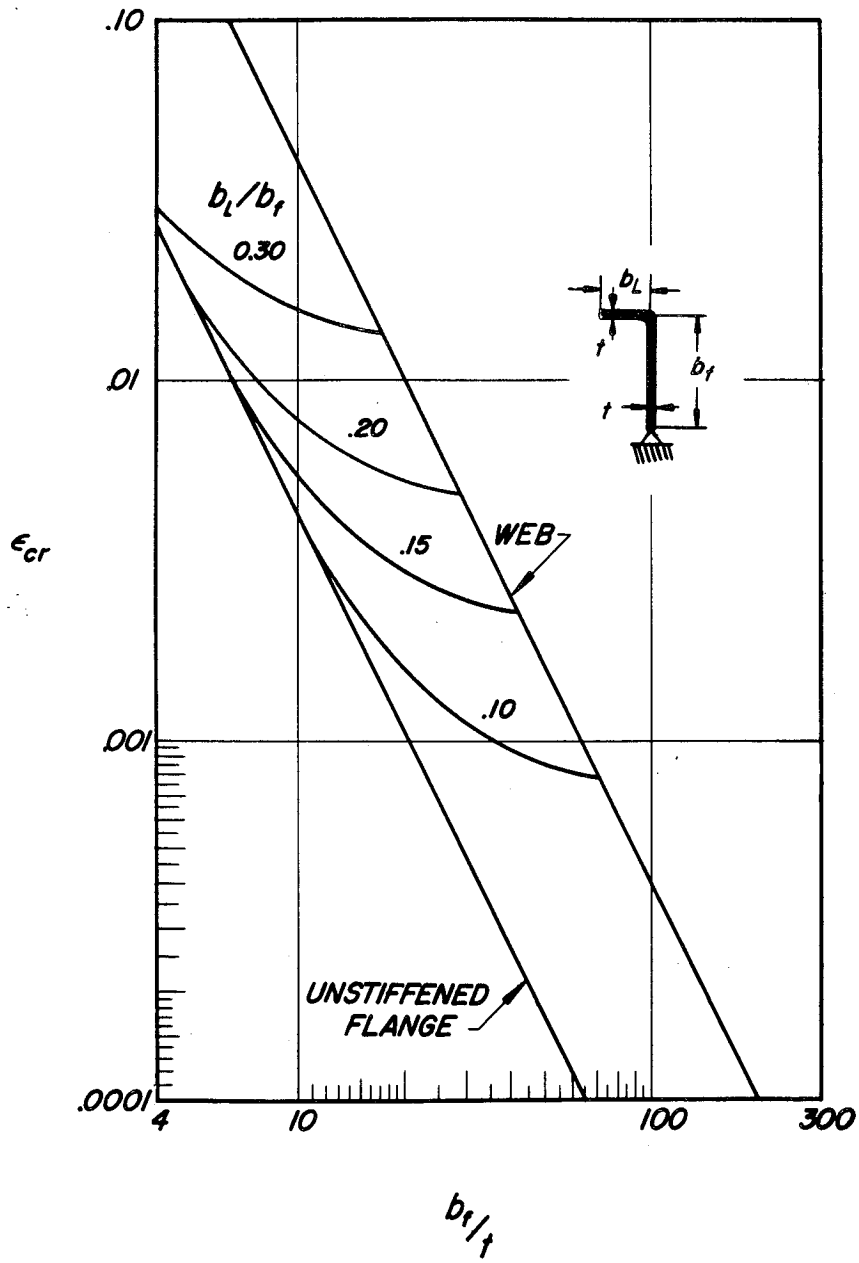

(a) Lip flanges.

Figure 3.- Buckling strain of hinged flanges. $L/b_f = 3.5$;

$$\epsilon_{cr} = \frac{k_f \pi^2}{12\left(1 - \nu_e^2\right)}\left(\frac{t}{b_f}\right)^2; \quad \nu_e = 0.3 \quad \text{(data of ref. 10).}$$

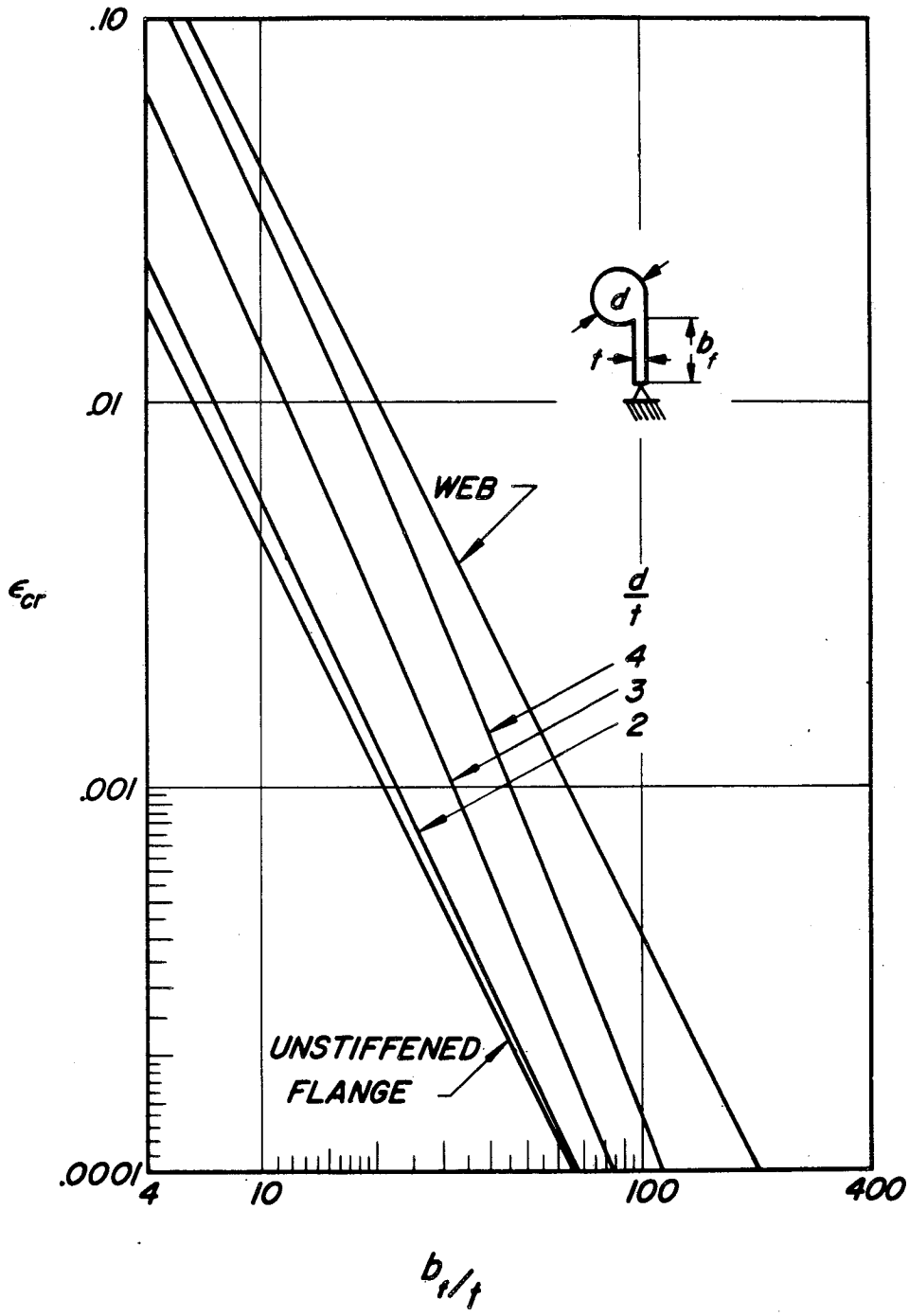

(b) Bulb flanges.

Figure 3.- Concluded.

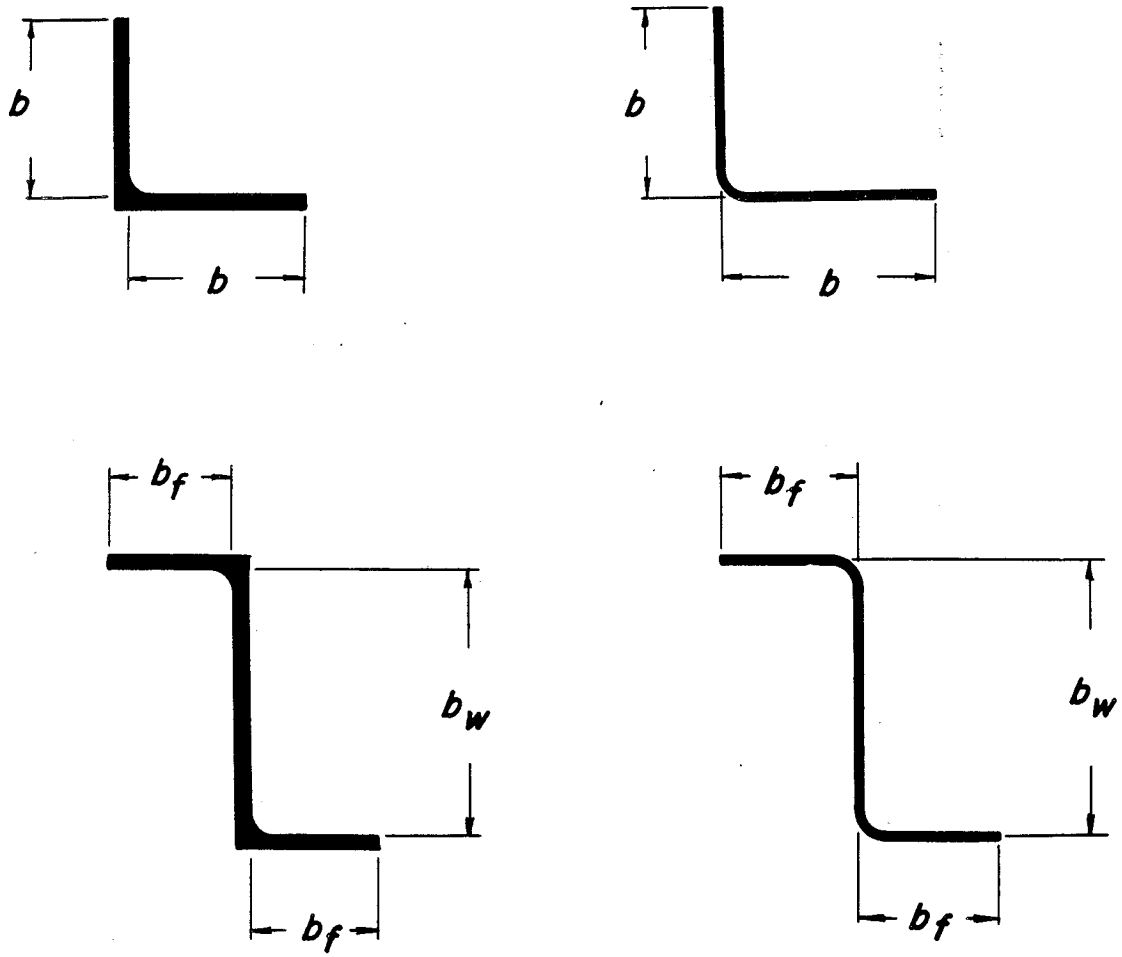

(a) Extruded sections. (b) Formed sections.

Figure 4.- Typical formed and extruded stiffeners.

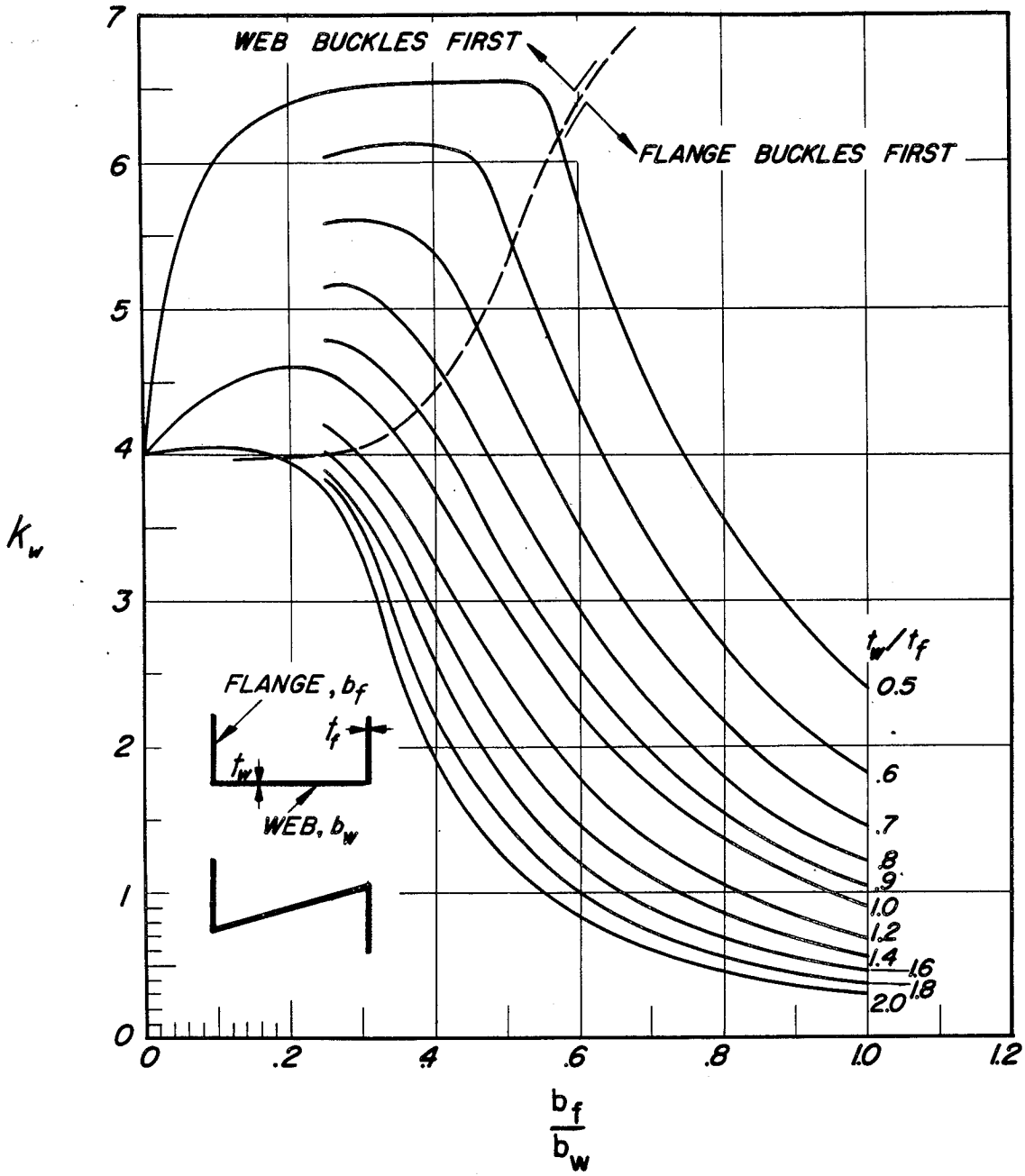

(a) Channel- and Z-section stiffeners. $\sigma_{cr} = \dfrac{k_w \pi^2 E}{12\left(1 - \nu_e^2\right)} \dfrac{t_w^2}{b_w^2}$.

Figure 5.- Buckling coefficients for stiffeners (data of ref. 5).

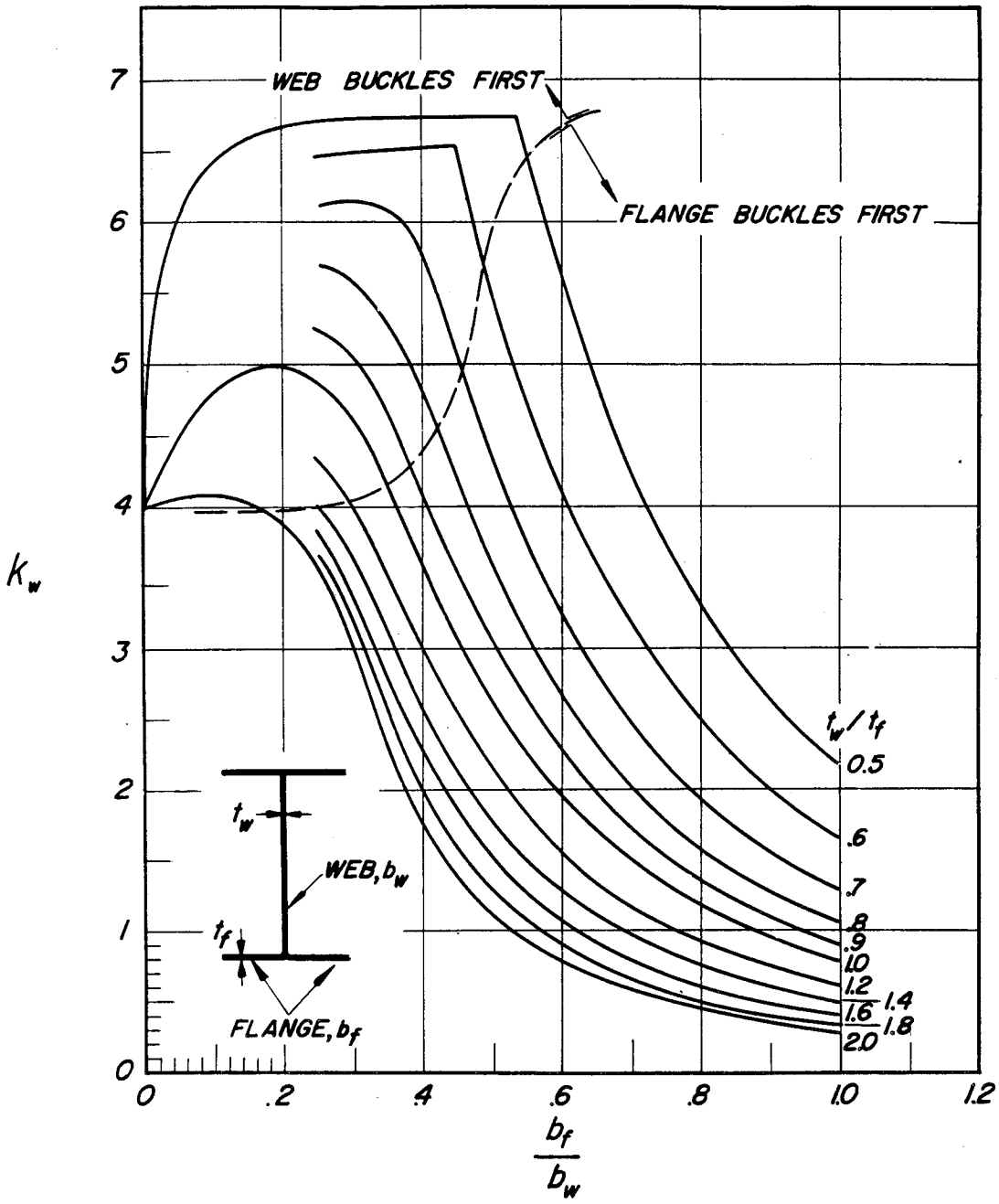

(b) H-section stiffeners. $\sigma_{cr} = \frac{k_w \pi^2 E}{12\left(1 - \nu_e^2\right)} \frac{t_w^2}{b_w^2}$.

Figure 5.- Continued.

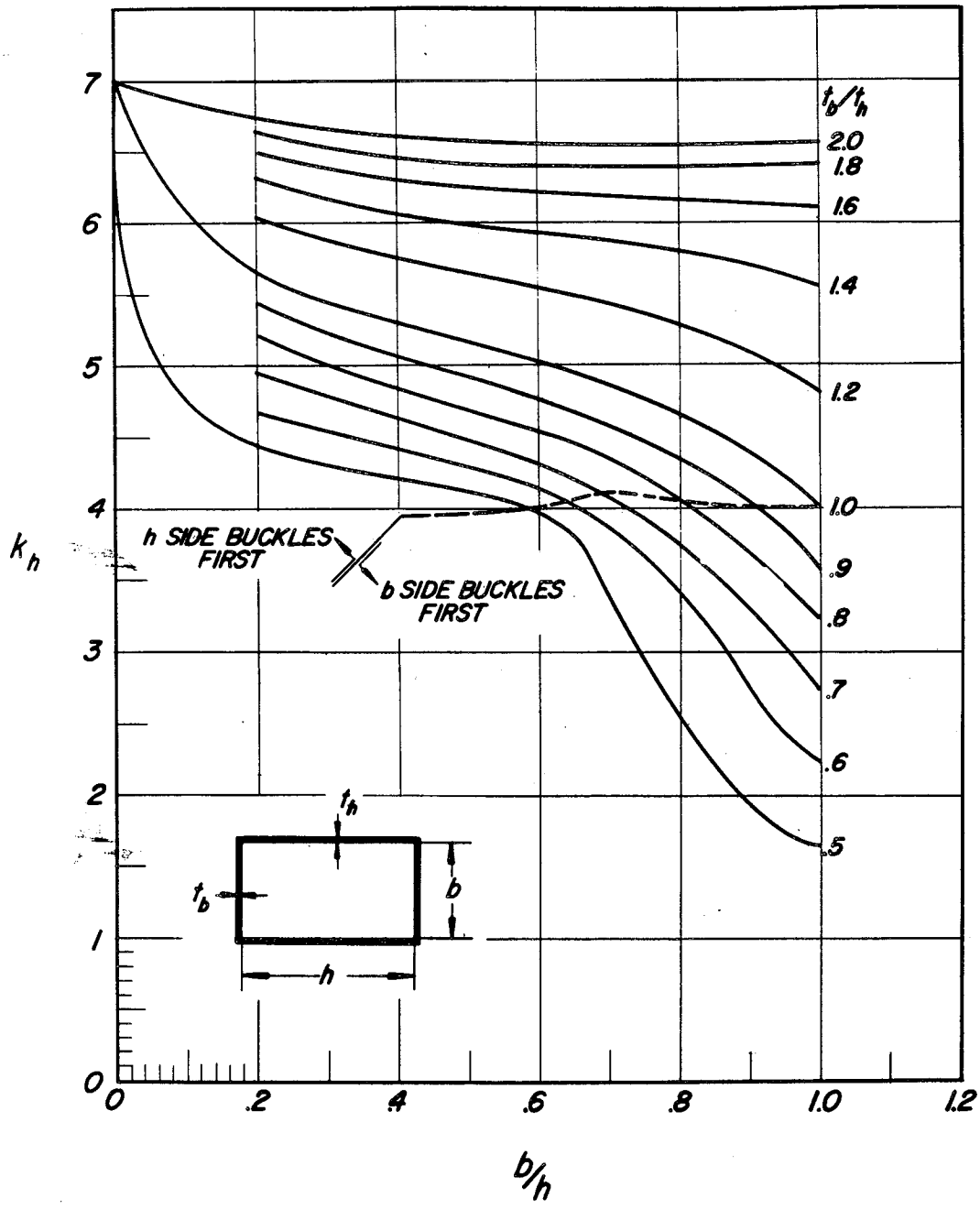

(c) Rectangular-tube-section stiffeners. $\sigma_{cr} = \dfrac{k_h \pi^2 E}{12\left(1 - \nu_e^2\right)}\left(\dfrac{t_h}{h}\right)^2$.

Figure 5.- Concluded.

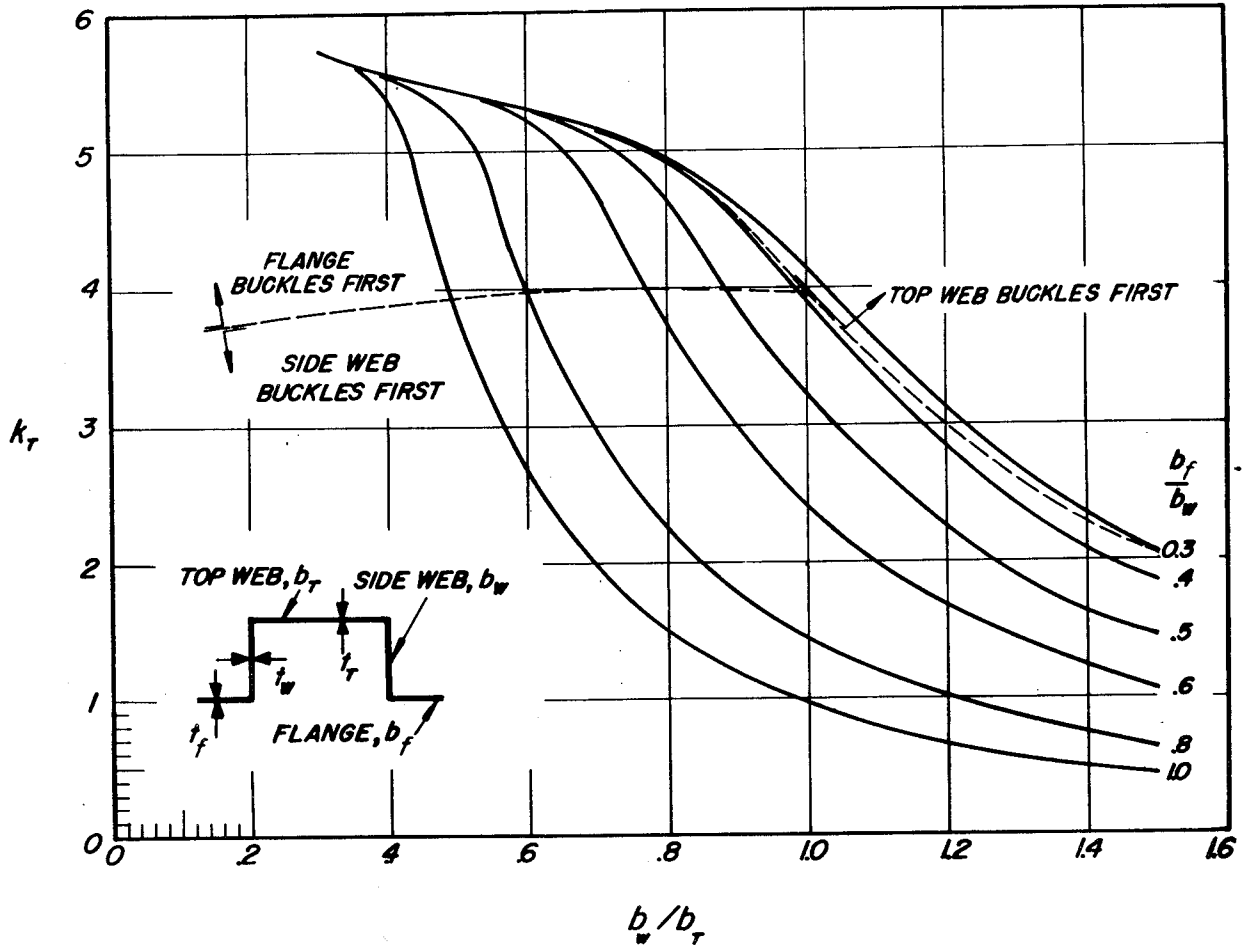

Figure 6.- Buckling stress for hat-section stiffeners. $t = t_f = t_w = t_T$;

$$\sigma_{cr} = \frac{k_T \pi^2 E}{12\left(1 - \nu_e^2\right)} \frac{t^2}{b_T^2}.$$ (Data of ref. 12.)

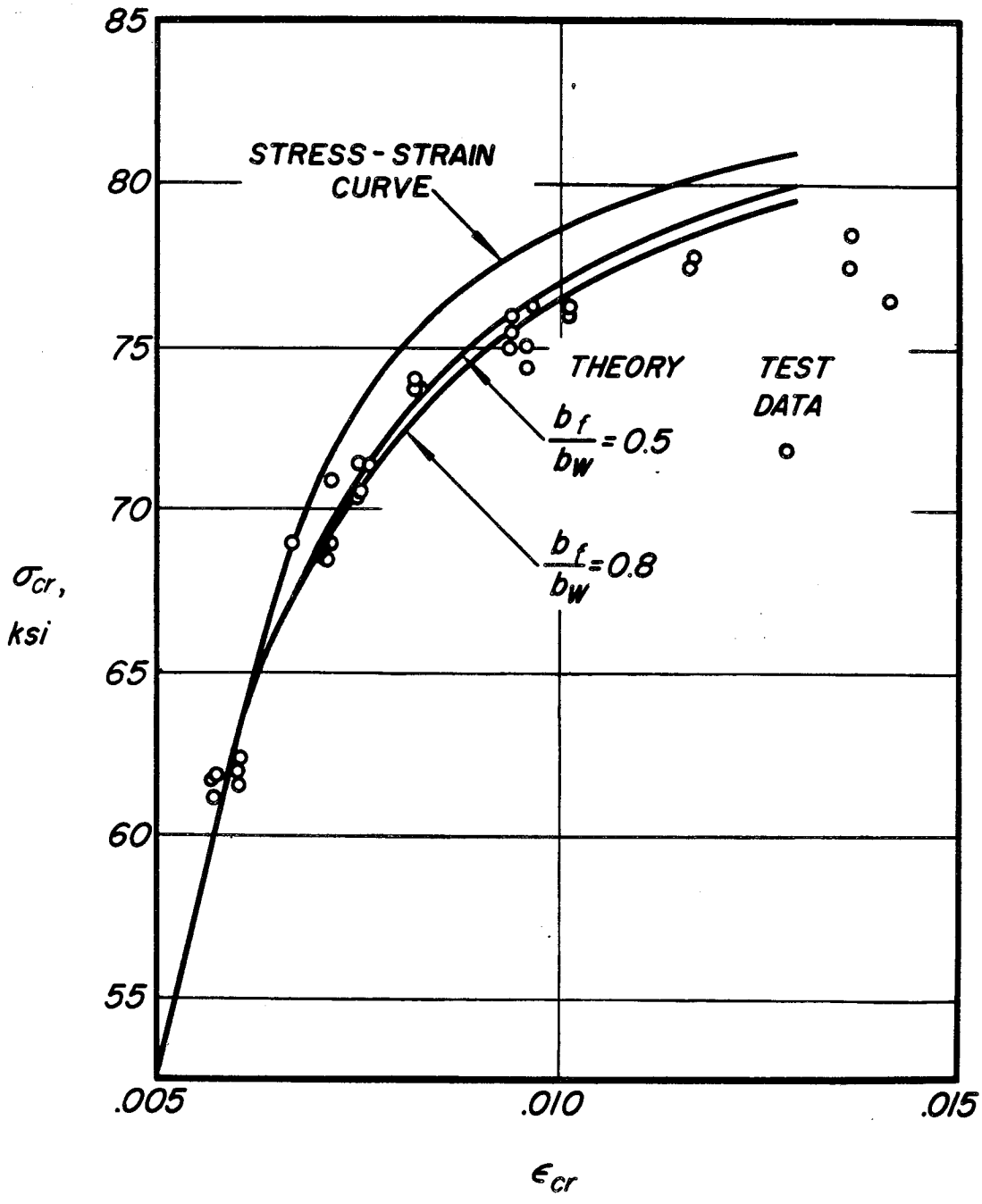

Figure 7.- Comparison of theory and test data for inelastic buckling of H-section stiffeners. $\epsilon_{cr} = \frac{k_w \pi^2 t_w^2}{12\left(1 - \nu_e^2\right) b_w^2}$; $\frac{t_f}{t_w} = 1.0$; $\frac{b_f}{b_w} = 0.5$ and 0.8. (Data of ref. 13.)

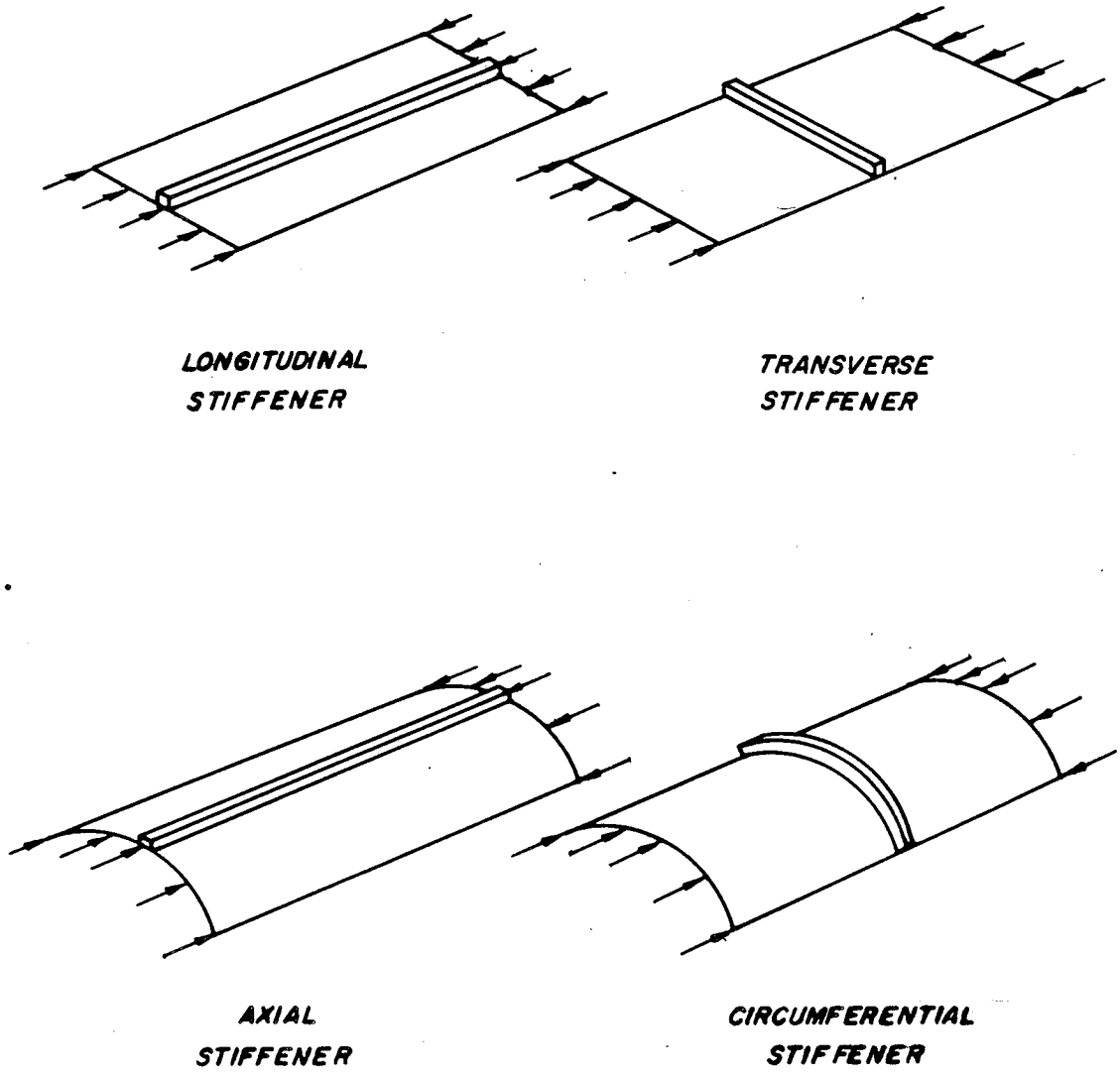

Figure 8.- Typical arrangements of plate stiffener combinations under longitudinal compression.

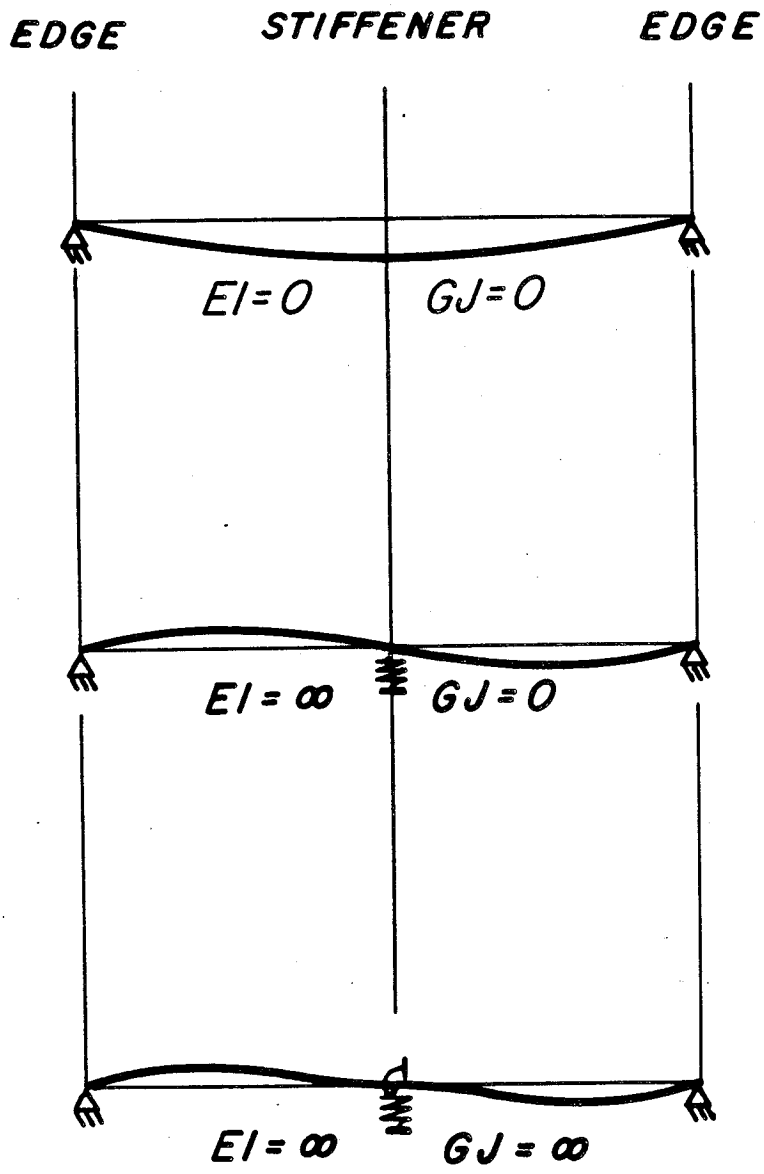

Figure 9.- Buckling behavior of axially compressed flat plate supported by deflectional and rotational springs.

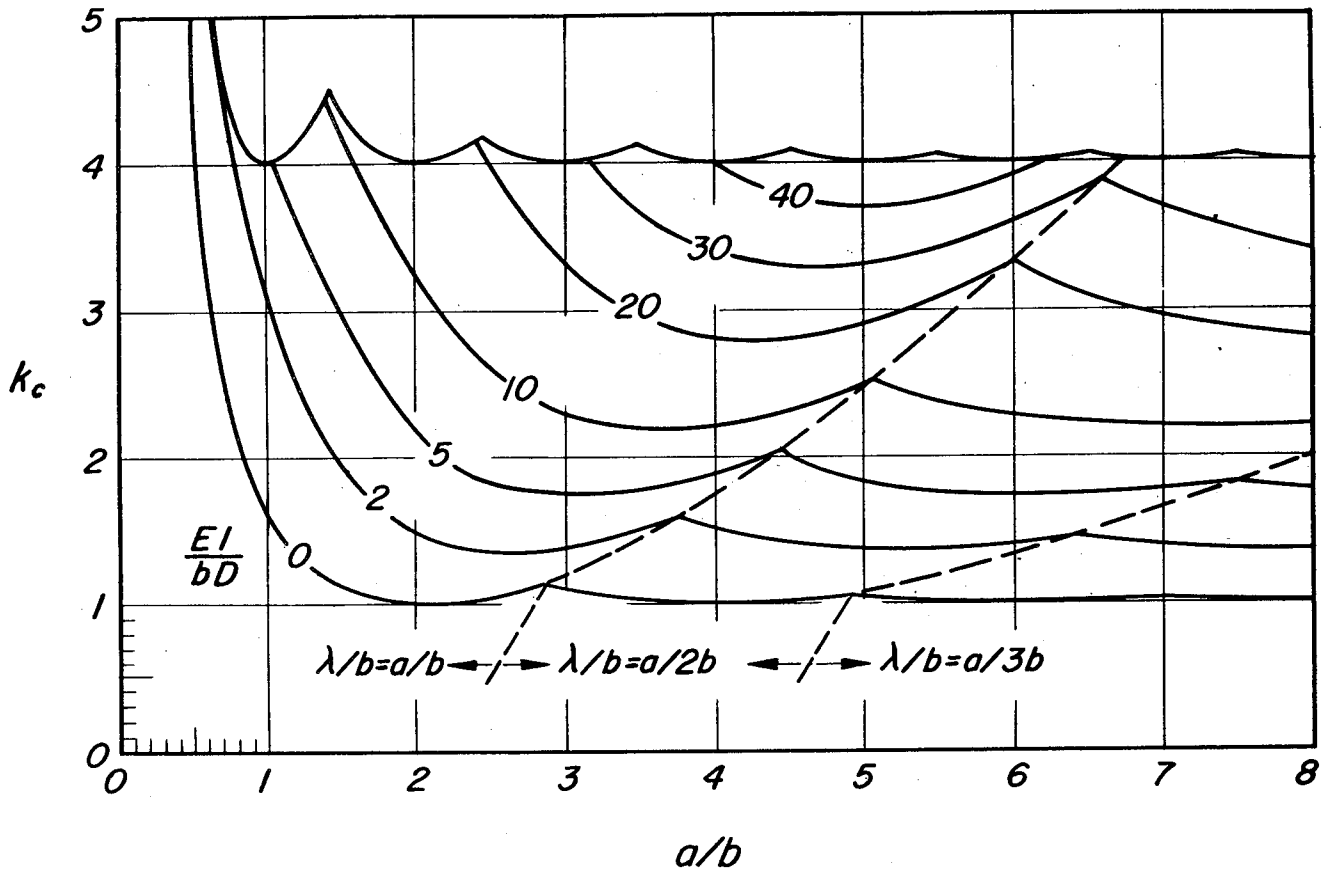

(a) One stiffener. A/bt = 0.

Figure 10.- Compressive-buckling coefficients for simply supported flat plates with longitudinal stiffeners. $\sigma_{cr} = \frac{k_c \pi^2 E}{12\left(1 - \nu_e^2\right)}\left(\frac{t}{b}\right)^2$. (Data of ref. 15.)

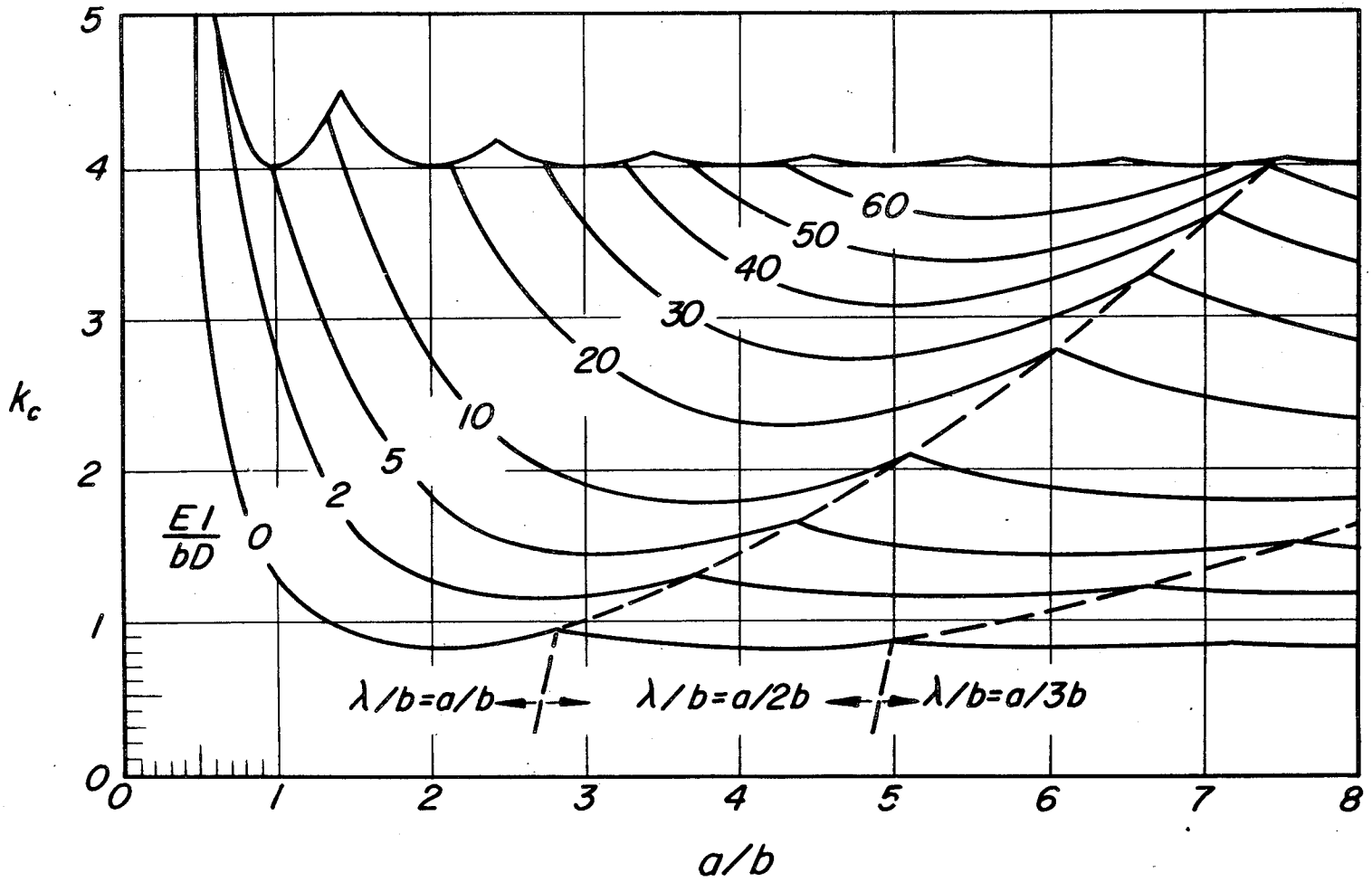

(b) One stiffener. A/bt = 0.2.

Figure 10.- Continued.

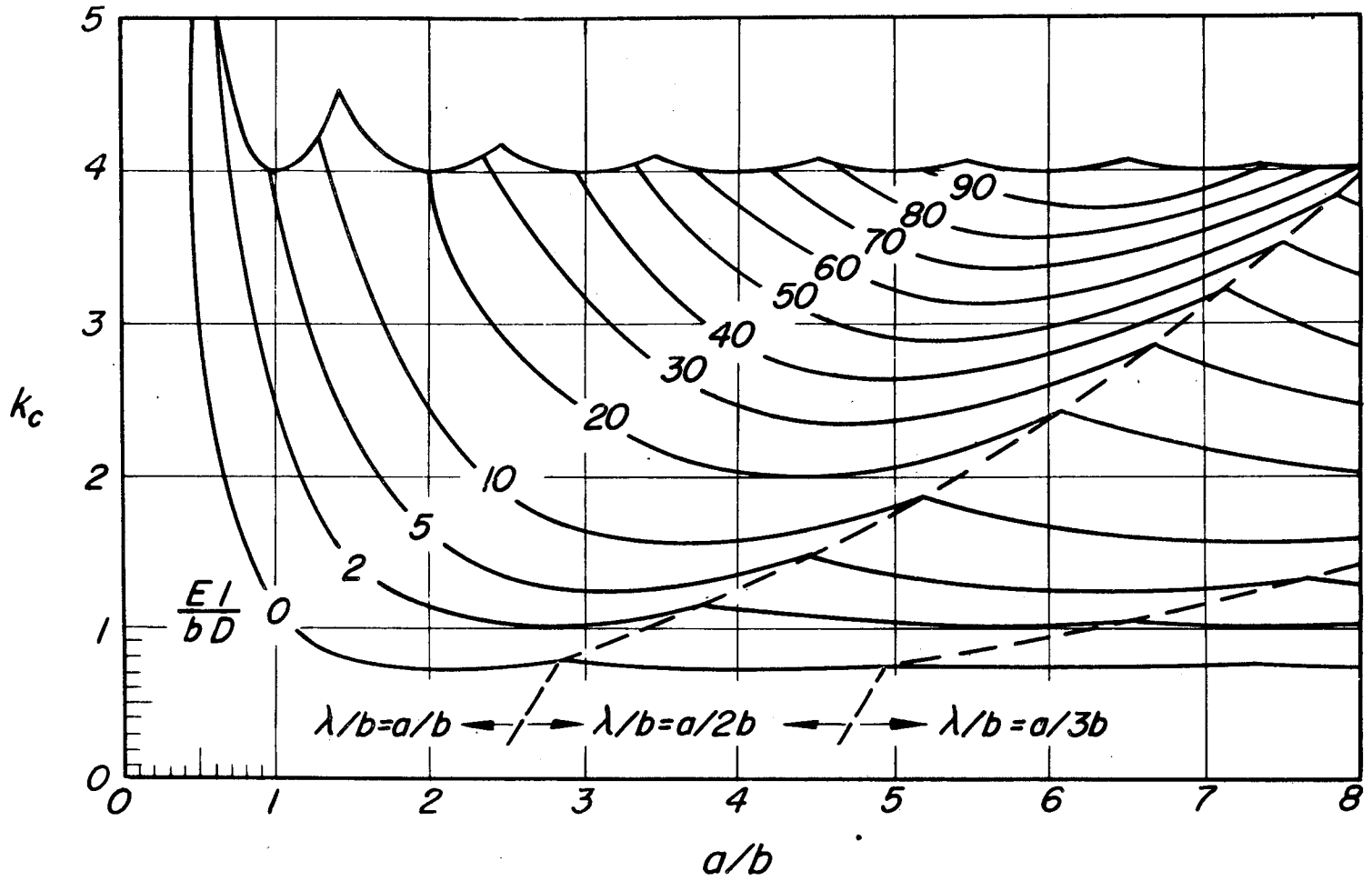

(c) One stiffener. A/bt = 0.4.

Figure 10.- Continued.

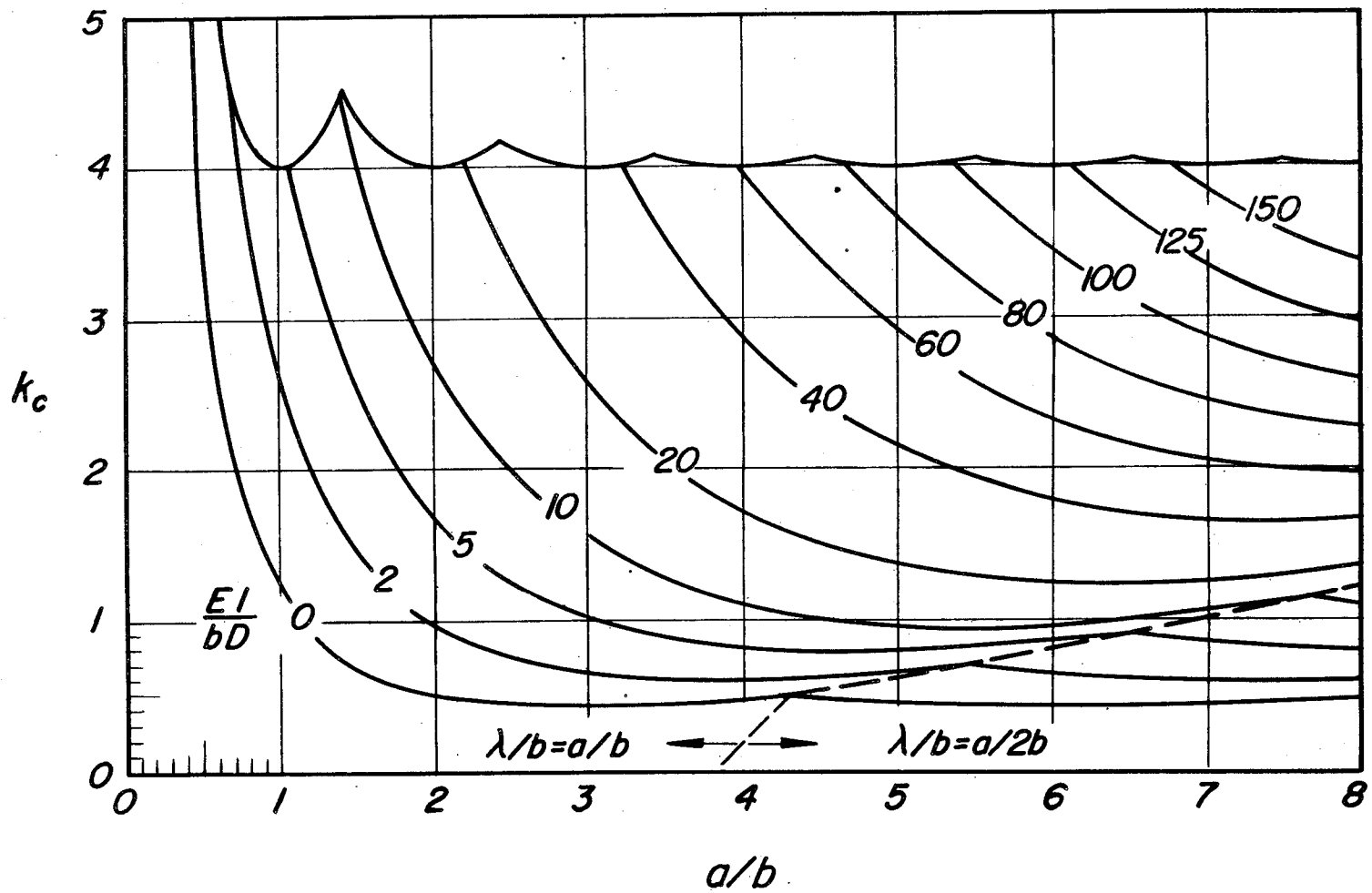

(d) Two stiffeners. A/bt = 0.

Figure 10.- Continued.

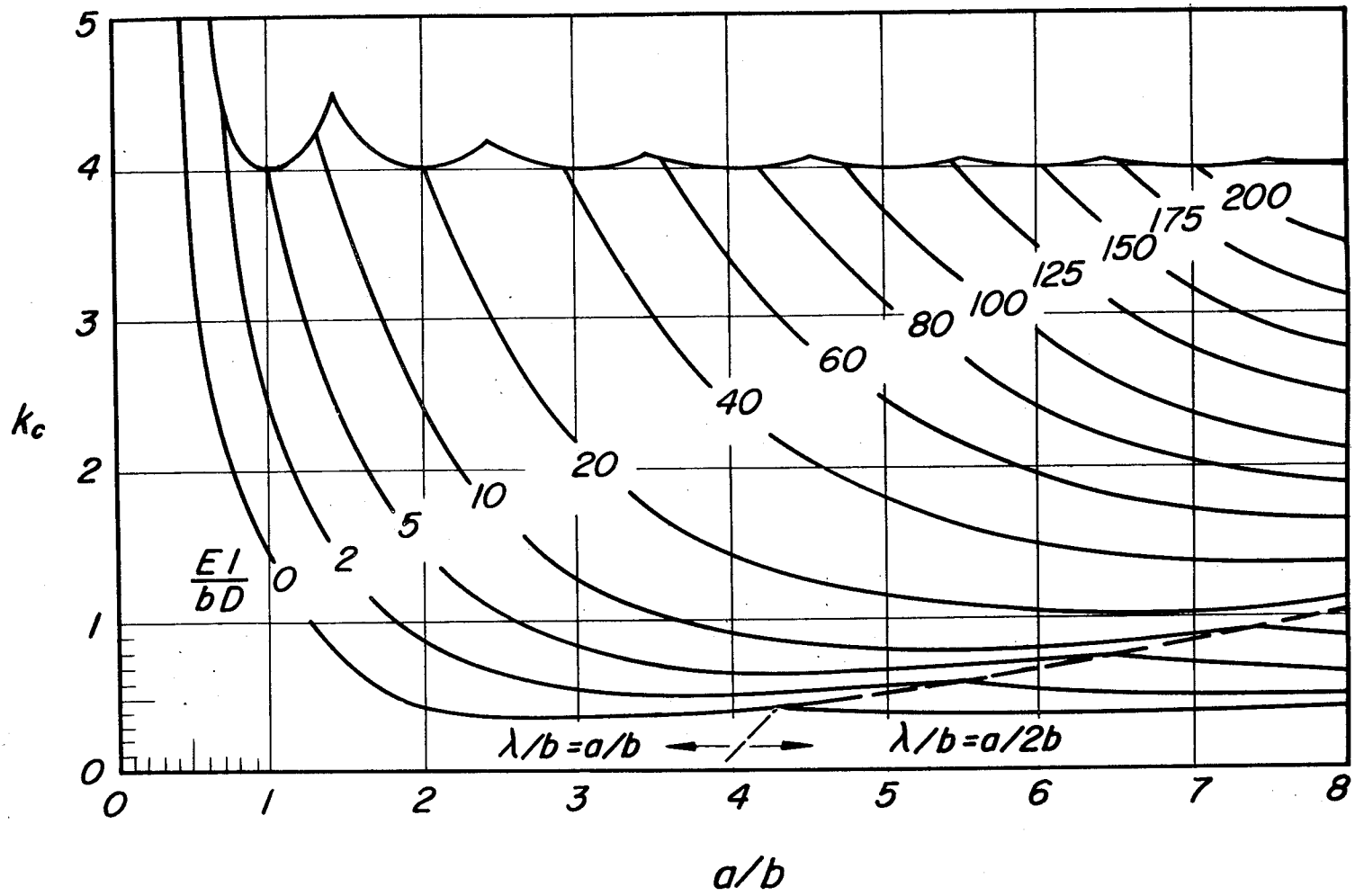

(e) Two stiffeners. A/bt = 0.2.

Figure 10.- Continued.

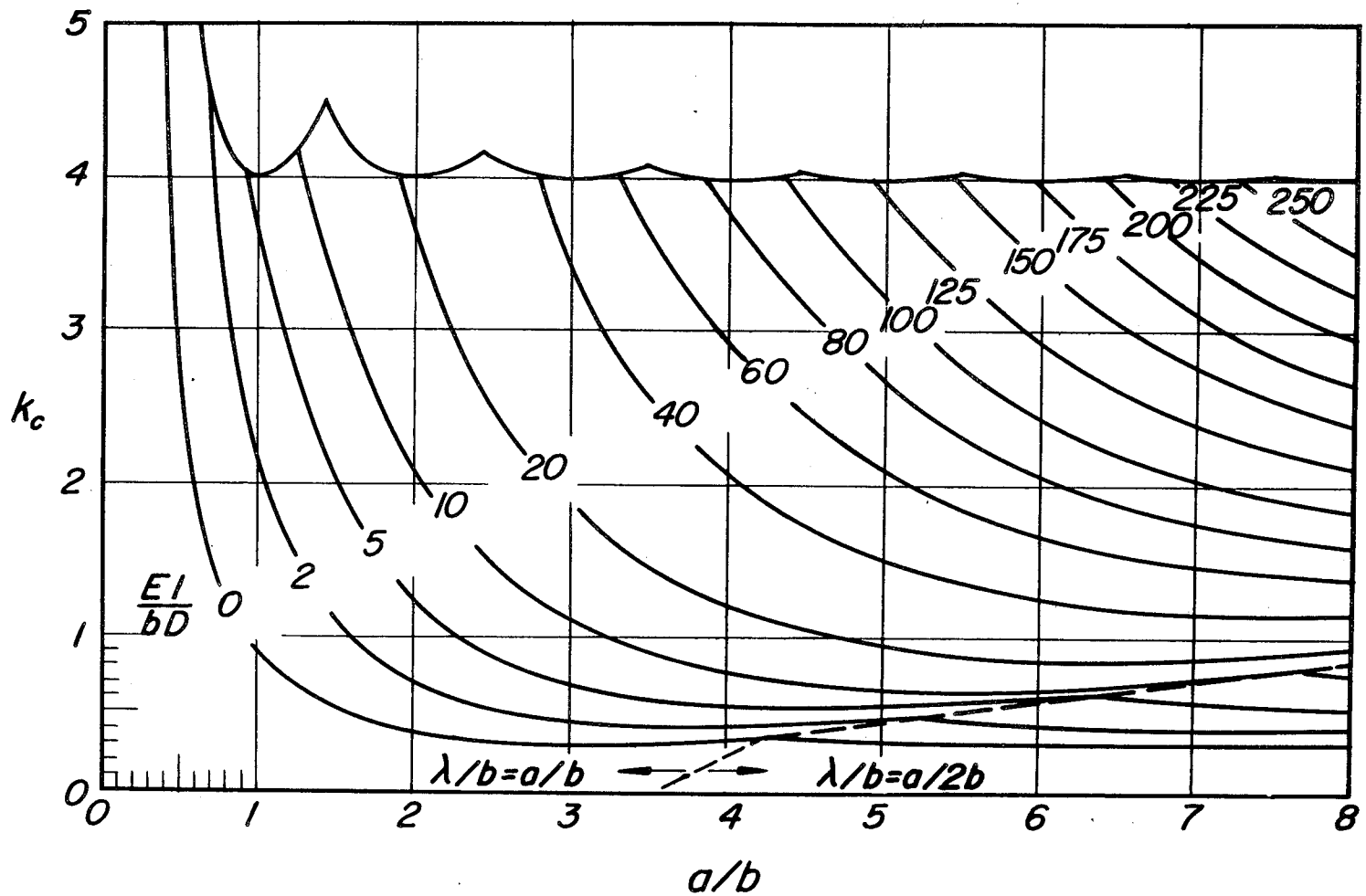

(f) Two stiffeners. A/bt = 0.4.

Figure 10.- Continued.

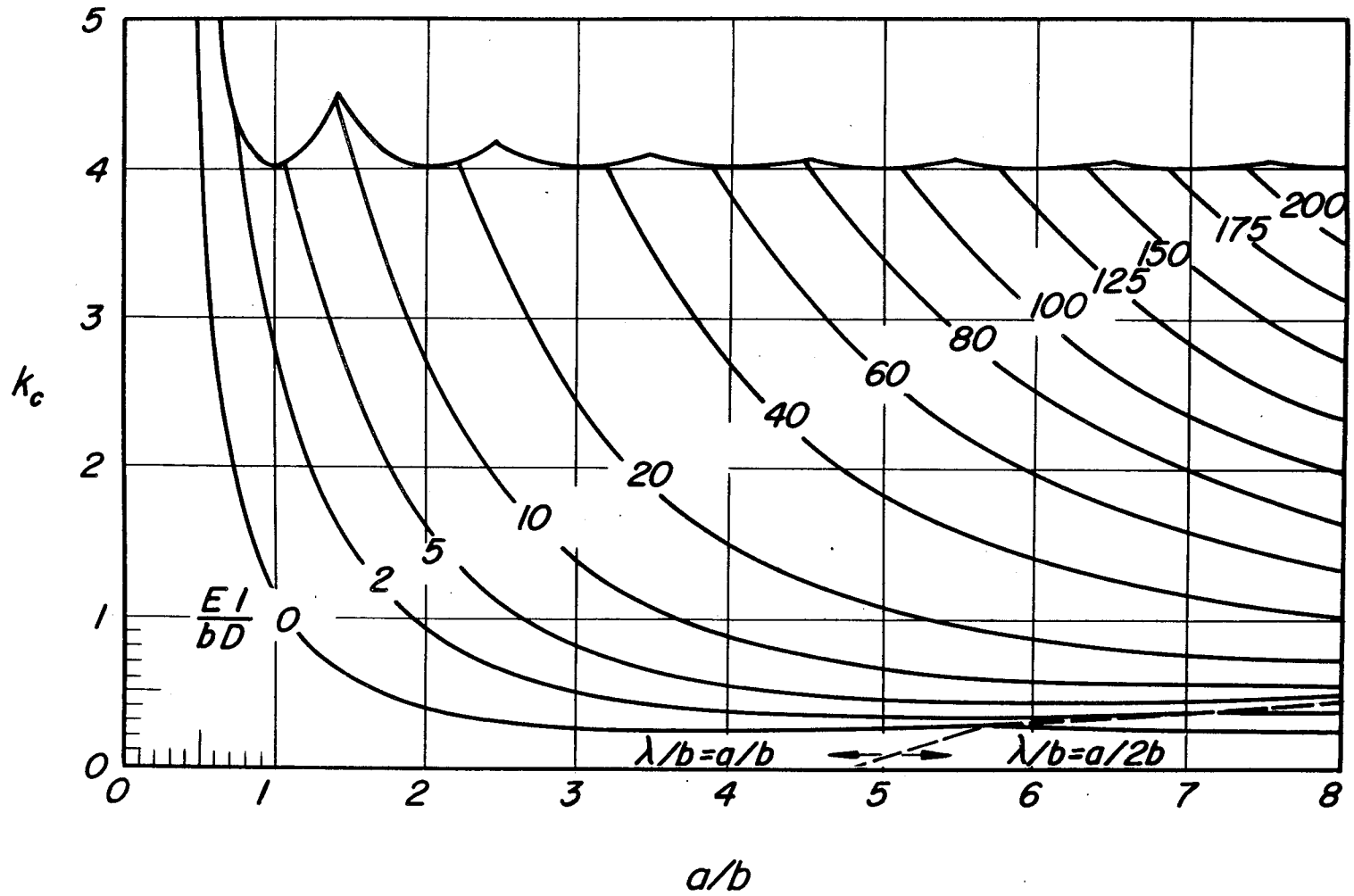

(g) Three stiffeners. A/bt = 0.

Figure 10.- Continued.

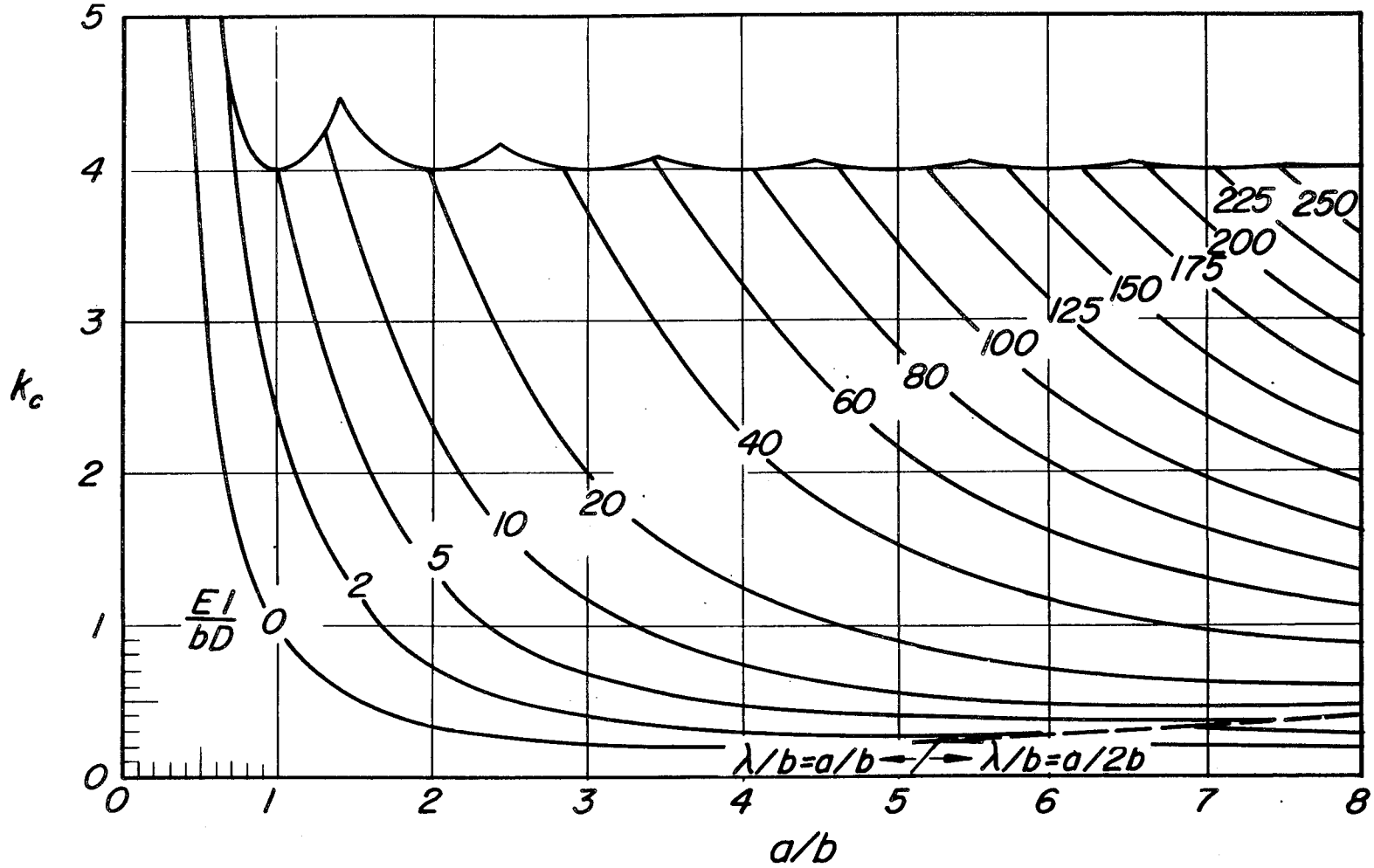

(h) Three stiffeners. A/bt = 0.2.

Figure 10.- Continued.

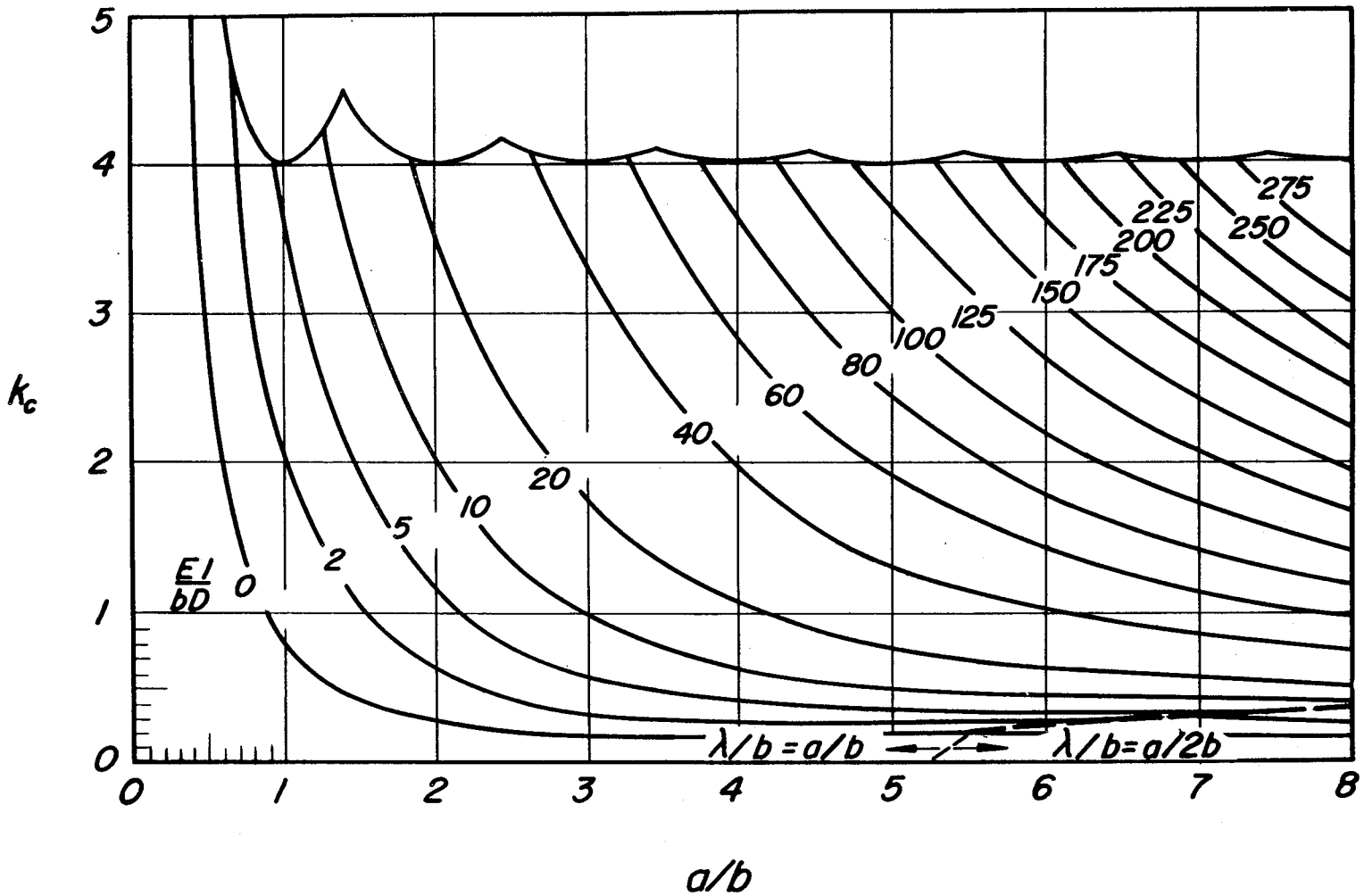

(i) Three stiffeners. A/bt = 0.4.

Figure 10.- Continued.

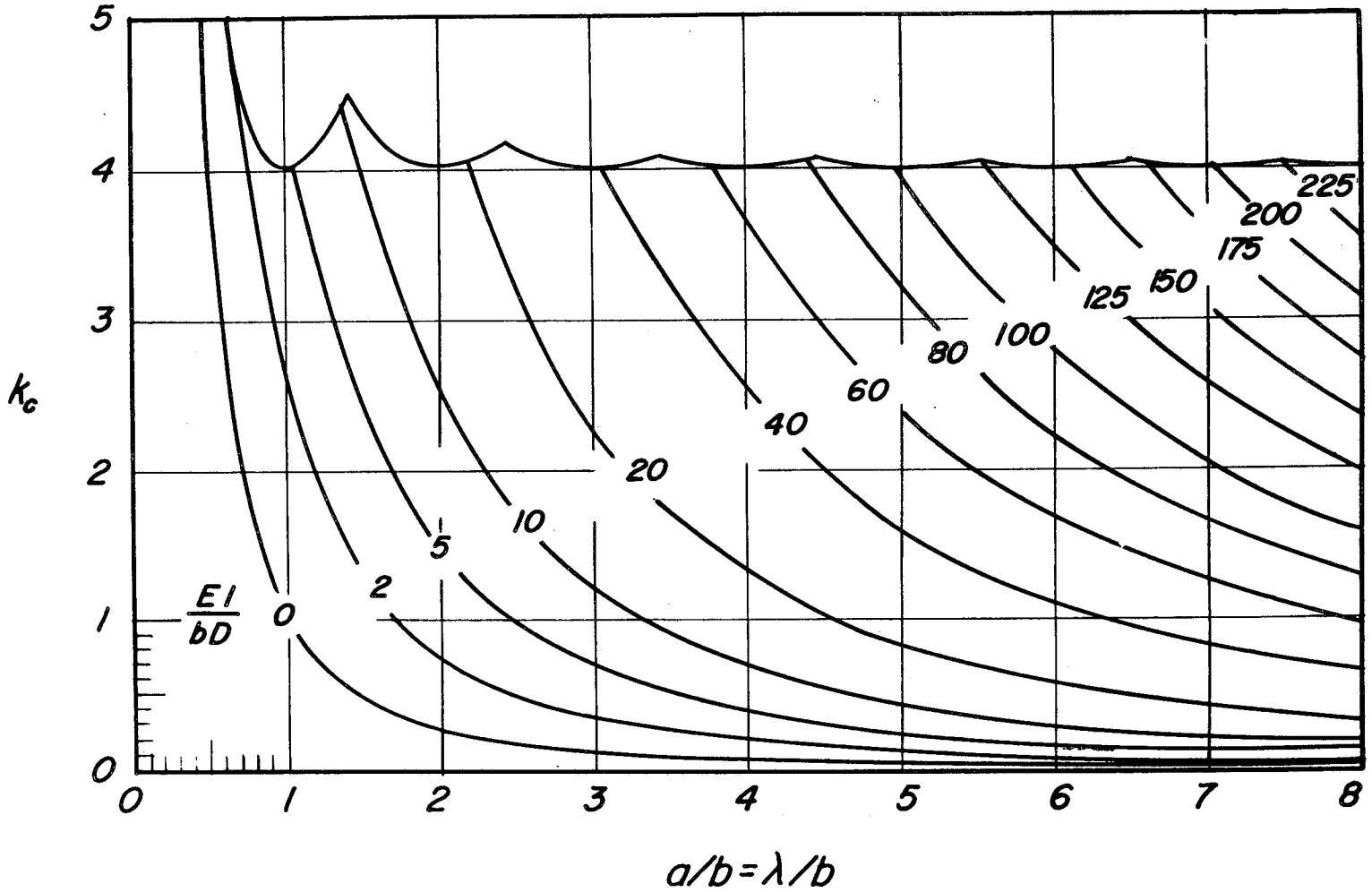

(j) Infinite number of stiffeners. A/bt = 0.

Figure 10.- Continued.

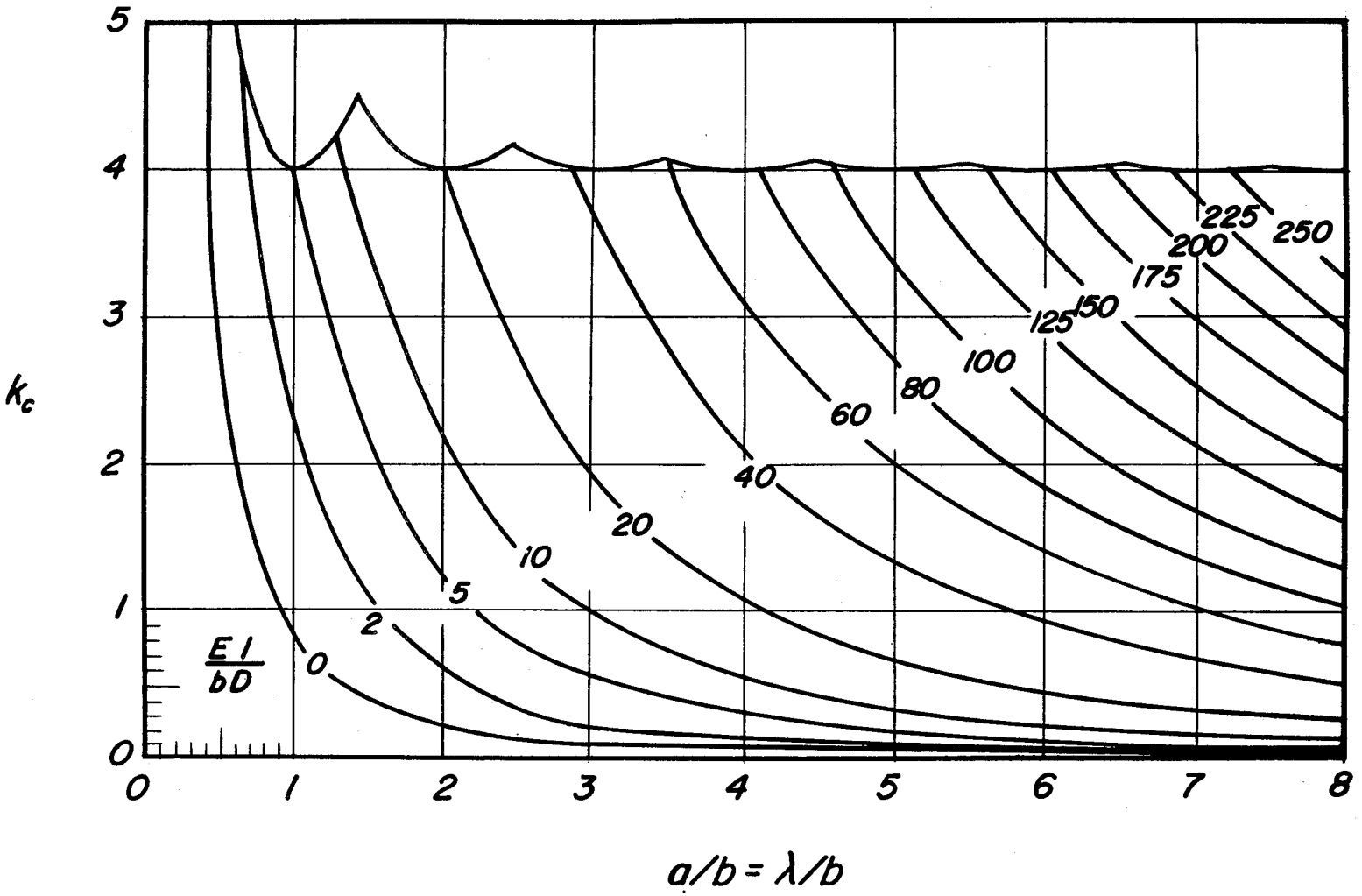

(k) Infinite number of stiffeners. A/bt = 0.2.

Figure 10.- Continued.

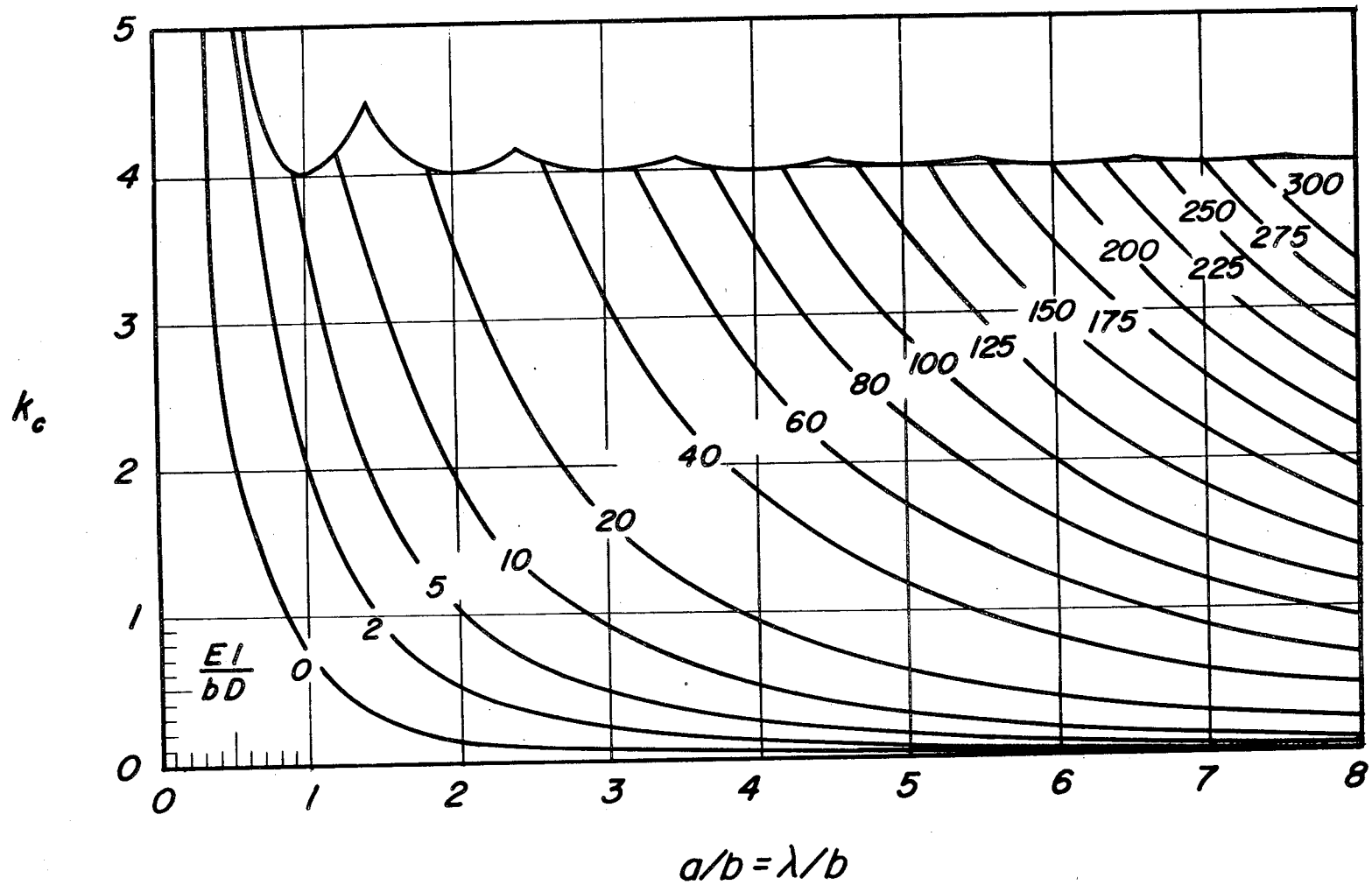

(l) Infinite number of stiffeners. A/bt = 0.4.

Figure 10.- Concluded.

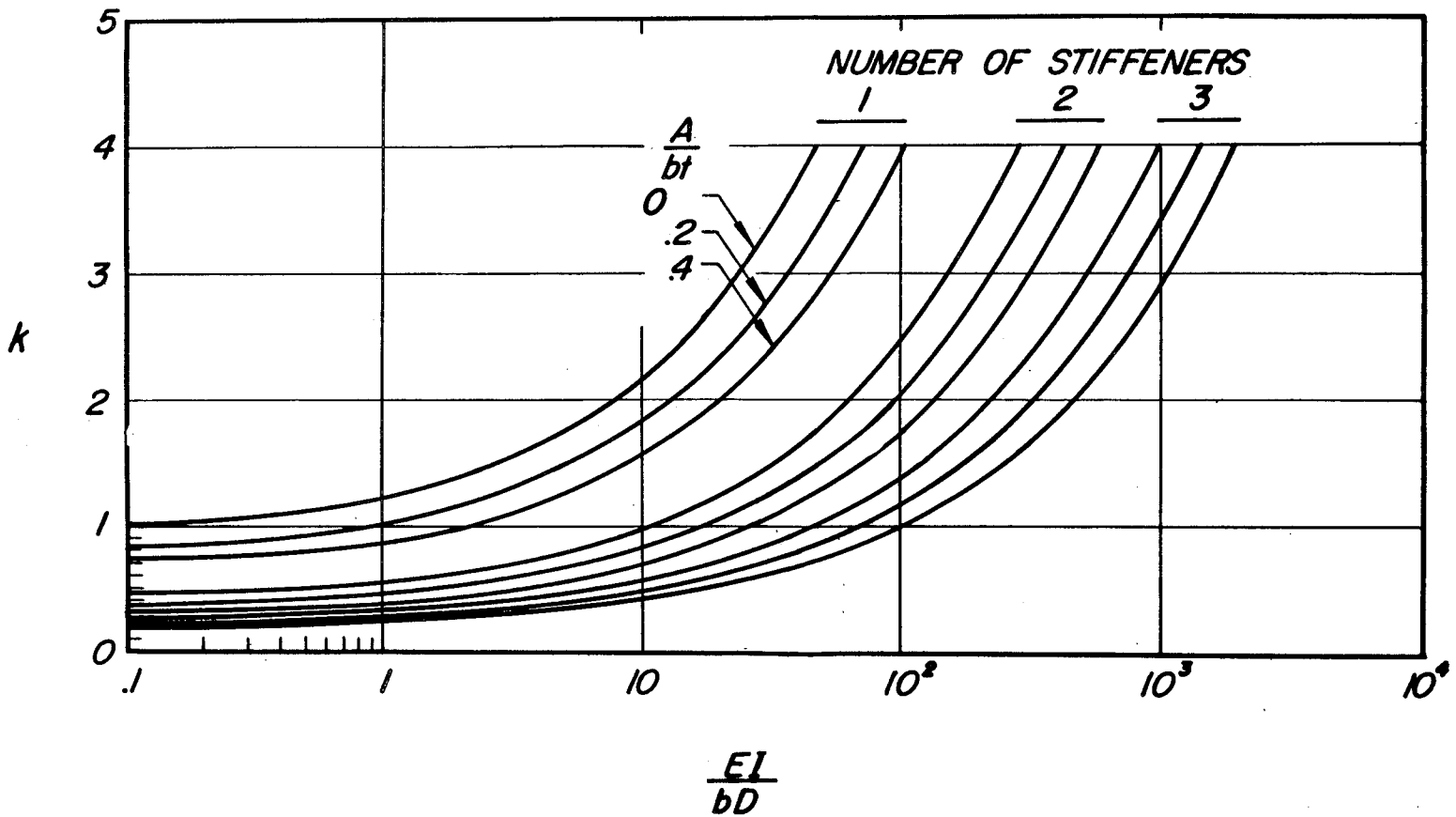

Figure 11.- Compressive-buckling coefficients for infinitely long simply supported flat plates with longitudinal stiffeners.

$$\sigma_{cr} = \frac{k_c \pi^2 E}{12\left(1 - \nu_e^2\right)}\left(\frac{t}{b}\right)^2.$$ (Data of ref. 15.)

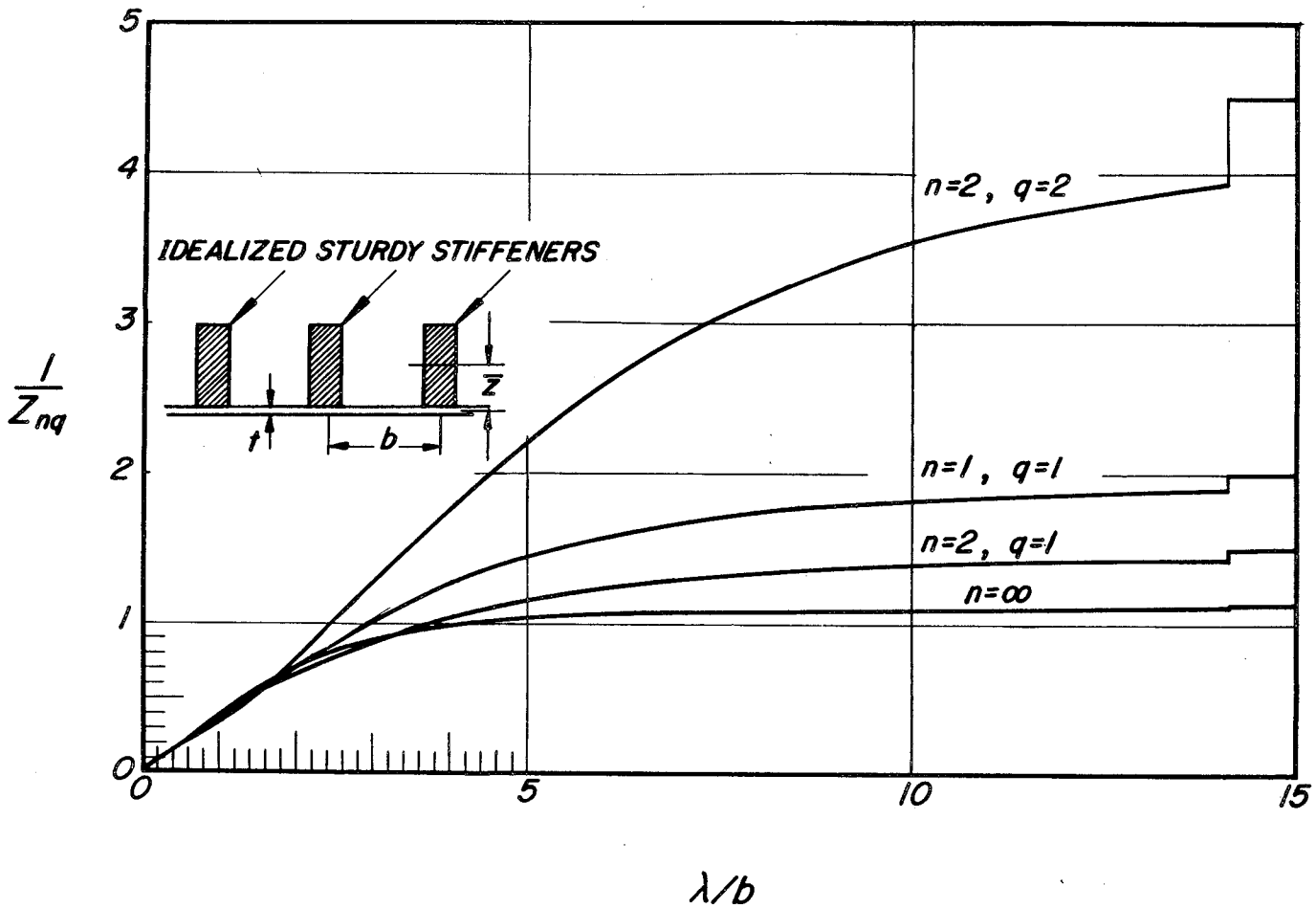

Figure 12.- $1/Z_{nq}$ as a function of stiffened plate proportions and buckle pattern. $r = \frac{(EI/bD)_e}{(EI/bD)} = 1 + \frac{A\bar{z}^2/I}{1 + \left(Z_{nq}A/bt\right)}$. A is area of stiffener cross section. (Data of ref. 17.)

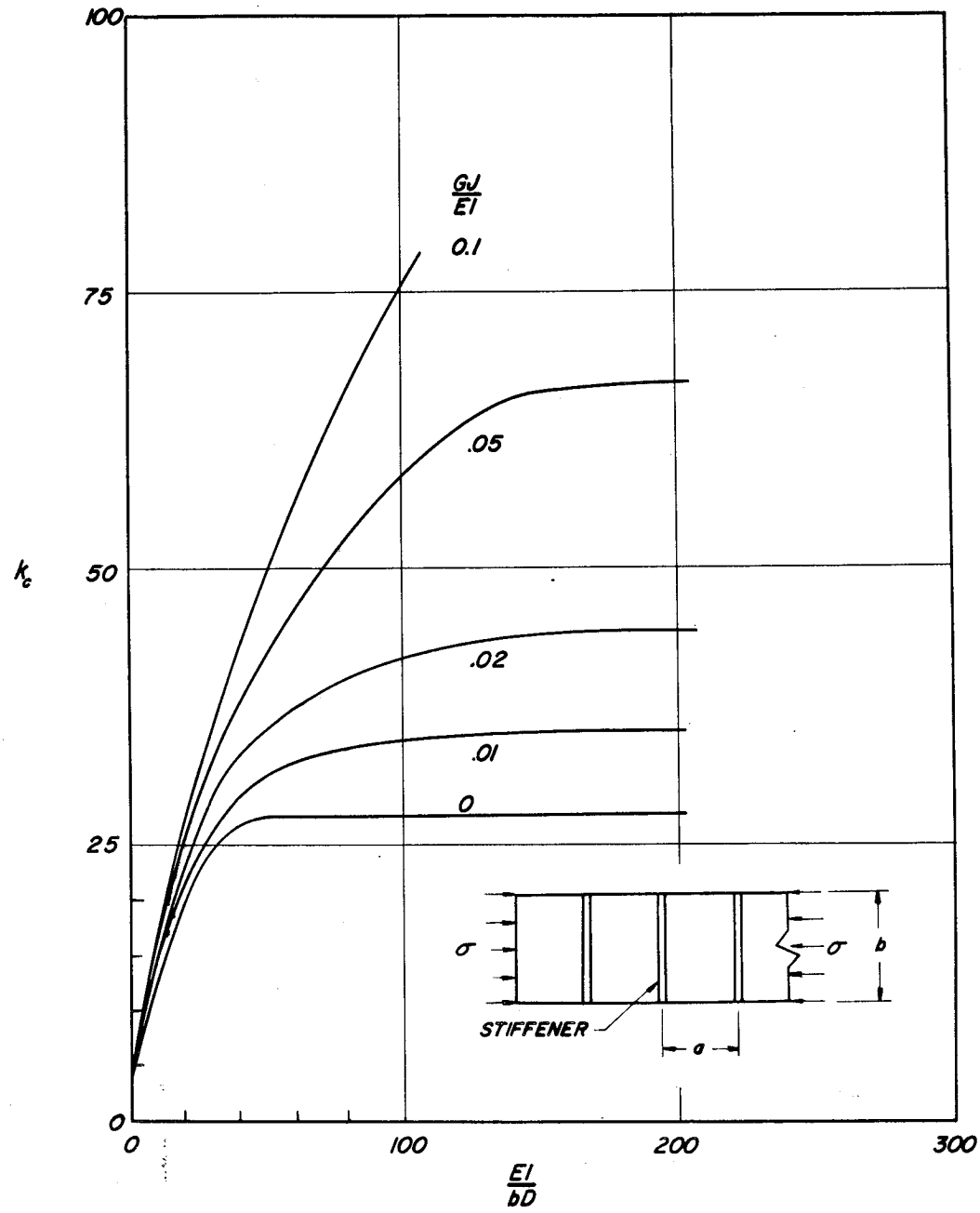

(a) a/b = 0.20.

Figure 13.- Longitudinal-compressive-buckling coefficients for simply supported plates with transverse stiffeners. $\tau_{cr} = \frac{k_c \pi^2 E t^2}{12\left(1 - \nu_e^2\right) b^2}$.

(Data of ref. 18.)

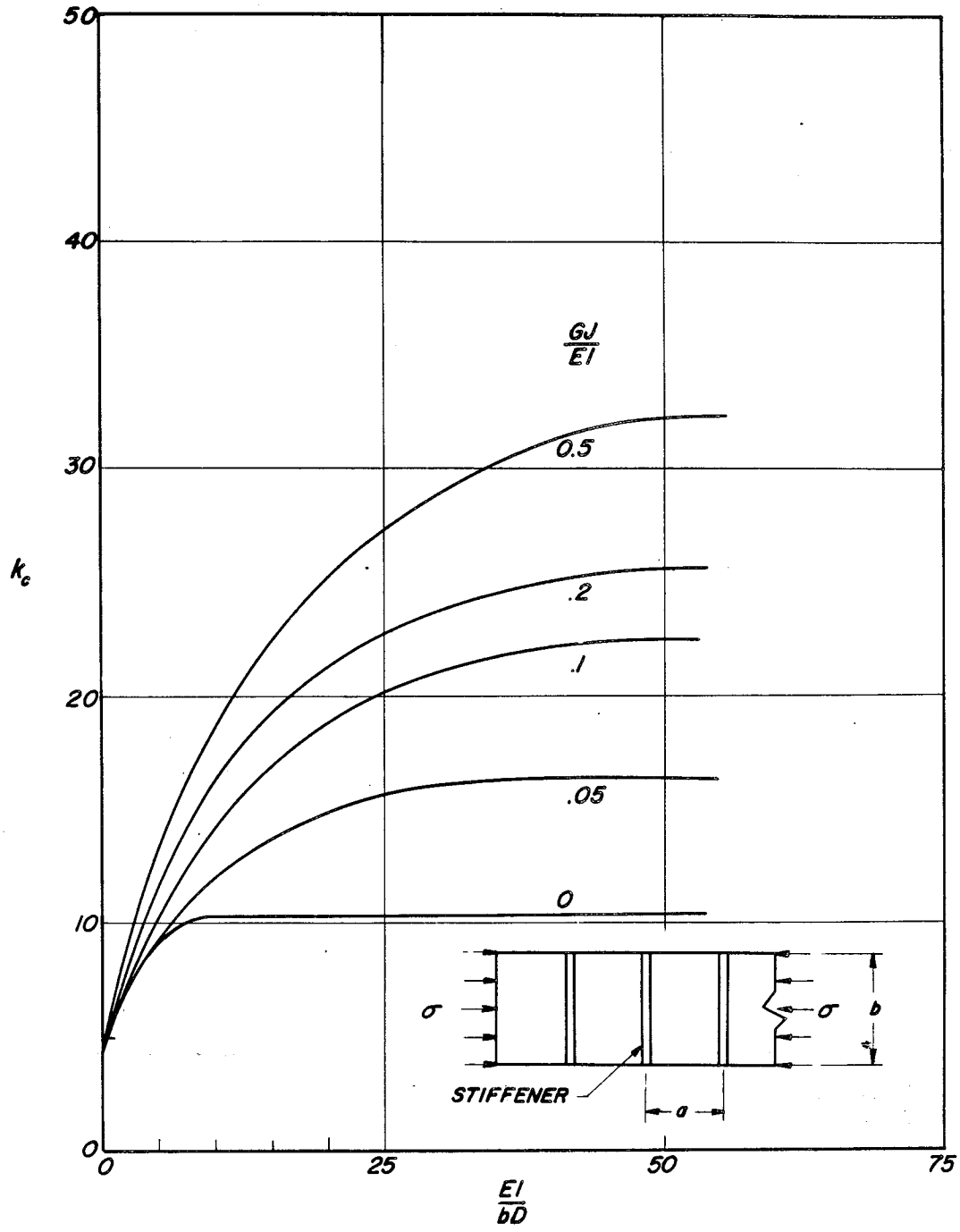

(b) a/b = 0.35.

Figure 13.- Continued.

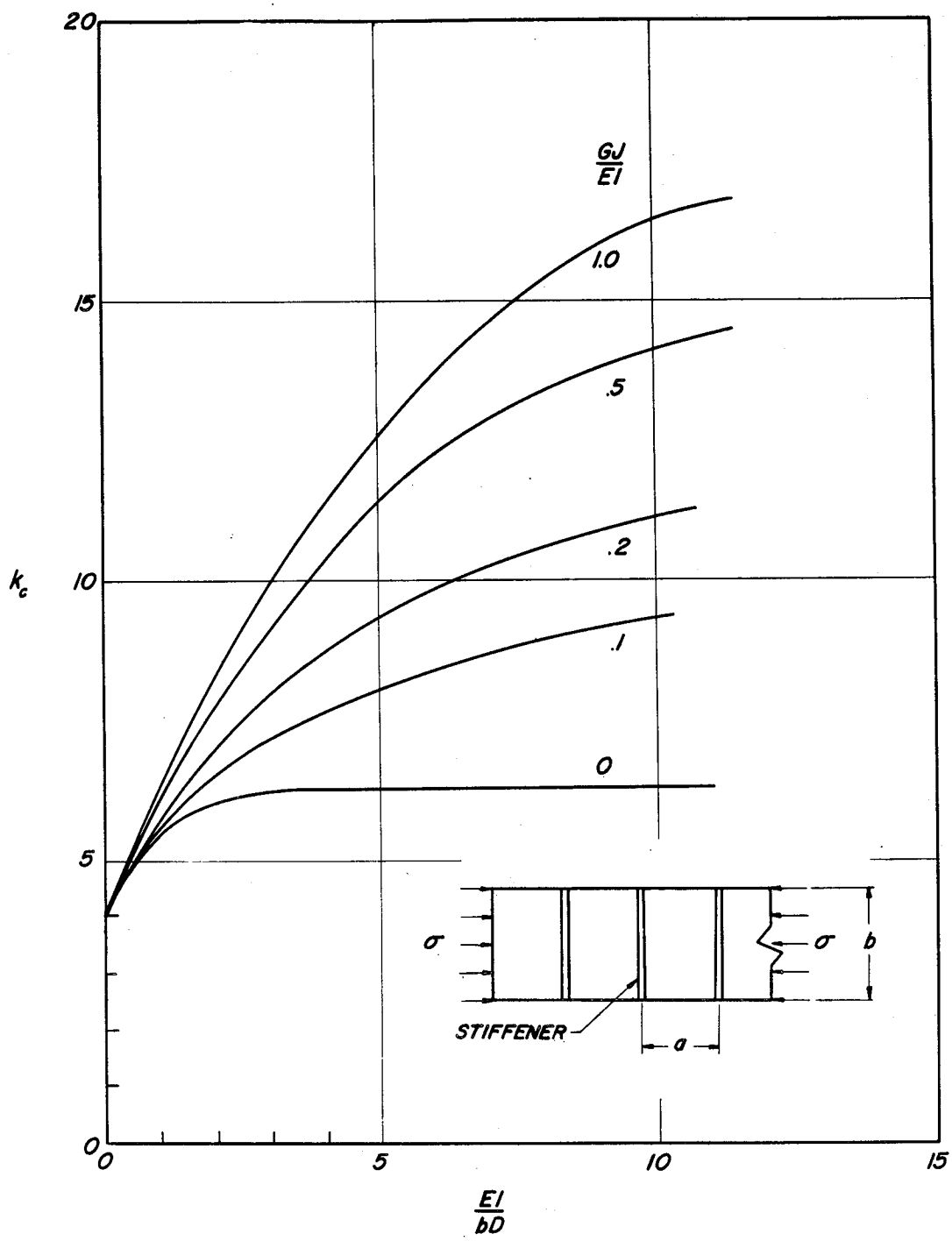

(c) a/b = 0.50.

Figure 13.- Concluded.

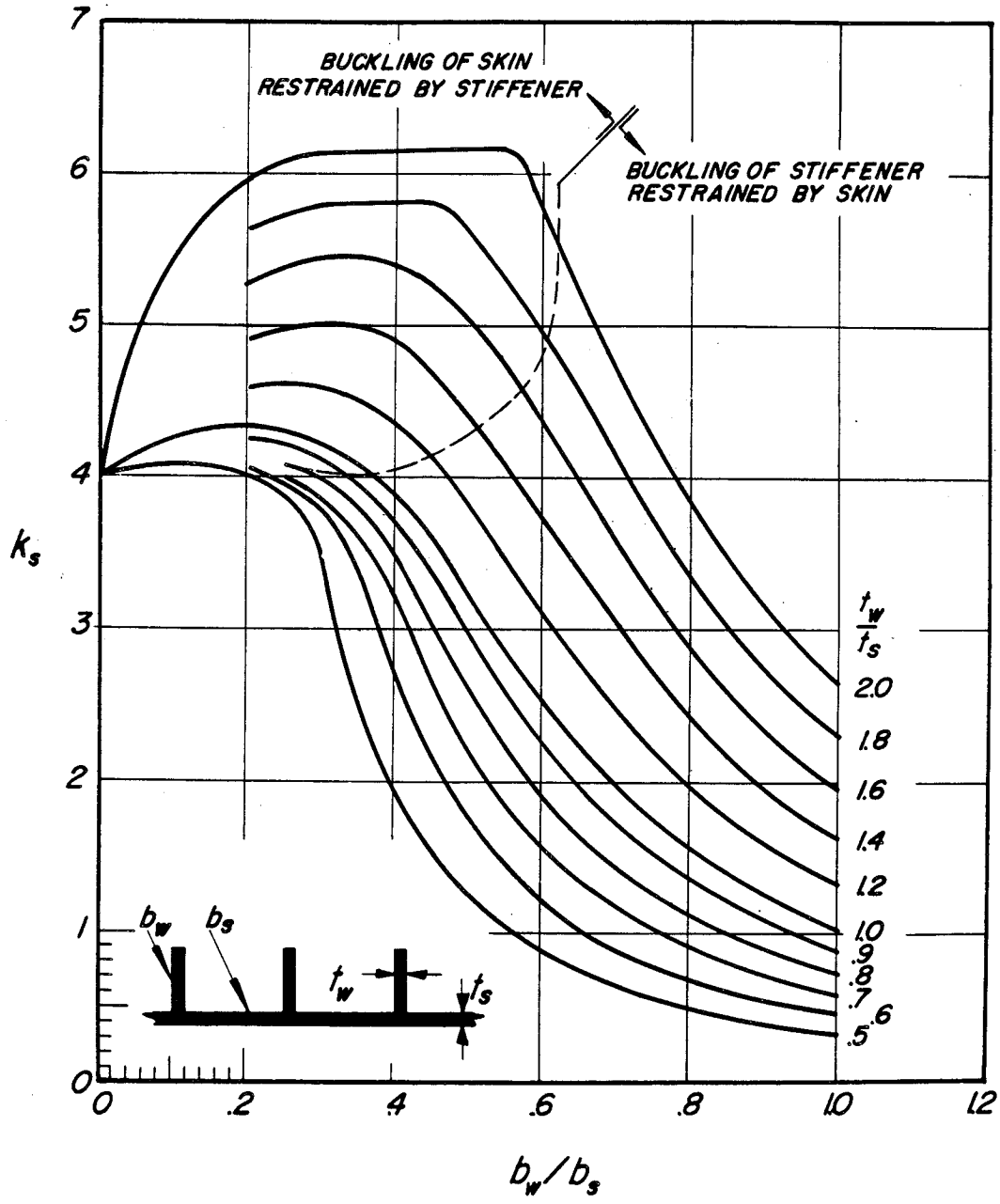

(a) Web stiffeners. $0.5 < t_w/t_s < 2.0$ (Data of ref. 20.)

Figure 14.- Compressive-local-buckling coefficients for infinitely wide idealized stiffened flat plates. $\sigma_{cr} = \frac{k_s \pi^2 E}{12\left(1 - \nu_e^2\right)}\left(\frac{t_s}{b_s}\right)^2$.

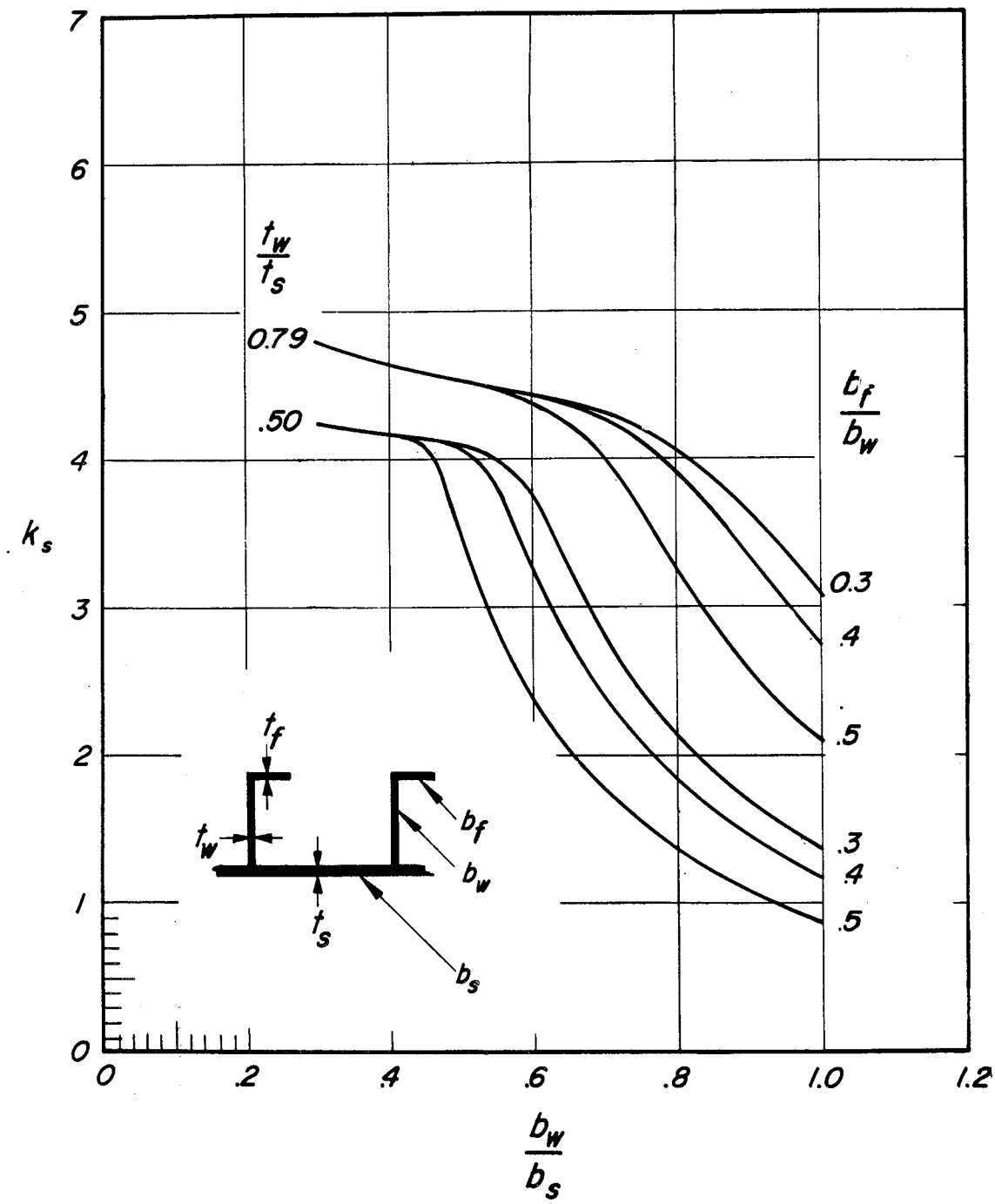

(b) Z-section stiffeners. t_w/t_s = 0.50 and 0.79. (Data of ref. 19.)

Figure 14.- Continued.

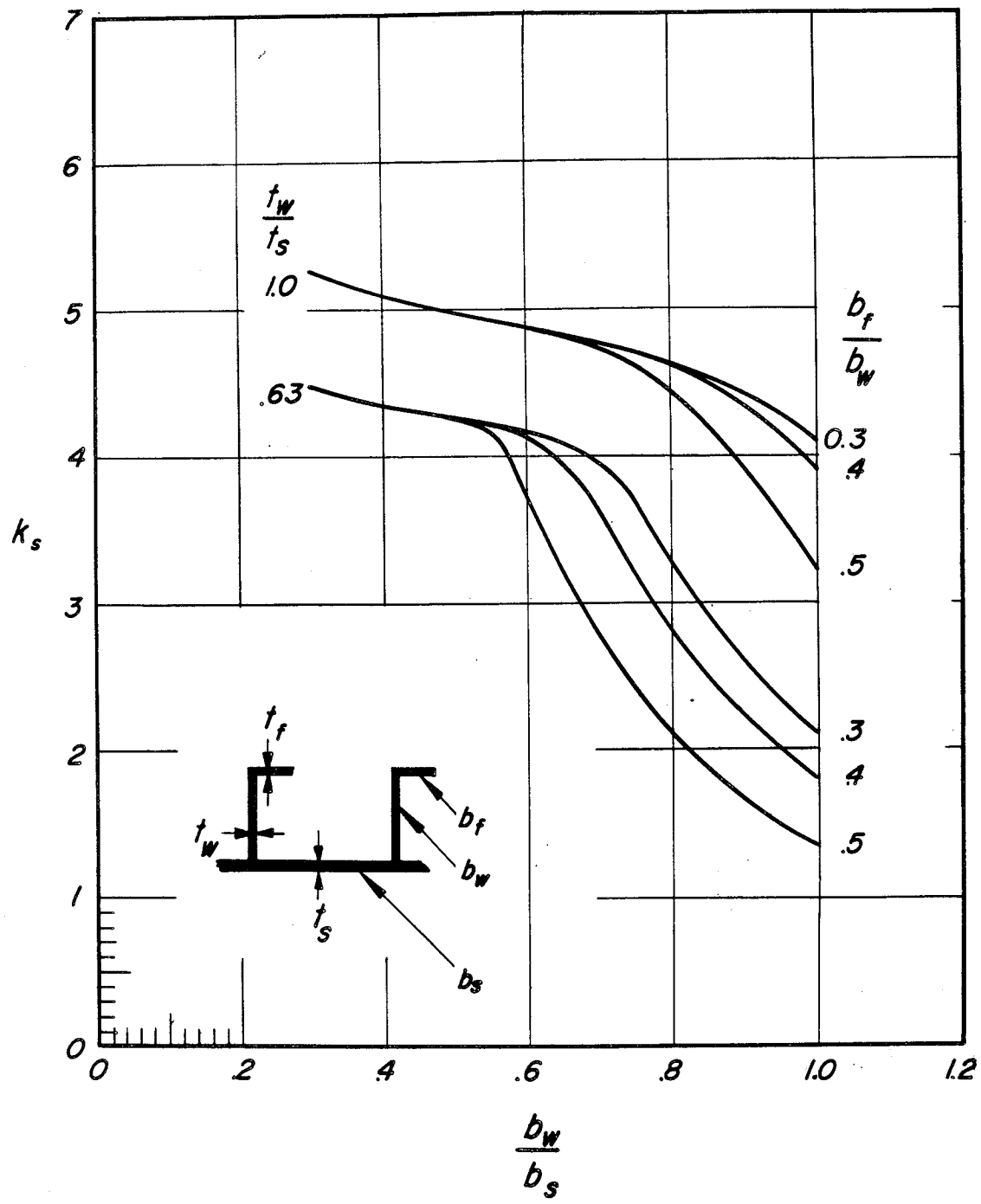

(c) Z-section stiffeners. t_w/t_s = 0.63 and 1.0. (Data of ref. 19.)

Figure 14.- Continued.

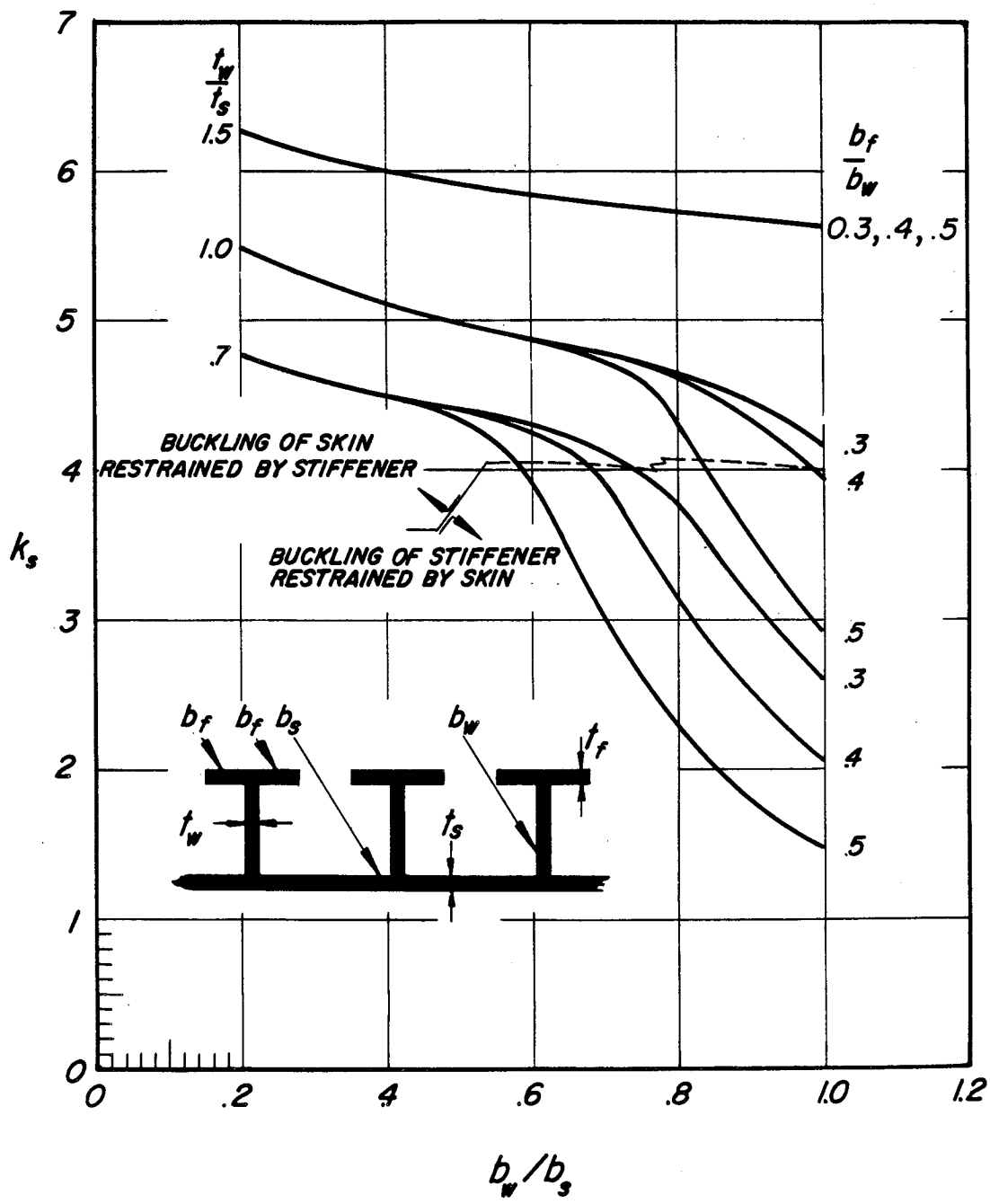

(d) T-section stiffeners. $t_w/t_f = 1.0$; $\frac{b_f}{t_f} > 10$; $\frac{b_w}{b_s} > 0.25$.

(Data of ref. 20.)

Figure 14.- Continued.

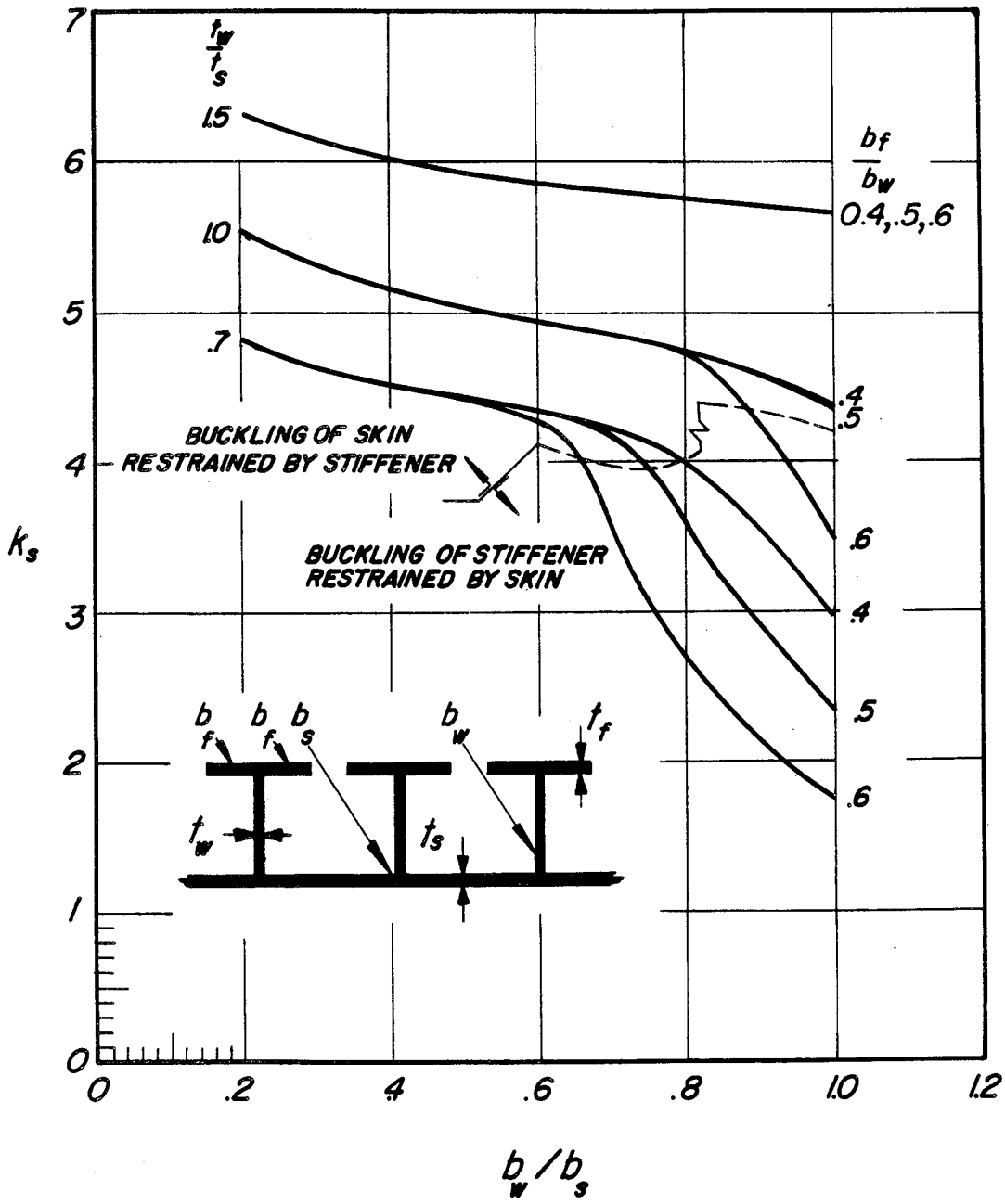

(e) T-section stiffeners. $t_w/t_f = 0.7$; $b_f/t_f > 10$; $b_w/b_s > 0.25$.

(Data of ref. 20.)

Figure 14.- Concluded.

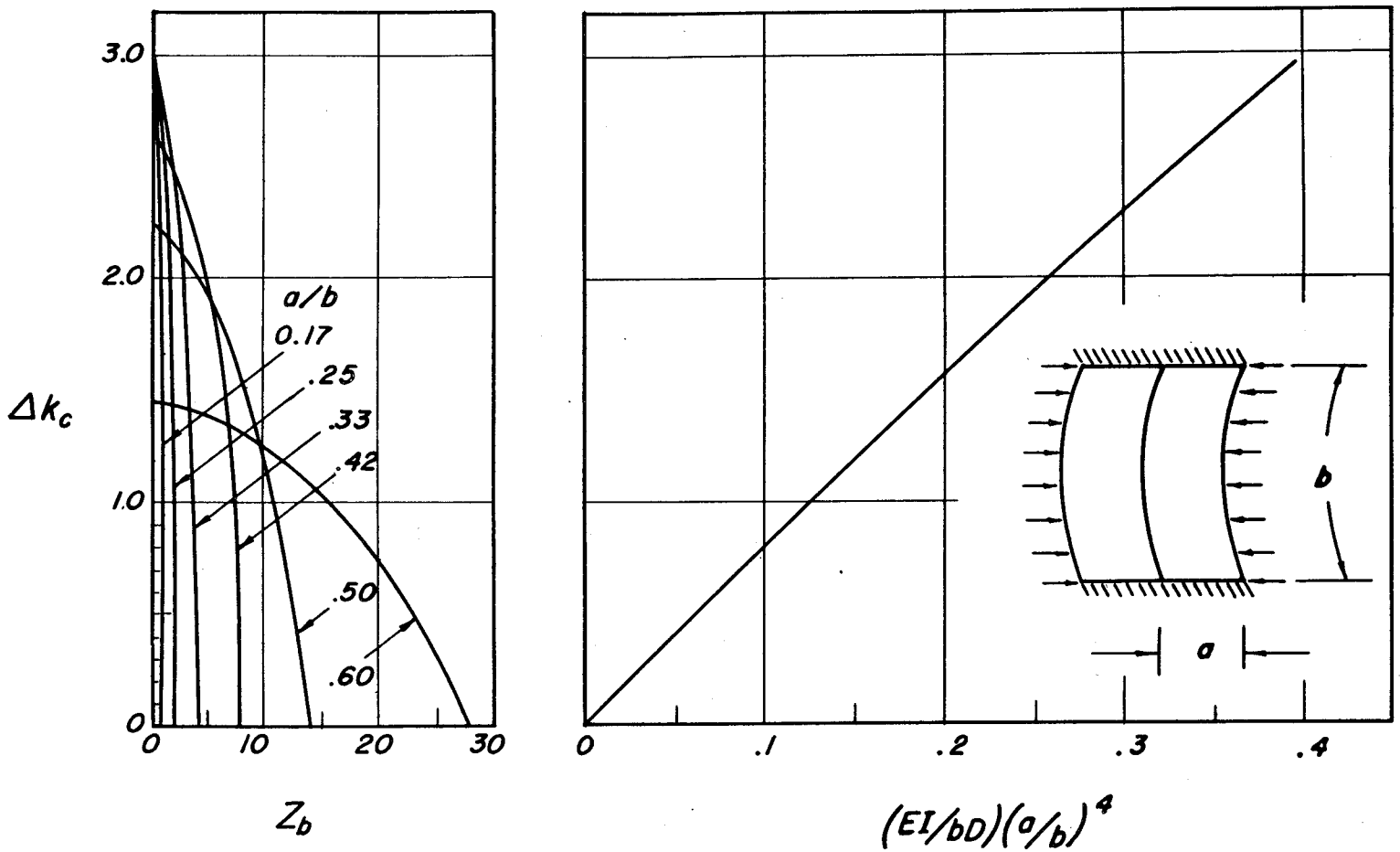

(a) Maximum increase.

(b) Increase for given stiffness.

Figure 15.- Increase in compressive-buckling stress for simply supported curved plates with a center circumferential stiffener. (Data of ref. 21.)

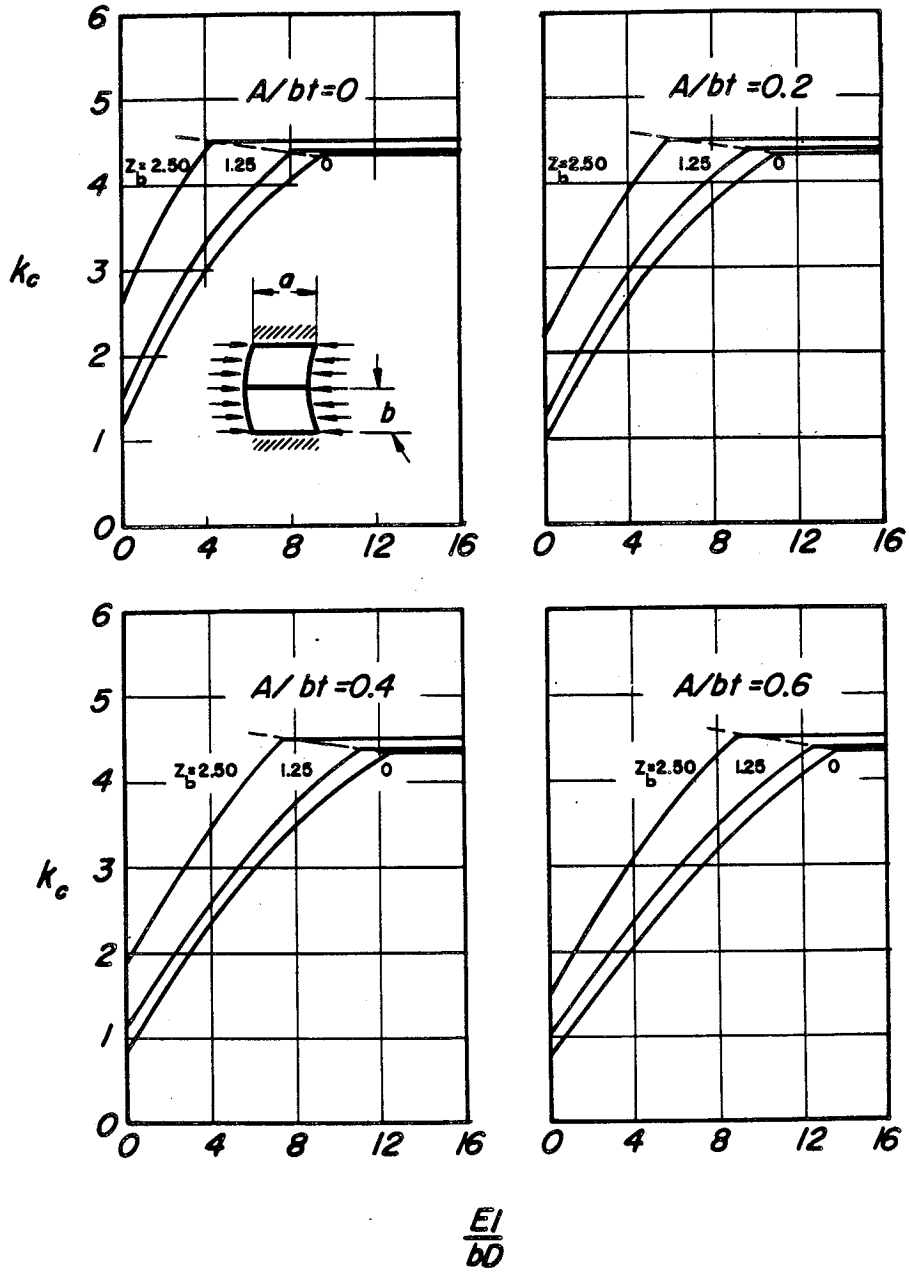

(a) a/b = 4/3.

Figure 16.- Compressive-buckling coefficients for simply supported curved plates with center longitudinal stiffener. $\sigma_{cr} = \dfrac{k_c \pi^2 E}{12\left(1 - \nu_e^2\right)}\left(\dfrac{t}{b}\right)^2$.

(Data of ref. 22.)

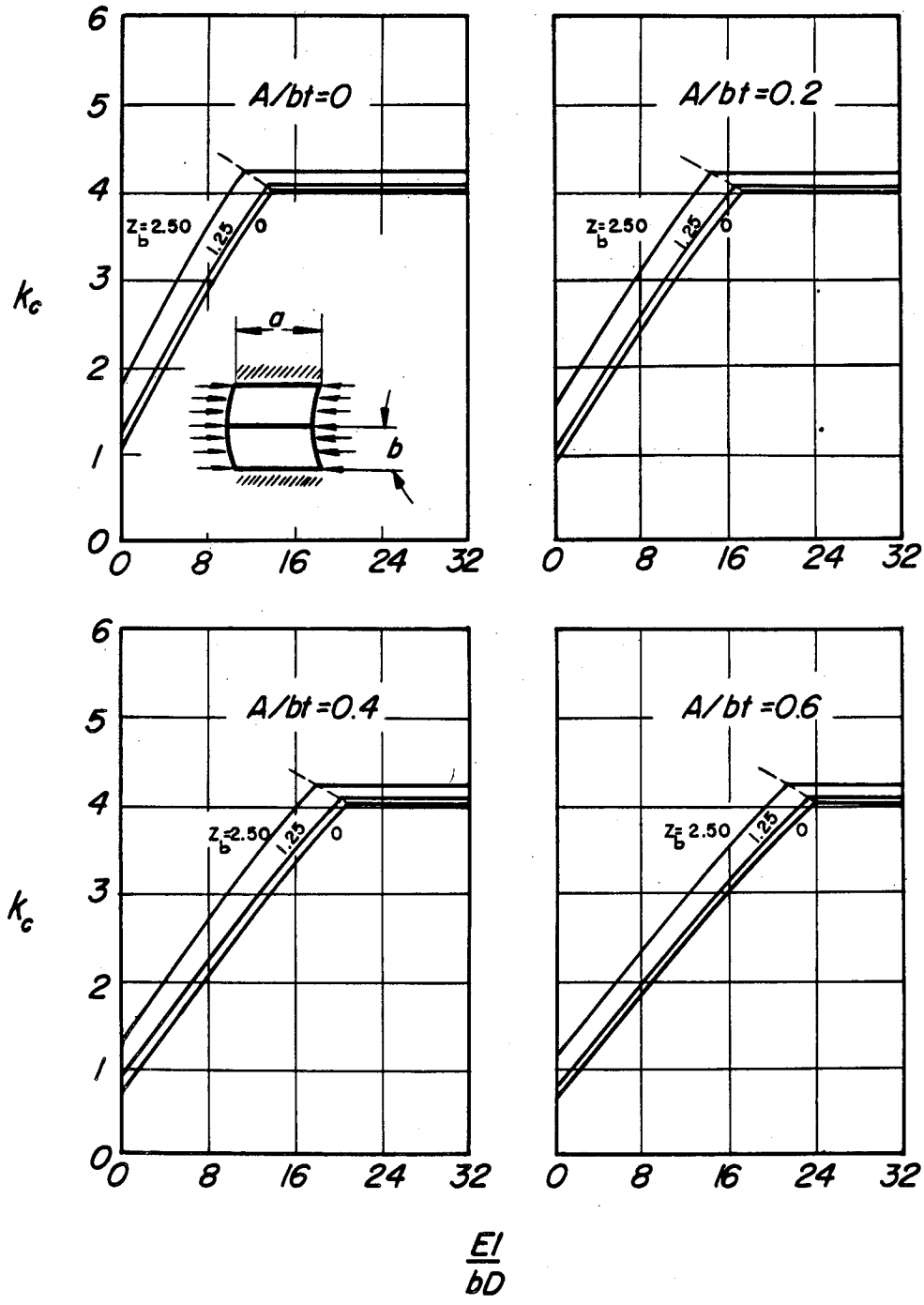

(b) a/b = 2.

Figure 16.- Continued.

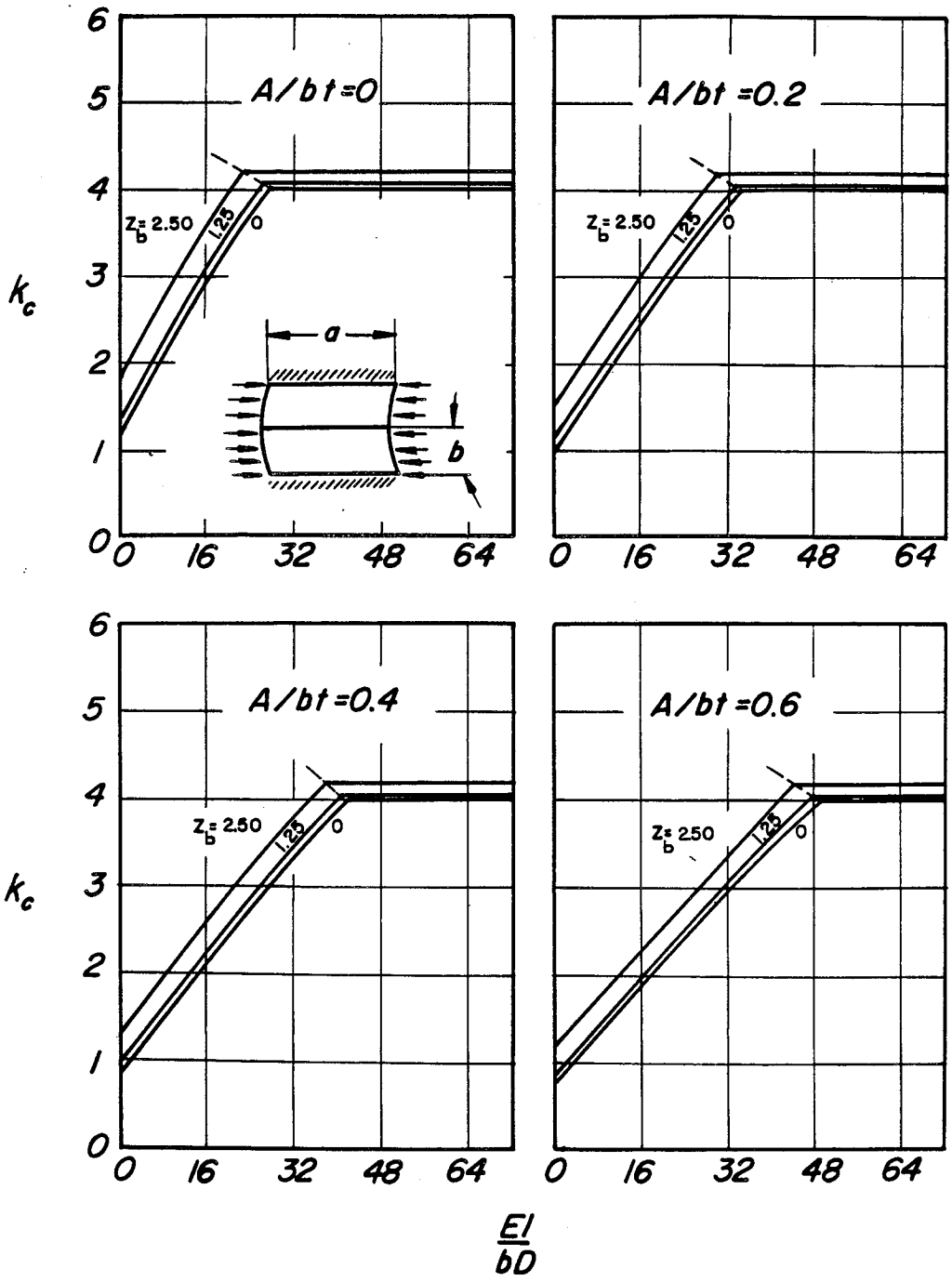

(c) a/b = 3.

Figure 16.- Continued.

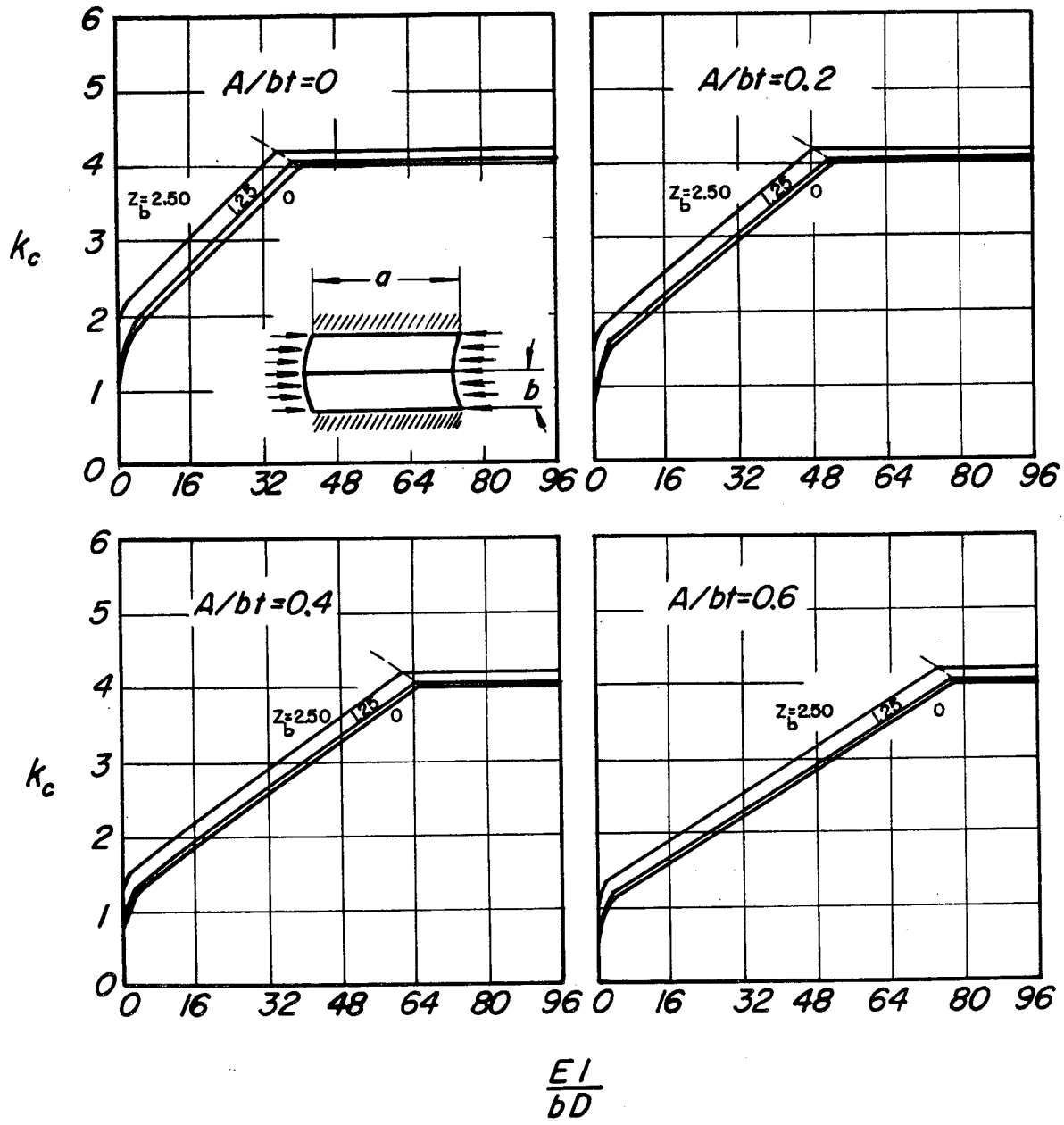

(d) a/b = 4.

Figure 16.- Concluded.

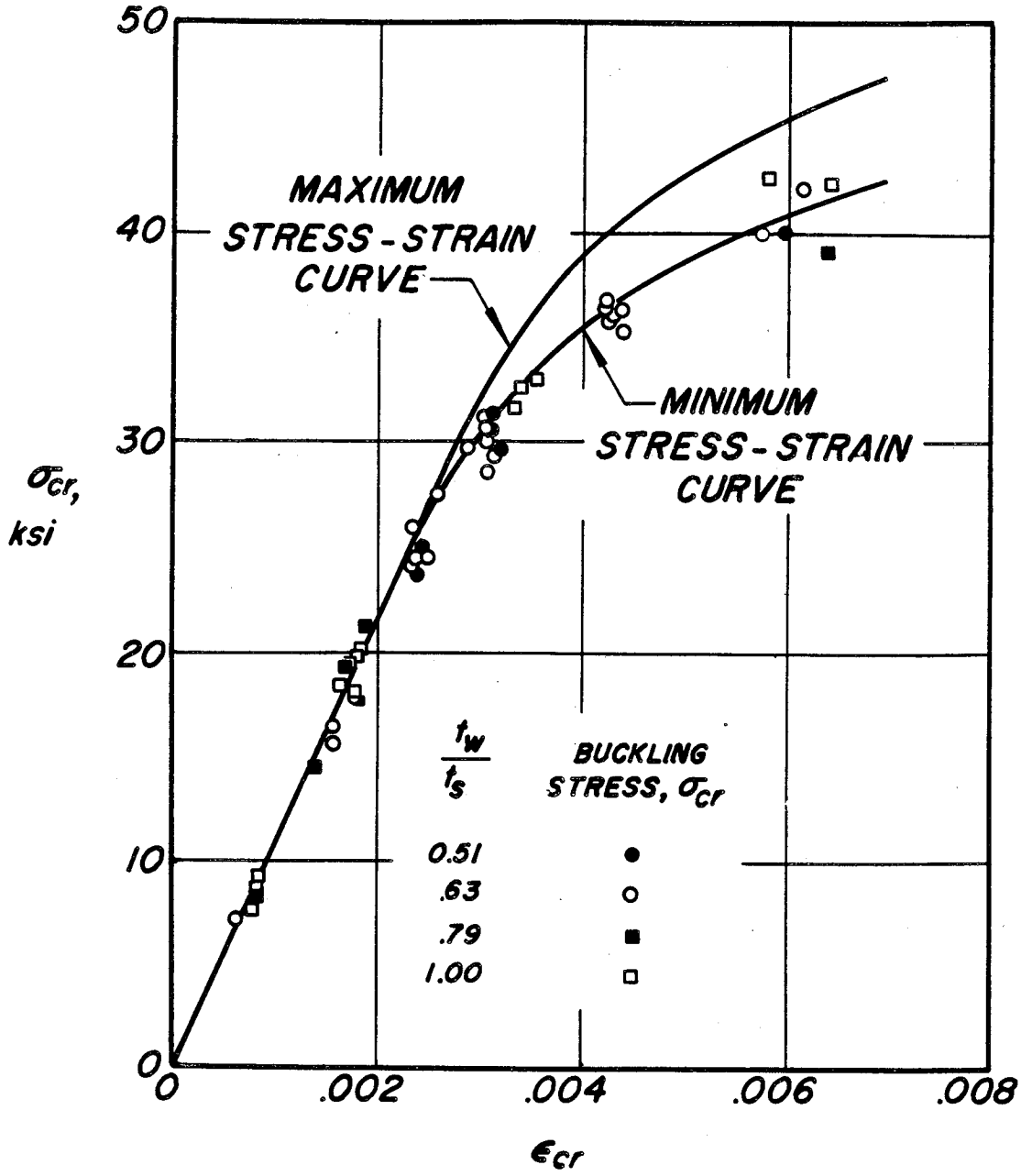

Figure 17.- Comparison of test data with secant-modulus theory for inelastic-local-buckling stress of Z-stiffened flat plates under compressive load. (Data of ref. 19.)

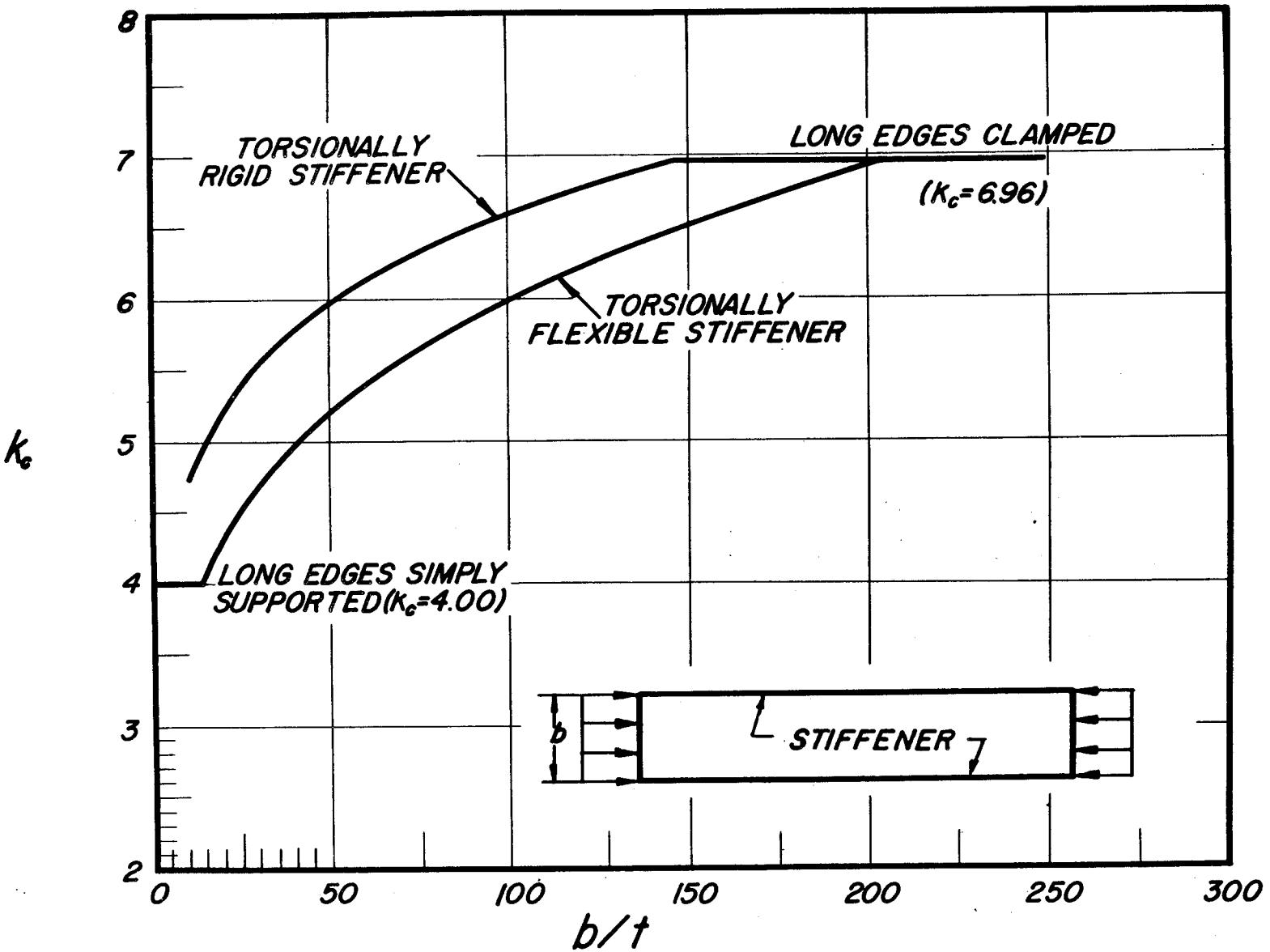

Figure 18.- Effect of torsional rigidity of stiffener on buckling coefficients for flat plates. (Data of ref. 1.)

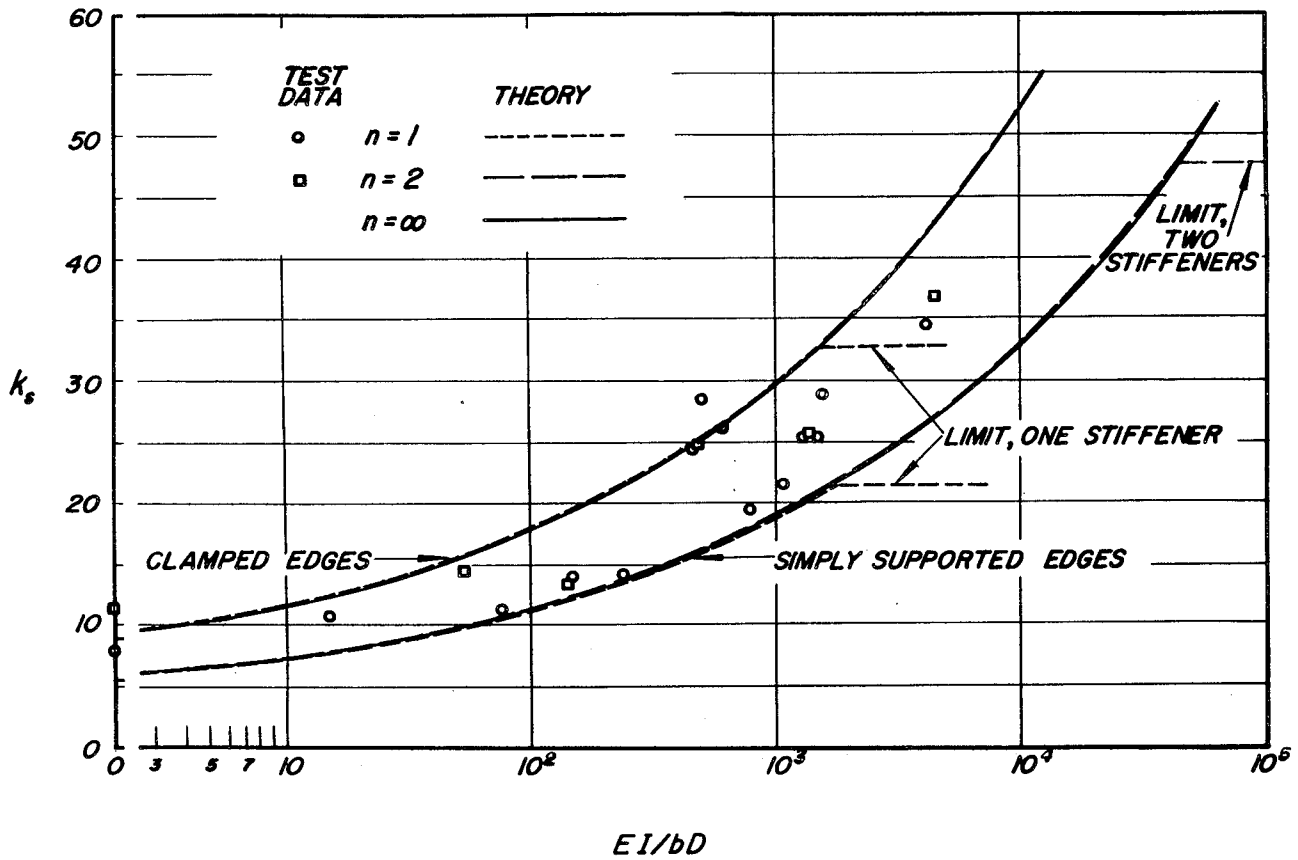

(a) Clamped and simply supported plates; longitudinal stiffeners.

Figure 19.- Comparison of theory and test data for shear-buckling coefficients of long flat plates with stiffeners.

$$\tau_{cr} = \frac{k_s \pi^2 E (n+1)^2}{12\left(1 - \nu_e^2\right)}\left(\frac{b}{t}\right)^2.$$ (Data of ref. 28.)

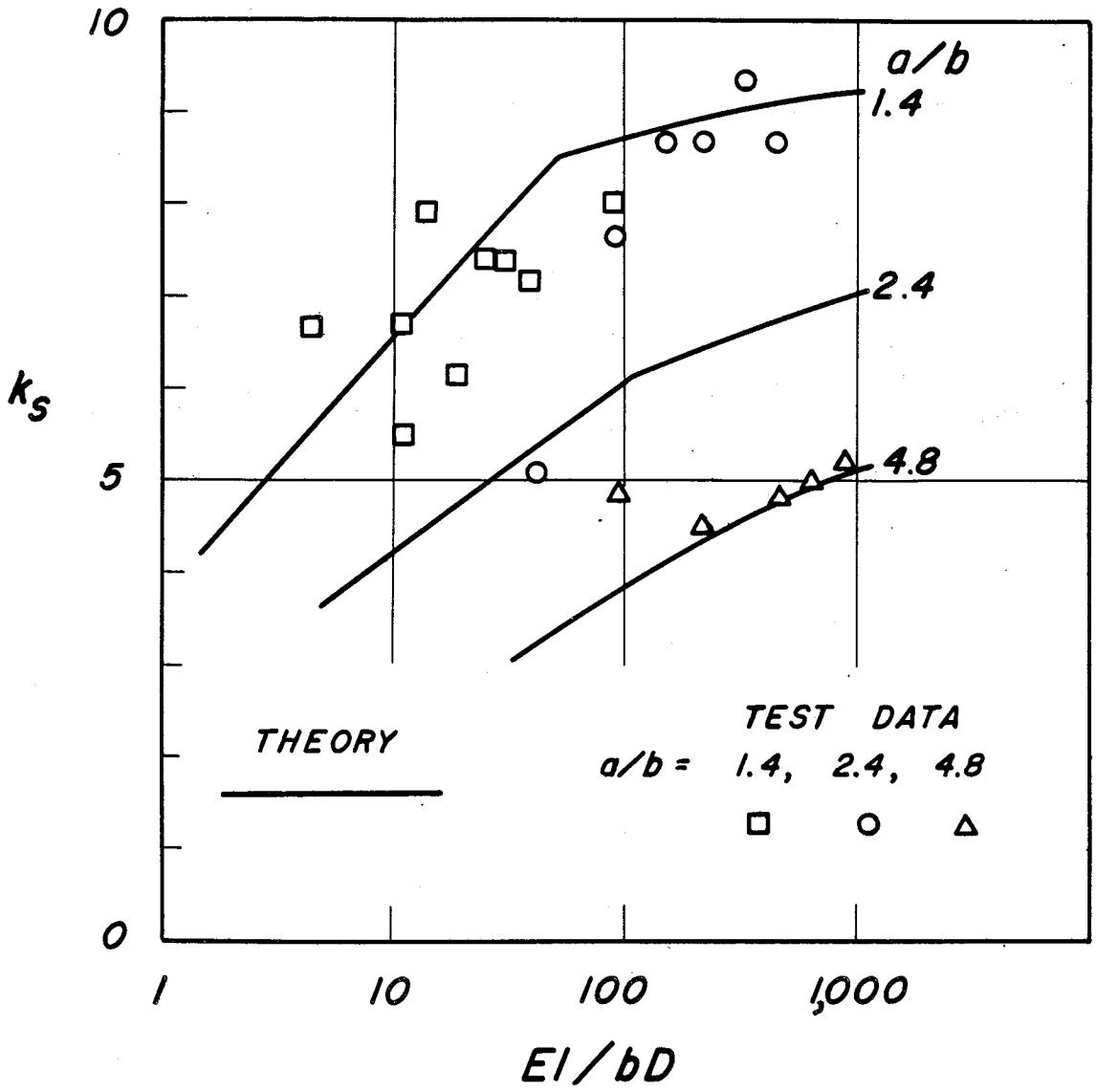

(b) Simply supported plates; transverse stiffeners.

Figure 19.- Concluded.

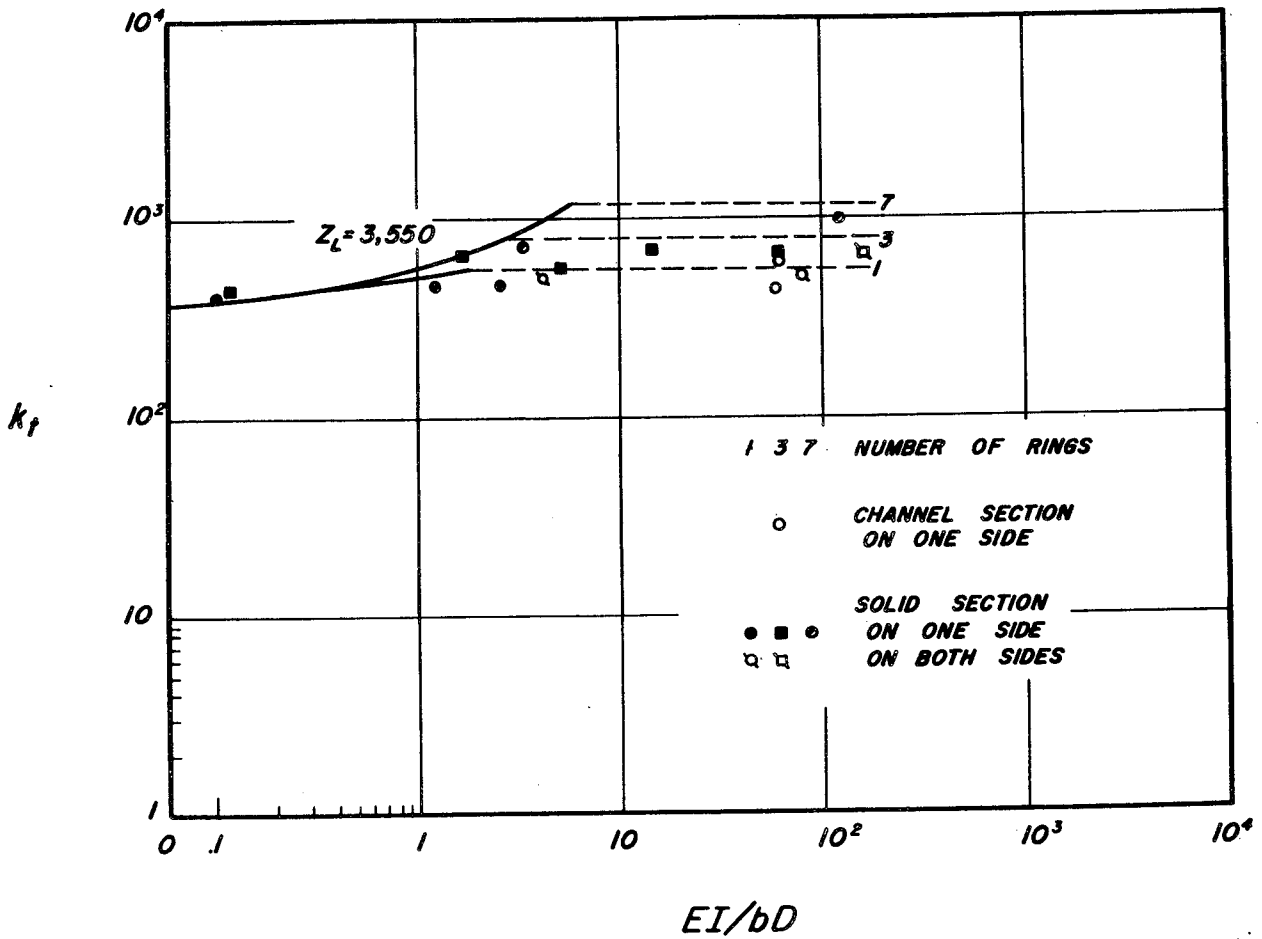

Figure 20.- Comparison of theory and test data for simply supported circular cylinders stiffened by rings and loaded in torsion.

$$\tau_{cr} = \frac{k_t \pi^2 E}{12\left(1 - \nu_e^2\right)}\left(\frac{t}{L}\right)^2.$$ (Data of ref. 30.)

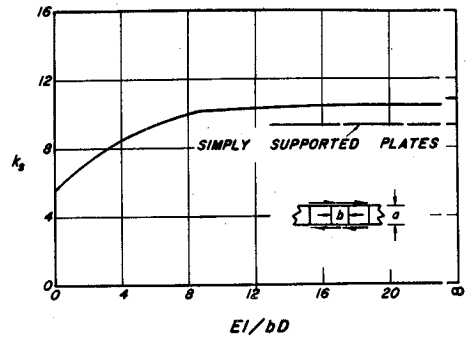

(a) a/b = 1.

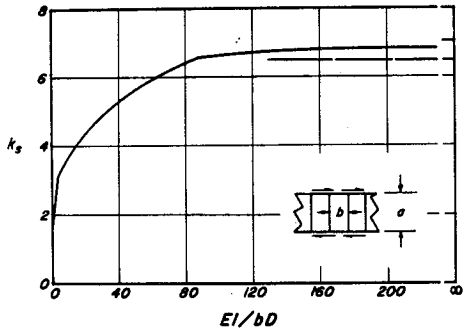

(b) a/b = 2.

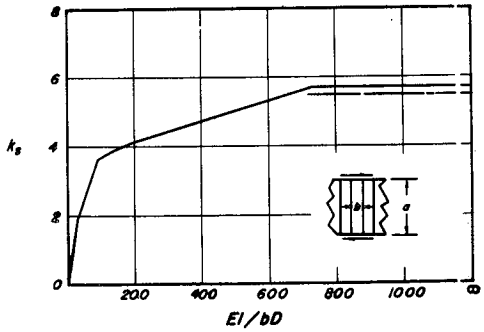

(c) a/b = 5.

Figure 21.- Shear-buckling coefficients for long simply supported flat plates with transverse stiffeners. $\tau_{cr} = \frac{k_s \pi^2 E}{12\left(1 - \nu_e^2\right)}\left(\frac{t}{b}\right)^2$.

(Data of ref. 28.)

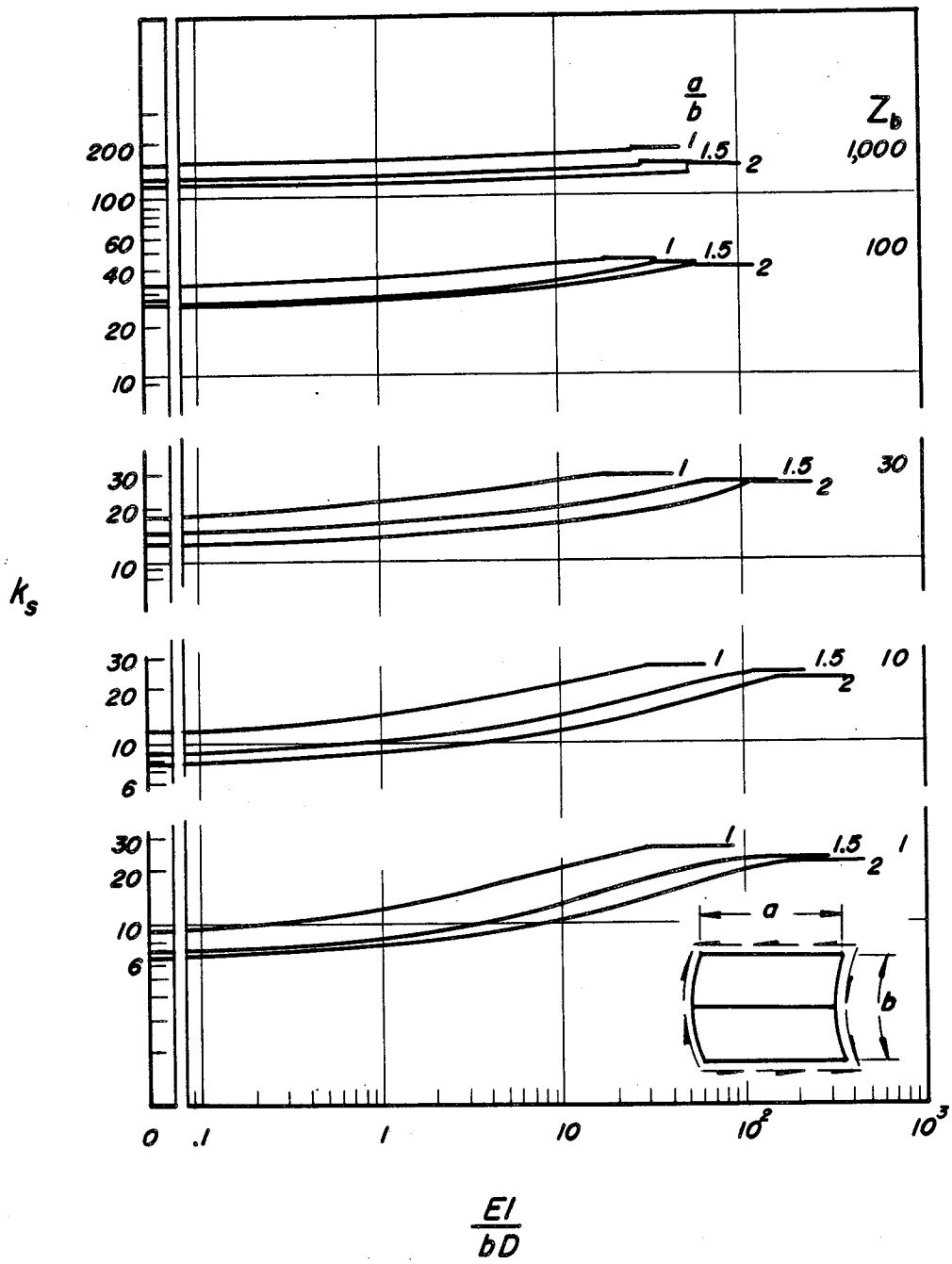

(a) Center axial stiffener; axial length greater than circumferential width.

Figure 22.- Shear-buckling coefficients for simply supported curved plates with center stiffener. (Data of ref. 29.)

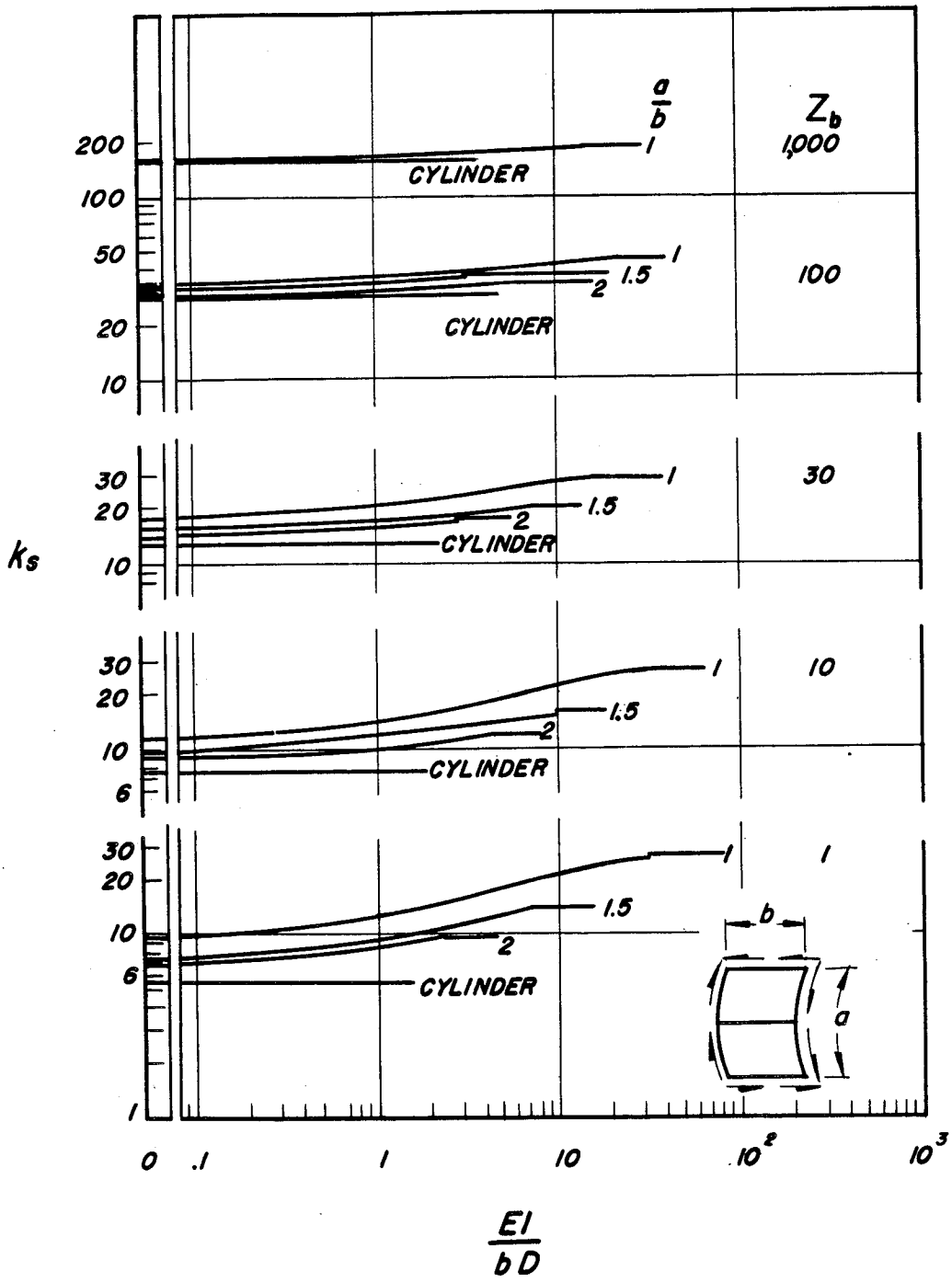

(b) Center axial stiffener; circumferential width greater than axial length.

Figure 22.- Continued.

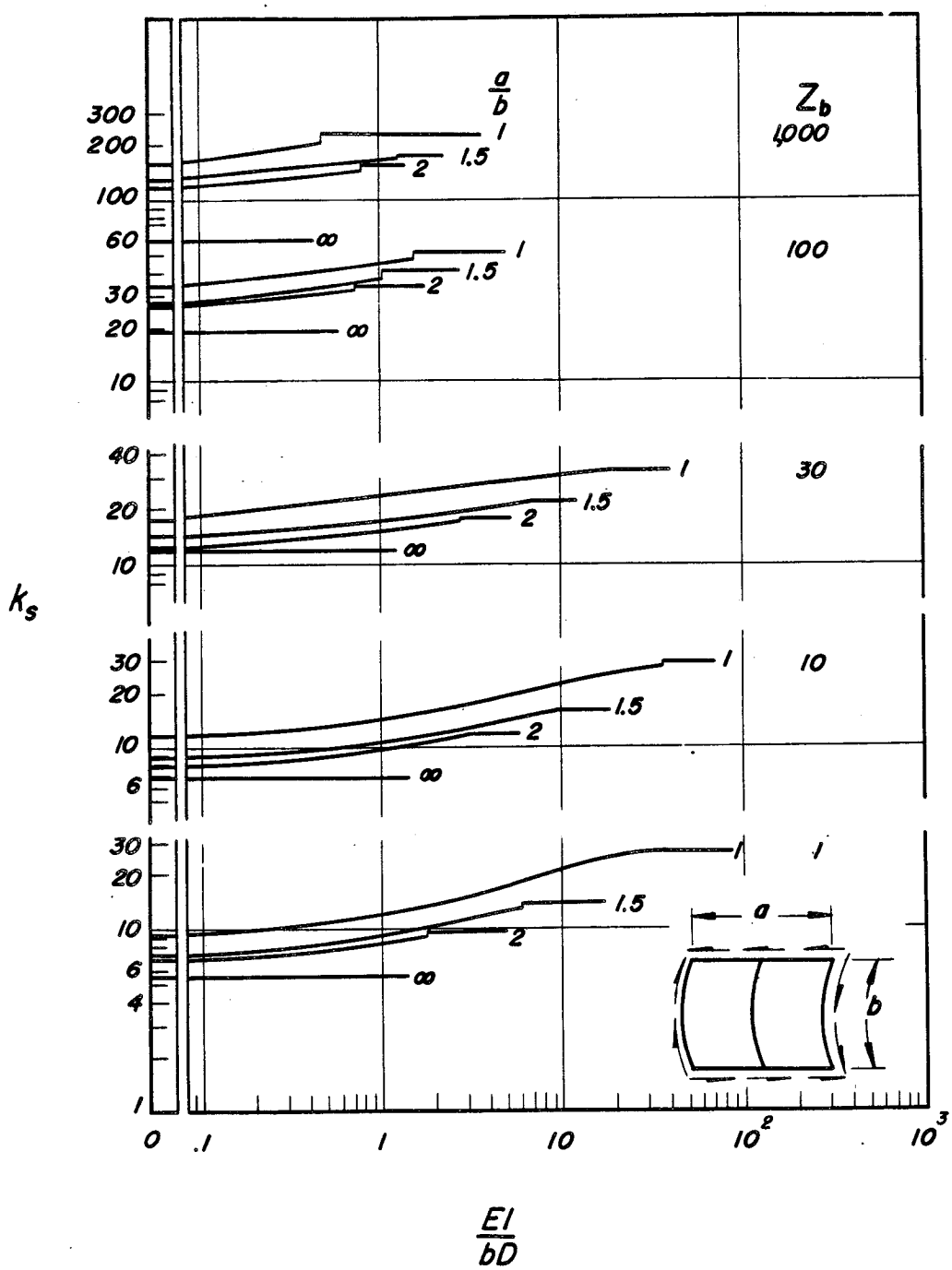

(c) Center circumferential stiffener; axial length greater than circumferential width.

Figure 22.- Continued.

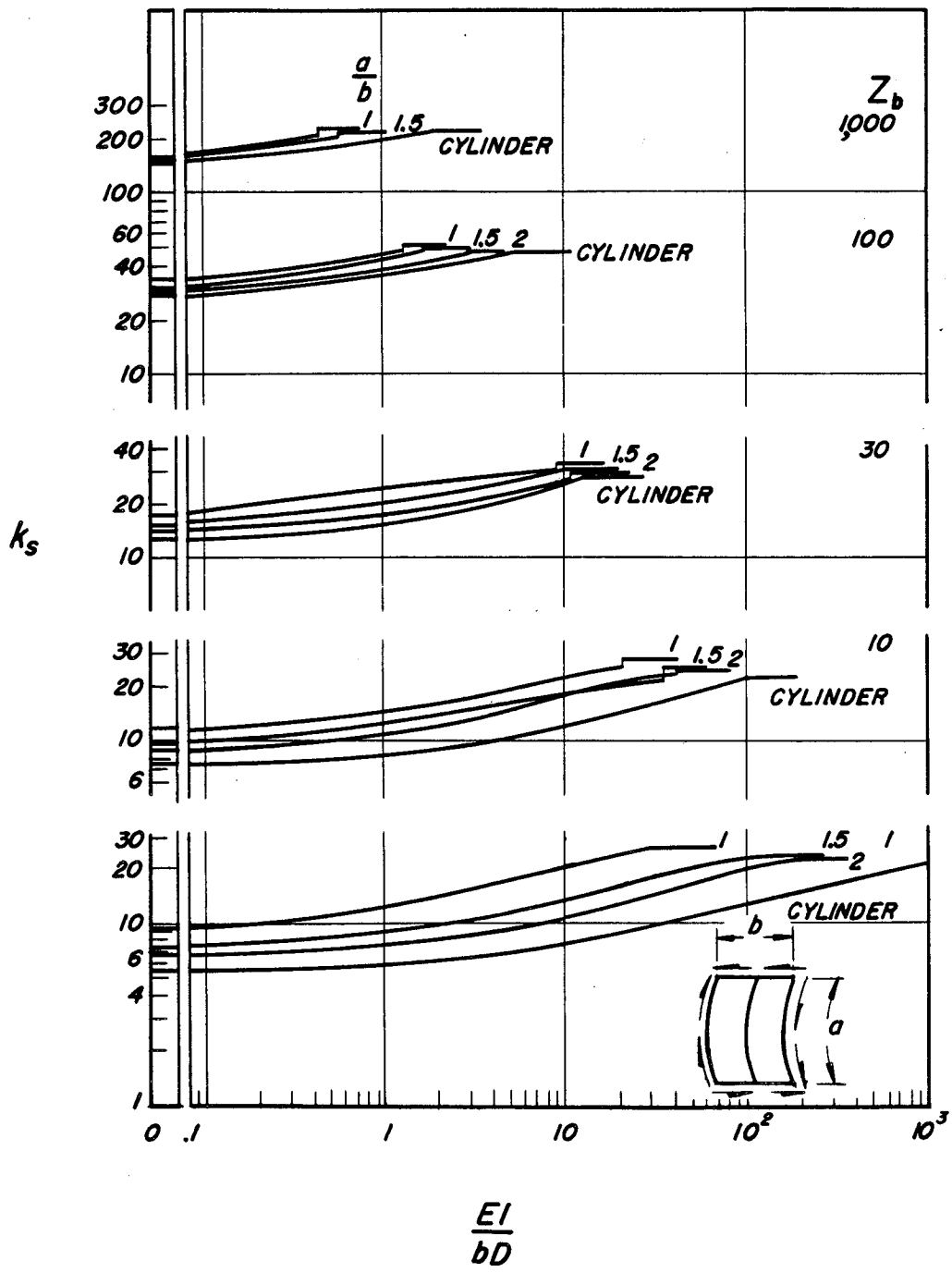

(d) Center circumferential stiffener; circumferential width greater than axial length.

Figure 22.- Concluded.

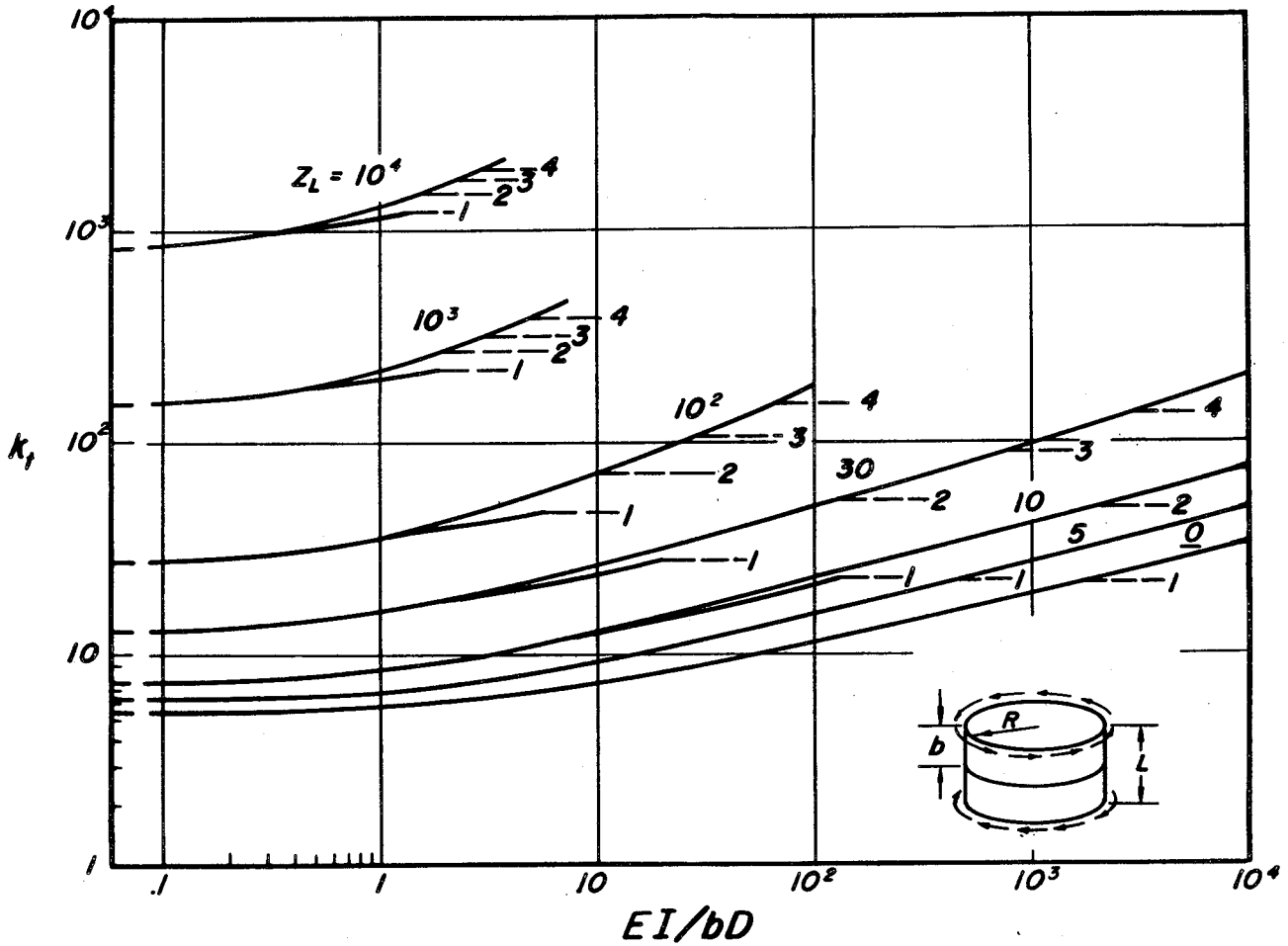

Figure 23.- Buckling coefficients for simply supported circular cylinders stiffened by rings and loaded in torsion. $\tau_{cr} = \dfrac{k_t \pi^2 E}{12\left(1 - \nu_e^2\right)}\left(\dfrac{t}{L}\right)^2$.

(Data of ref. 30.)